

MICROBIAL PRODUCTIVITY IN THE NEUSE RIVER AND PAMLICO SOUND  
ESTUARINE SYSTEM: PATTERNS AND PERTURBATIONS

Benjamin Lewis Peierls

A dissertation submitted to the faculty of the University of North Carolina at Chapel Hill  
in partial fulfillment of the requirements for the degree of Doctor of Philosophy in the  
Department of Marine Sciences.

Chapel Hill  
2009

Approved by:

Hans W. Paerl

Marc J. Alperin

Robert R. Christian

Rachel T. Noble

Frederic K. Pfaender

© 2009  
Benjamin Lewis Peierls  
ALL RIGHTS RESERVED

## **ABSTRACT**

**BENJAMIN LEWIS PEIERLS: Microbial Productivity in the Neuse River and**

**Pamlico Sound Estuarine System: Patterns and Perturbations**

(Under the direction of Hans W. Paerl)

The spatiotemporal patterns of estuarine microbial communities under a variety of conditions is essential to a better understanding of overall ecosystem function and its influence on adjacent coastal areas. In 1999, three sequential hurricanes impacted the Neuse River and Pamlico Sound system and the effects on water quality and the phytoplankton community in the sound were followed for over two years. Pre-storm conditions returned after a month for nutrients and after from 6–8 months for salinity and phytoplankton biomass. Phytoplankton community structure appeared to be still changing at the end of the study. The storm floods generated 2–3 times the annual nitrogen loading to the sound, bypassing the sub-estuary filtration. The patterns and controls of bacterioplankton were examined during 2002–2005 along the salinity gradient in the same system. Bacterioplankton productivity (BP) was similar to measurements from other temperate estuaries and had about 50% of its variation explained by temperature. Dissolved and particulate organic matter showed a small interactive effect with temperature, but much of the remaining variation was left unexplained. Overall, there was a mid-estuarine peak in BP that corresponded to peak phytoplankton productivity and biomass, and the location of these peaks related to annual discharge. This pattern

disappeared at the scale of individual research trips and when the system was impacted by another major hurricane. Variation with depth was large and BP was often higher in bottom or pycnocline waters, correlating with stratification intensity and particulate carbon concentrations. The effect of temperature varied by location, with the upstream, freshwater station having a lower effect than the rest, possibly due to substrate limitation. Data from this study fit the phytoplankton–bacterioplankton relationship seen in cross-system analyses, although the freshwater site again appeared independent of the other sites. Water column respiration was found to be similar to benthic respiration rates and was used to calculate bacterial growth efficiency and carbon demand (BCD). At all the downstream marine stations, BCD was approximately equal to phytoplankton production, whereas it was several times that at the freshwater site indicating support of bacteria by allochthonous organic matter

Dedicated to the memory of Ronald and Julie Peierls.

## **ACKNOWLEDGEMENTS**

I need to begin by thanking my advisor, Dr. Hans Paerl, for his support, encouragement, and patience. His dedication to study of these estuaries is inspiring. I also want to thank the rest of my committee, Dr. Marc Alperin, Dr. Robert Christian, Dr. Rachel Noble, and Dr. Frederic Pfaender for their patience and their many helpful comments and words of support. This work was supported by grants and funding from EPA, NC DENR, NC Sea Grant, NSF, and WRRI.

I am indebted to the fine staff and faculty at both the Department and Institute of Marine Sciences. In particular I would like to recognize Mary Campbell and Naadii Salaam at the Department and Stacy Davis, Claude Lewis, Joe Purifoy, Jean Stack, and Laura White at the Institute.

None of this would have been possible without the help of many dedicated laboratory technicians. Cell count data was graciously provided by Denene Blackwood and other Noble lab personnel. A very special thanks goes to all Paerl Lab technicians, past and present, for superb field and lab support, as well as friendship and camaraderie, including Jeremy Braddy, Lou Anne Cheshire, Scott Ensign, Malia Go, Rodney Guajardo, Alan Joyner, Lois Kelly, Melissa Leonard, Karen Rossignol, Patrick Sanderson, Christina Tallent, Suzanne Thompson, Rich Weaver, Valerie Wunderly, Pam Wyrick.

I want to thank some of the many fellow graduate students I have met along the way for fellowship, support, and helpful discussions: Liz Calandrino, Erika Clesceri,

Julie Dyble, John Fear, Janelle and Jason Fleming, Ken Fortino, Tom Gallo, Alicia Gaulke, Galen Johnson, Nathan Hall, Jennifer Joyner, Sara McMillan, Pia Moisander, Amy Poe, Tim Steppe, Amy Waggener, and David Whitall. I have also had wonderful interactions and much help from many post-doctoral researchers at the Institute, including Chris Buzzelli, Dina Leech, Mike Piehler, Jay Pinckney, Tammi Richardson, Chris Taylor, Luke Twomey, Tony Yannarell, Lexia Weaver, Mike Wetz.

I am grateful for the much needed distraction provided by the Morehead Brass Consortium, the Carteret Community Sunshine Band, and Lookout Ultimate.

To my family, thank you for your patience and understanding. My four-legged family, Rosie, Ozy, Emmy, and Rohan, also helped me through this venture.

Finally, I wish to give loving thanks to Kar for her tolerance, understanding, humor, and support through this sometimes trying process. I guess it took a little longer than we expected...

## TABLE OF CONTENTS

|   |     |
|---|-----|
| LIST OF TABLES .....  | xi  |
| LIST OF FIGURES .....   | xii |
| LIST OF ABBREVIATIONS.....  | xix |
| CHAPTER   |     |
| 1. INTRODUCTION AND BACKGROUND .....  | 1   |
| 2. WATER QUALITY AND PHYTOPLANKTON AS INDICATORS OF<br>HURRICANE IMPACTS ON A LARGE ESTUARINE ECOSYSTEM ..... | 6   |
| 2.1 Abstract .....  | 6   |
| 2.2 Introduction.....   | 7   |
| 2.3 Materials and Methods.....  | 10  |
| 2.3.1 System Description and Study Location.....  | 10  |
| 2.3.2 Field Sampling .....  | 12  |
| 2.3.3 Laboratory Analyses .....   | 13  |
| 2.3.4 Network Analysis.....   | 15  |
| 2.3.5 Statistics .....  | 16  |
| 2.4 Results.....  | 17  |
| 2.4.1 Temporal Patterns .....   | 17  |
| 2.4.2 Spatial Patterns.....   | 26  |
| 2.4.3 N Loading .....   | 29  |
| 2.5 Discussion .....  | 30  |
| 2.6 Acknowledgements.....   | 41  |
| 3. TEMPORAL PATTERNS AND CONTROLS OF BACTERIOPLANKTON .....   | 43  |
| 3.1 Introduction.....   | 43  |
| 3.2 Methods and Analysis.....   | 44  |



|  |     |
|--|-----|
| 3.2.1 Stations and collection .....                        | 44  |
| 3.2.2 Chemistry and phytoplankton .....                    | 46  |
| 3.2.3 Bacterioplankton .....                               | 46  |
| 3.2.4 Statistics and analysis .....                        | 48  |
| 3.3 Results.....   | 48  |
| 3.3.1 Summary .....  | 48  |
| 3.3.2 Interannual Patterns .....                           | 50  |
| 3.3.3 Monthly Patterns .....                               | 55  |
| 3.3.4 Effect of Temperature .....                          | 62  |
| 3.3.5 Multiple regression analyses.....                    | 65  |
| 3.3.6 Impact of Events .....                               | 66  |
| 3.4 Discussion .....                                       | 70  |
| 3.5 Conclusions.....                                       | 77  |
| 4. SPATIAL PATTERNS AND CONTROLS OF BACTERIOPLANKTON ..... | 79  |
| 4.1 Introduction.....                                      | 79  |
| 4.2 Methods.....   | 81  |
| 4.2.1 Field measurements and water collection .....        | 81  |
| 4.2.2 Lab and data analyses .....                          | 82  |
| 4.3 Results.....   | 83  |
| 4.3.1 Summaries by station.....                            | 83  |
| 4.3.2 Effect of discharge .....                            | 92  |
| 4.3.3 Property–salinity relationships.....                 | 95  |
| 4.3.4 Effect of location.....                              | 98  |
| 4.3.5 Vertical scale variability .....                     | 100 |
| 4.3.6 Cross system comparison.....                         | 103 |

|   |     |
|---|-----|
| 4.4 Discussion .....                    | 106 |
| 4.5 Conclusions.....                    | 110 |
| 5. RESPIRATION AND CARBON FLUXES .....  | 112 |
| 5.1 Introduction.....                   | 112 |
| 5.2 Methods.....                        | 114 |
| 5.3 Results and Discussion .....        | 116 |
| 5.3.1 Respiration Values .....          | 116 |
| 5.3.2 Bacterial Growth Efficiency ..... | 118 |
| 5.3.3 Bacterial Carbon Demand.....      | 119 |
| 5.3.4 Oxygen Deficits .....             | 121 |
| 5.4 Conclusions.....                    | 124 |
| 6. SUMMARY .....                        | 125 |
| APPENDIX: LEUCINE UPTAKE KINETICS.....  | 131 |
| LITERATURE CITED .....                  | 134 |

## LIST OF TABLES

|           |  |    |
|-----------|--|----|
| Table 2.1 | Group comparisons for Pamlico Sound data pooled by time period. Flood period is October 1999–March 2000 compared against the same months in the succeeding two years. Fall is September, October, and November. Numbers are median values for each group. Significant difference between groups as determined by the Kruskal–Wallis rank-sum test is indicated by italics ( $p < 0.05$ ), italics + bold ( $p < 0.01$ ), and bold ( $p < 0.0001$ ). Salinity = surface salinity; $\Delta$ Sal. = bottom salinity–surface salinity; DOC = dissolved organic carbon; C:N = molar carbon to nitrogen ratio; $\text{NO}_3$ = nitrate + nitrite; $\text{NH}_4$ = ammonium; $\text{PO}_4$ = orthophosphate; DO = bottom dissolved oxygen; Chl $a$ = fluorometrically determined chl $a$ . .... | 21 |
| Table 2.2 | As in Table 2.1, but for algal taxonomic groups determined from diagnostic photopigments. All units are $\mu\text{g chl } a \text{ L}^{-1}$ . BD = below detection. ....   | 25 |
| Table 2.3 | As in Table 2.1 and Table 2.2, but for data pooled by station groups. Spatial comparisons were conducted for three different seasons during 1999 and 2000 and for all available data. ....   | 28 |
| Table 3.1 | Summary of surface physical, chemical, and biological variables measured during 2002–2005 in the NRPS. IQR is interquartile range (third quartile minus first quartile) and N is the number of samples. BD = below detection (reported as method detection limit/3, DIN: 0.14, Phos.: 0.004). ....   | 49 |
| Table 3.2 | Correlation coefficients for selected parameters versus BP. The coefficient was determined using the Spearman rank correlation test. ....  | 66 |
| Table 4.1 | Correlation with salinity for measured chemical and biological variables. $\text{BP}_{20}$ is BP normalized to 20 °C. Coefficient is from the Spearman’s rank correlation test. ....   | 95 |
| Table 4.2 | Results of multiple regression analysis by station with BP as the response factor. Fitted model is $\ln\text{BP} = B_0 + B_1\text{Temp} + B_2\ln\text{DOC} + B_3\ln\text{PON}$ . Coefficients significantly different from zero are indicated with * ( $p < 0.05$ ) or ** ( $p < 0.001$ ). ....  | 99 |

## LIST OF FIGURES

|  |    |
|--|----|
| Figure 2.1. Map of study area including sampling stations and coverage dates. Station groups, identified by West (W), Middle (M), and East (E) are used for spatial comparisons.....   | 12 |
| Figure 2.2 Box and whisker plots of surface salinity; $\Delta S$ (difference between bottom and surface salinity); surface and bottom water nitrate plus nitrite (top), ammonium (middle), and orthophosphate (bottom); The diamond symbol is the median value, shaded boxes indicate interquartile range (25th to 75th percentile), and the whiskers are the minimum and maximum values ( $n = 9-10$ or $18-20$ ). The flow data comes from the USGS gauging station at Kinston, North Carolina (station no. 02089500, $N35^{\circ} 15' 29''$ , $W77^{\circ} 35' 09''$ ), and is daily mean stream flow in $m^3 s^{-1}$ ..... | 18 |
| Figure 2.2 (Continued) Box and whisker plots of diffuse light attenuation coefficient, $K_d$ ( $m^{-1}$ ); surface and bottom dissolved organic carbon (DOC) (dotted line represents the long-term median concentration for October 1999–April 2002); the molar ratio of POC to PN in surface and bottom water samples (the dotted line is the Redfield C:N ratio).....  | 19 |
| Figure 2.2 (Continued) Box and whisker plots of surface and bottom chl <i>a</i> ; group-specific algal biomass; and bottom water DO in $mg L^{-1}$ (upper dashed line is EPA criterion continuous concentration [ $4.8 mg L^{-1}$ ] and the lower dotted line is the criterion minimum concentration [ $2.3 mg L^{-1}$ ; USEPA 2000]. These limits signify critical hypoxic conditions) in Pamlico Sound over time.....  | 20 |
| Figure 2.3 Spatial distribution of $\Delta S$ (psu), bottom DO ( $mg L^{-1}$ ), and surface chl <i>a</i> ( $\mu g L^{-1}$ ) from October 6, 1999–February 22, 2000. Closed circles indicate actual station locations and each bar indicates the value for a specific date at that station. A scale bar is in the upper right corner. ....  | 27 |
| Figure 2.4 Relationship of total N (TN, in $mmol m^{-2} season^{-1}$ ) exported to Pamlico Sound as a function of TN loaded to the Neuse River estuary as determined by network analysis. Each point represents one season from the 16 consecutive seasonal networks for the period 1985–1989. The most extreme import and export values occurred as a result of major storms in winter 1987. Lines are least squares linear and non-linear (2nd order polynomial) regression. Dotted sections of lines indicate extrapolation beyond the data. ....   | 30 |
| Figure 3.1 Map of study area showing station locations. Station labels are prefixed with the station group indicator NR (Neuse River) or PS (Pamlico Sound). Inset shows the extent of the map in context with the southeastern U.S. ....  | 45 |

|             |  |    |
|-------------|--|----|
| Figure 3.2  | Daily mean Neuse River discharge (top) and surface salinity in NRPS (bottom) by year. Discharge data came from the USGS gage at Fort Barnwell (# 02091814). Solid diamond is the median, light grey box is the interquartile range (IQR), and whiskers are drawn to the last value within the span from the quartiles ( $1.5 \times \text{IQR}$ ). Values outside of the span are considered outliers and are indicated by open circles. The dark grey box indicates 95% confidence intervals around the median..... | 51 |
| Figure 3.3  | Surface DOC (top) and DON (bottom) in NRPS by year. Symbols as in Figure 3.2.....  | 52 |
| Figure 3.4  | Surface DIN (top) and phosphate (bottom) in NRPS by year. Symbols as in Figure 3.2. ....   | 52 |
| Figure 3.5  | Surface chlorophyll <i>a</i> in NRPS by year. Symbols as in Figure 3.2. Outliers outside of the axis scale are indicated by the number and an arrow. ....  | 53 |
| Figure 3.6  | Surface phytoplankton productivity in NRPS by year. Symbols as in Figure 3.2.....  | 54 |
| Figure 3.7  | Surface bacterioplankton productivity in NRPS by year. Symbols as in Figure 3.2.....   | 54 |
| Figure 3.8  | Surface water temperature in NRPS by month for the period 2002 through 2005. Symbols as in Figure 3.2.....   | 55 |
| Figure 3.9  | Daily mean Neuse River discharge for the period 2002 through 2005. Data from the USGS gage near Fort Barnwell, NC. Symbols as in Figure 3.2.....   | 56 |
| Figure 3.10 | Surface DOC (top) and DON (bottom) concentration in NRPS by month for the period 2002 through 2005. Symbols as in Figure 3.2. ....   | 57 |
| Figure 3.11 | Surface DIN (top) and phosphate (bottom) in NRPS by month for the period 2002 through 2005. DIN is the sum of nitrate/nitrite and ammonium concentrations. Symbols as in Figure 3.2. ....  | 57 |
| Figure 3.12 | Surface chlorophyll <i>a</i> concentrations in NRPS by month for the period 2002 through 2005. Symbols as in Figure 3.2. Outliers outside of the axis scale are indicated by the number and an arrow. ....   | 59 |
| Figure 3.13 | Surface primary productivity in NRPS by month for the period 2002 through 2005. Symbols as in Figure 3.2.....  | 59 |
| Figure 3.14 | Median surface phytoplankton productivity and chlorophyll <i>a</i> concentration by month in NRPS. ....  | 60 |

|  |    |
|--|----|
| Figure 3.15 Surface bacterioplankton abundance in NRPS by month for the period 2002 through 2005. Symbols as in Figure 3.2. ....   | 61 |
| Figure 3.16 Surface bacterioplankton productivity in NRPS by month for the period 2002 through 2005. Symbols as in Figure 3.2.....   | 61 |
| Figure 3.17 Surface bacterioplankton productivity (BP) and water temperature in NRPS versus date. Filled circles are BP measured at individual stations. Dotted line is a smoothed line through the temperature data using a LOESS (locally weighted regression) smoothing function. ....  | 62 |
| Figure 3.18 Linear regression of natural log-transformed surface BP versus temperature. The solid line is the least squared regression and the dashed lines are the 95 % confidence limits for the regression. Bracketed numbers in equation are coefficient standard errors.....  | 63 |
| Figure 3.19 Linear regressions of natural log-transformed surface BP versus temperature, for temperature $\leq 25^{\circ}\text{C}$ (solid line) and $> 25^{\circ}\text{C}$ (long dashed line). The short dashed lines are the 95 % confidence limits for the regression. Bracketed numbers in equations are coefficient standard errors. ....  | 64 |
| Figure 3.20 Linear regression of natural log-transformed surface BP (top) and PP (bottom) versus the inverse of absolute temperature (T) times the Boltzmann constant (k). Lines and equations as in Figure 3.18.....  | 65 |
| Figure 3.21 Map of study area showing tracks of storms that impacted during the period of study. Line type indicates category of storm: dashed = tropical storm; dash-1 dot = cat. 1 hurricane, dash-2 dots = cat. 2 hurricane. Inset shows the extent of the map in context with the southeastern U.S. Storm tracks courtesy of NOAA Coastal Services Center ( <a href="http://maps.csc.noaa.gov/hurricanes/">maps.csc.noaa.gov/hurricanes/</a> ). ....               | 68 |
| Figure 3.22 Surface bacterioplankton productivity (BP) in NRPS and daily mean Neuse River discharge at Fort Barnwell versus date. Filled circles are BP measured at individual stations and solid line is the discharge data.....  | 69 |
| Figure 3.23 Surface bacterioplankton productivity (BP) in NRPS and daily mean Neuse River discharge at Fort Barnwell versus date. Filled circles are BP measured at individual stations, solid line is the discharge data, and the dashed line is the 12 year mean discharge by day. ....  | 70 |
| Figure 4.1 Surface salinity and $\Delta$ salinity by station in NRPS during 2002-2005. $\Delta$ salinity is the difference between near bottom and surface salinity. Value below station label is number of samples. Solid diamond is the median, light grey box is the interquartile range (IQR), and whiskers are drawn to the last value within the span from the quartiles ( $1.5 \times \text{IQR}$ ). Values outside of the span are considered outliers and are |    |

|             |   |    |
|-------------|---|----|
|             | indicated by open circles. The dark grey box indicates 95% confidence intervals around the median. ....   | 84 |
| Figure 4.2  | Surface dissolved oxygen percent saturation (DO, top) and pH (bottom) by station in NRPS during 2002-2005. Symbols as in Figure 4.1 .....   | 85 |
| Figure 4.3  | Surface dissolved organic carbon (DOC, top) and dissolved organic nitrogen (DON, bottom) in $\mu\text{mol L}^{-1}$ by station in NRPS during 2002-2005. Symbols as in Figure 4.1. ....  | 86 |
| Figure 4.4  | Surface DOC to DON ratio (molar, top) and chromophoric dissolved organic matter (CDOM) in $\mu\text{g quinine sulfate L}^{-1}$ (QS, bottom) by station in NRPS during 2002-2005. Symbols as in Figure 4.1. ....                                       | 86 |
| Figure 4.5  | Surface dissolved inorganic nitrogen (DIN, top) and phosphate (bottom) in $\mu\text{mol L}^{-1}$ by station in NRPS during 2002-2005. Symbols as in Figure 4.1 .....  | 87 |
| Figure 4.6  | Surface chlorophyll <i>a</i> in $\mu\text{g L}^{-1}$ by station in NRPS during 2002-2005. Outliers at station NR70 indicated by values next to arrow. Symbols as in Figure 4.1. ....  | 88 |
| Figure 4.7  | Surface particulate organic carbon (POC, top) and nitrogen (PON, bottom) in $\mu\text{mol L}^{-1}$ by station in NRPS during 2002-2005. Outliers at station NR70 indicated by values next to arrows. Symbols as in Figure 4.1 .....                   | 89 |
| Figure 4.8  | Surface phytoplankton productivity in $\mu\text{g C L}^{-1} \text{ h}^{-1}$ by station in NRPS during 2002-2005. Symbols as in Figure 4.1 .....   | 89 |
| Figure 4.9  | Surface bacterioplankton abundance in $\text{cells mL}^{-1}$ by station in NRPS during 2002-2005. Outlier at station NR0 indicated by arrow. Symbols as in Figure 4.1. Note that Pamlico Sound stations are based on only one or two data points..... | 91 |
| Figure 4.10 | Surface bacterioplankton productivity in $\mu\text{g C L}^{-1} \text{ h}^{-1}$ by station in NRPS during 2002-2005. Outlier at station NR0 indicated by arrow. Symbols as in Figure 4.1. ....   | 91 |
| Figure 4.11 | Surface bacterioplankton productivity normalized to 20 °C in $\mu\text{g C L}^{-1} \text{ h}^{-1}$ by station in NRPS during 2002-2005. Outlier at station NR0 indicated by arrow. Symbols as in Figure 4.1. ....                                     | 92 |
| Figure 4.12 | Surface bacterioplankton productivity in $\mu\text{g C L}^{-1} \text{ h}^{-1}$ by station and year in the NRPS. Symbols as in Figure 4.1, except 95% confidence limits are not shown. Vertical scale limit is less than maximum value of 24.6 .....   | 93 |

|   |     |
|---|-----|
| Figure 4.13 Surface phytoplankton productivity in $\mu\text{g C L}^{-1} \text{ h}^{-1}$ by station and year in the NRPS. Symbols as in Figure 4.12.....   | 94  |
| Figure 4.14 Surface DOC concentrations in $\mu\text{mol L}^{-1}$ by station and year in the NRPS. Symbols as in Figure 4.12. ....   | 94  |
| Figure 4.15 Property–salinity plot for bacterioplankton productivity (BP), phytoplankton productivity (PP), and DOC on 22 February 2005, units as before. Error bars for BP when visible indicate the 95% confidence interval around the mean. ....   | 96  |
| Figure 4.16 Property–salinity plot on 1 November 2004. All else as in Figure 4.15 .....   | 97  |
| Figure 4.17 Property–salinity plot on 22 September 2003, four days after Hurricane Isabel crossed the system. Note change in BP and DOC scale. All else as in Figure 4.15 .....   | 97  |
| Figure 4.18 Linear regression of natural log-transformed surface BP versus temperature in the NRPS during 2002–2005. Symbols indicate either the freshwater station (NR0, triangles and dashed line) or the marine stations (all others, open circles and solid line). Bracketed numbers in equations are coefficient standard errors. ....   | 99  |
| Figure 4.19 Location by date of BP profiles in Neuse River. The middle station of each grouping by date is the location of the chlorophyll maximum. The profiles collected 16–17 June were in the same location for a day and night sampling.....   | 101 |
| Figure 4.20 Vertical profiles of BP ( $\mu\text{g C L}^{-1} \text{ h}^{-1}$ ), salinity (ppt), and in vivo chlorophyll fluorescence ( $\mu\text{g L}^{-1}$ ) at three stations in the Neuse River estuary on 16–17 June 2005 at mid-morning and just past midnight. Station 3 was at the location of the chlorophyll maximum for the estuary and Stations 1 and 5 were located upstream and downstream, respectively, from Station 3..... | 101 |
| Figure 4.21 Comparison of BP versus $\Delta$ salinity (bottom minus surface) in 12 vertical profiles in the Neuse River estuary during June 2005. Symbol type indicates sample depth location. ....   | 102 |
| Figure 4.22 Comparison of BP versus POC in 12 vertical profiles in the Neuse River estuary during June 2005. Symbols as for Figure 4.21 .....   | 102 |
| Figure 4.23 Relationship between daily surface bacterioplankton and phytoplankton productivity using station mean values. Shown is the regression line from Cole et al. 1988 for all data points excluding the validation data (their Fig. 1). Dotted and dashed lines are confidence and prediction limits respectively for the regression calculated from statistics in Cole et al. 1988 (their Table 2). Neuse River and Pamlico       |     |



|  |     |
|--|-----|
| Sound stations are indicated by symbols and the most upstream station is labeled by NR0.....   | 104 |
| Figure 4.24 Relationship between daily surface bacterioplankton productivity and chlorophyll <i>a</i> using station mean values. Shown is the regression line from Cole et al. 1988 for all data points (solid, <i>n</i> = 41) and the regression line from White et al. 1991 (dashed, <i>n</i> = 412). Symbols as in Figure 4.23.....   | 105 |
| Figure 4.25 Relationship between bacterioplankton abundance and chlorophyll <i>a</i> using station mean values. Shown is the regression line from Cole et al. 1988 for all data points. Symbols as in Figure 4.23. Note <i>n</i> = 1 to 2 for the Pamlico Sound station.....   | 105 |
| Figure 5.1 Daily volumetric respiration ( $\text{mmol O}_2 \text{ m}^{-3} \text{ d}^{-1}$ ) versus temperature in the Neuse River. Stations indicated by symbols and error bars are the standard errors of the oxygen change slope. Line is the exponential curve fit. Regression results are for the semi-log form and bracketed numbers are coefficient standard errors..... | 117 |
| Figure 5.2 Linear regression of hourly volumetric respiration versus bacterioplankton productivity both in units of $\mu\text{g L}^{-1} \text{ hr}^{-1}$ in the Neuse River. Line is the linear fit. Error bars for BP are standard deviations. All else as in Figure 5.1. ....  | 117 |
| Figure 5.3 Bacterial growth efficiency versus temperature in the Neuse River. Error bars represent propagated errors from respiration and BP. All else as in Figure 5.1. ....  | 118 |
| Figure 5.4 Ratio of daily bacterioplankton productivity (BP) to daily phytoplankton productivity (PP) by station in the NRPS. Ratios were calculated for each trip. Dotted line indicates a ratio of one. Some of the outliers (maximum ratio of 24) have been cut of by the y-axis scaling. ....  | 120 |
| Figure 5.5 Ratio of daily bacterioplankton carbon demand (BCD) to daily phytoplankton productivity (PP) by station in the NRPS. Ratios were calculated for each trip. Dotted line indicates a ratio of one. Some of the outliers have been cut of by the y-axis scaling. ....  | 121 |
| Figure 5.6 Integrated dissolved oxygen (DO) deficit in $\text{mmol m}^{-2}$ by station in the NRPS. Dotted line indicates a deficit of zero, which means the whole water column was at saturation.....   | 123 |
| Figure 5.7 Integrated dissolved oxygen (DO) deficit in $\text{mmol m}^{-2}$ by date at two stations in the Neuse River. Dotted line indicates a deficit of zero, which means the whole water column was at saturation. Significant tropical storms striking the area are indicated by vertical lines.....  | 123 |

|            |  |     |
|------------|--|-----|
| Figure 6.1 | Conceptual model of dissolved organic matter (DOM) sources available to bacterioplankton (Bact) that explains the peak in productivity in the mid-estuary. DIN = dissolved inorganic N, Phyto = phytoplankton, POM = particulate organic matter. Solid lines are DOM fluxes, dashed lines are DIN fluxes, dashed plus dotted line is POM flux, and dotted lines represent the variable location of pycnocline..... | 129 |
| Figure A.1 | Examples of $^3\text{H}$ -leucine uptake kinetics using Neuse River water. Dotted lines are the non-linear least square regressions model fits. Estimated maximum uptake rate, $V_{\text{max}}$ , is indicated for each date. ....   | 132 |
| Figure A.2 | Isotope dilution (ID) versus $^3\text{H}$ -leucine concentration from 44 uptake kinetic experiments. ID is the ratio of maximum uptake ( $V_{\text{max}}$ ) to measured uptake for each experimental replicate. The solid line is the non-linear least squares regression line with the model and estimated parameters shown. The dotted line is $\text{ID} = 1$ . ....  | 133 |

## LIST OF ABBREVIATIONS

|                 |                                       |
|-----------------|---------------------------------------|
| BA              | bacterioplankton abundance            |
| BCD             | bacterial carbon demand               |
| BGE             | bacterial growth efficiency           |
| BP              | bacterioplankton productivity         |
| C               | carbon                                |
| CDOM            | chromophoric dissolved organic matter |
| Chl <i>a</i>    | chlorophyll <i>a</i>                  |
| CO <sub>2</sub> | carbon dioxide                        |
| CV              | coefficient of variation              |
| DIN             | dissolved inorganic nitrogen          |
| DIP             | dissolved inorganic phosphorus        |
| DO              | dissolved oxygen                      |
| DOC             | dissolved organic carbon              |
| DOM             | dissolved organic matter              |
| DON             | dissolved organic nitrogen            |
| ID              | isotope dilution factor               |
| K <sub>d</sub>  | diffuse light attenuation coefficient |
| N               | nitrogen                              |
| NO <sub>2</sub> | nitrite                               |
| NO <sub>3</sub> | nitrate                               |
| NH <sub>4</sub> | ammonium                              |
| NRPS            | Neuse River and Pamlico Sound         |

|                 |                                     |
|-----------------|-------------------------------------|
| P               | phosphorus                          |
| PAR             | photosynthetically active radiation |
| PO <sub>4</sub> | phosphate                           |
| POC             | particulate organic carbon          |
| POM             | particulate organic matter          |
| PON             | particulate organic nitrogen        |
| PP              | phytoplankton productivity          |
| ppt             | parts per thousand                  |
| TDN             | total dissolved nitrogen            |
| TN              | total nitrogen                      |
| μM              | μmol L <sup>-1</sup>                |

## **CHAPTER 1**

### **INTRODUCTION AND BACKGROUND**

Estuaries are highly complex and productive aquatic ecosystems that form the interface between terrestrial, fresh water, oceanic, and atmospheric environments (Day et al. 1989). As the transition zone between rivers and oceans, estuaries receive and concentrate terrestrial particulate and dissolved matter, which is then either transformed, transported, or stored depending on the inherent biogeochemical properties and hydrologic and geomorphic features. Much of the material processing is done by the endogenous autotrophic and heterotrophic microorganisms, which utilize and recycle nutrients and organic matter. Resolving the spatiotemporal dynamics of this microbial community under a variety of conditions is essential to a better understanding of overall estuarine function and its influence on adjacent coastal ecosystems.

The intrinsic complexity of estuaries stems from the physico-chemical features that help define it as an ecological boundary (Strayer et al. 2003) or an ecocline (Attrill and Rundle 2002) within the landscape. The feature most often used to define an estuarine system is the salinity gradient caused by the mixing of river and ocean waters, although this definition does not cover all cases (Elliott and Mclusky 2002). River flow, geomorphology, tides, and wind combine to create a salinity gradient and pattern of estuarine circulation specific to each estuary and this is further complicated by temporal variation in those physical drivers. It has been suggested that these variable conditions are

naturally stressful, but also that the resident biota have developed resilience to the stress leading to environmental homeostasis (Elliott and Quintino 2007).

Each combination of the physical forces in concert with microbial processes determines how estuaries function as both producer and processor of particulate and dissolved matter (Heip et al. 1995). For example, in highly flushed river-dominated estuaries, inorganic nutrients and organic matter tend to be exported to and utilized or processed in nearby coastal waters. Lagoonal estuaries, at the other extreme, tend to have much longer water residence times, so microbial production and processing of organic matter occurs within the system. While estuaries can be broadly categorized by physical and geomorphic characteristics, the lack of consensus on a definition for the term estuary (Elliott and McIlusky 2002) is evidence that making generalizations about estuaries can be difficult and that system-specific studies are a necessary part of estuarine science.

In addition to having natural complexity and variability, estuaries experience stresses from human actions within the estuary/watershed complex and from large-scale meteorological or climatological events. Increased human population densities and altered land use patterns in watersheds have caused increased inputs of contaminants, nutrients, and sediment to estuarine waters (Peierls et al. 1991; Cloern 2001). Estuarine eutrophication caused by excessive N inputs (Nixon 1995) is one of the world's foremost water quality problems. Coastal development and overfishing can lead to the loss of critical habitat and the reduction of commercially valuable species (Wilson 2002). Tropical storms can cause large flooding events, washing even more material into the estuary and changing the circulation patterns (Paerl et al. 2001; Peierls et al. 2003; Mallin and Corbett 2006; Paerl et al. 2006a).

Much of the estuarine response to natural and anthropogenic stressors is tied to the activity of the resident microbial community, in particular phytoplankton and bacterioplankton. A good deal of the early ecological work in estuaries focused on the dynamics of primary producers and higher trophic levels (Day et al. 1989), with a focus on light and nutrient supply as controls of primary production. The microbial loop paradigm (Azam et al. 1983) revealed that heterotrophic bacteria also play an essential role in the biogeochemical function and trophic structure of aquatic ecosystems (Kirchman 2000a). Populations within natural bacterial communities control the transformation of carbon, nitrogen, and phosphorus throughout freshwater and marine benthic and pelagic environments. Marine and freshwater bacteria also provide a food source for protistan and crustacean grazers, thereby providing an alternative to the classical food chain model of trophic transfer. The importance of the microbial loop was extended to estuaries, although gaps in understanding still remain (Ducklow and Shiah 1993; Kirchman 2000a). For instance, does the coupling between bacterioplankton and phytoplankton, reported from experimental (Hobbie and Cole 1984) and cross system analysis (Cole et al. 1988), occur in estuarine systems, despite the significant inputs of allochthonous organic matter? Microbial communities are major drivers of overall ecosystem metabolism, and their metabolic process control the extent to which an estuary is a carbon source or sink.

The Neuse River and Pamlico Sound (North Carolina) make up a large portion of the Albemarle-Pamlico Estuarine System (APES), the largest lagoonal estuary and second largest estuarine complex in the U.S (Steel 1991). Pamlico Sound serves as critical habitat for many juvenile and adult finfish and shellfish species, several of which

make up commercially significant fisheries (Epperly and Ross 1986; Eby and Crowder 2002). The shallow, microtidal sound is bounded by a system of barrier islands connected to the coastal ocean through only a few inlets. The Neuse River is a major tributary of Pamlico Sound and drains a 14500 km<sup>2</sup> watershed (Giese et al. 1985) containing growing urbanized areas and a variety of crop, forest, and livestock agriculture, including many concentrated animal feeding operations. Nutrient sources to the river have increased over the past century and particularly in the last few decades (Stow et al. 2001; Paerl et al. 2006b). Average freshwater discharge is 112 m<sup>3</sup> s<sup>-1</sup> (1997-2008; USGS Gage No. 02091814 near Ft. Barnwell, NC) and average depth is 3.8 m for the Neuse River and 4.9 m for Pamlico Sound (Giese et al. 1985). Circulation in the system is driven primarily by wind and river discharge (Luettich et al. 2002; Reynolds-Fleming et al. 2004) and the system is usually classified as partially mixed, with conditions varying from completely mixed to strongly stratified.

The Neuse River has been the subject of much research over the past several decades, in part because of a well documented history of nuisance algal bloom, hypoxia/anoxia, and fish kill events thought to be symptoms of eutrophication driven by human activities in the watershed (Paerl et al. 1998; Paerl 2006). A multi-institutional program to monitor Neuse River water quality and evaluate environmental management actions began in the mid 1990s and continues to the present (ModMon; Luettich et al. 2000; Paerl 2006). Less is known about Pamlico Sound and an extension of the monitoring program was started in 1999, following the landfall of three major hurricanes (Paerl et al. 2001). Heterotrophic bacterioplankton productivity was studied only briefly in the Neuse River (Christian et al. 1984) and never in Pamlico Sound.



The goal of the following work was to improve the understanding of estuarine microbial function by focusing on spatiotemporal patterns of the bacterioplankton and phytoplankton community and their response to system-wide perturbations in the impaired (Summers 2001) Neuse River and Pamlico Sound estuarine systems. The first part of this study (Chapter 2) focuses on the impact of the 1999 storms and floods on phytoplankton and water quality in Pamlico Sound. The goal of this work was to evaluate the temporal and spatial patterns of water quality and phytoplankton in the two and a half years following the storms and to use those patterns to assess recovery to pre storm conditions. The remaining sections focus on bacterioplankton metabolism along the salinity gradient in the Neuse River and Pamlico Sound. Chapters 3 and 4 are a characterization of the temporal and spatial patterns of bacterioplankton productivity and related environmental and biological variables, such as temperature and phytoplankton. Here, the underlying goals were to identify the major controls of bacterioplankton productivity and to assess the coupling between heterotrophic and phytoplankton productivity. Chapter 5 is an examination of planktonic microbial respiration in the system. The goal was to use respiration measurements to estimate bacterial growth efficiency, which when combined with bacterioplankton production produces an estimate of carbon flux through the heterotrophic community. This flux was then compared to internal carbon production by phytoplankton.

## **CHAPTER 2**

### **WATER QUALITY AND PHYTOPLANKTON AS INDICATORS OF HURRICANE IMPACTS ON A LARGE ESTUARINE ECOSYSTEM**

With kind permission from Springer Science + Business Media: Estuaries, Water quality and phytoplankton as indicators of hurricane impacts on a large estuarine ecosystem, volume 26, 2003, pages 1329–1343, Benjamin L. Peierls, Robert R. Christian, and Hans W. Paerl, figures 1–4, © 2003 Estuarine Research Federation.

#### **2.1 ABSTRACT**

Three sequential hurricanes in the fall of 1999 provided the impetus for assessing multi-annual effects on water quality and phytoplankton dynamics in southwestern Pamlico Sound, North Carolina. Two and a half years of post-hurricane data were examined for short- and long-term impacts from the storms and >100 year flooding. Salinity decreased dramatically and did not recover until May 2000. Inorganic nitrogen and phosphorus concentrations were briefly elevated during the flooding, but thereafter returned to background levels. Dissolved organic carbon concentrations declined through the whole study period, but did not appear to peak as was observed in the Neuse River estuary, a key tributary of the sound. Light attenuation was highest in the fall to spring following the storms and was best correlated with chlorophyll *a* concentrations. Phytoplankton biomass (chl *a*) increased and remained elevated until late spring 2000 when concentrations returned to pre-storm levels and then cycled seasonally. Phytoplankton community composition varied throughout the study, reflecting the

complex interaction between physiological optima and combinations of salinity, residence time, nutrient availability, and possibly grazing activity. Floodwater advection or dilution from upstream maxima may have controlled the spatial heterogeneity in total and group-specific biomass. The storms produced areas of short-term hypoxia, but hypoxic events continued during the following two summers, correlating strongly with water column stratification. Nitrogen loading to the southwestern sound was inferred from network analysis of previous nitrogen cycling studies in the Neuse River estuary. Based on these analyses, nutrient cycling and removal in the sub-estuaries would be decreased under high flow conditions, confirming observations from other estuaries. The inferred nitrogen load from the flood was 2-3 times the normal loading to the sound; this estimate was supported by the substantial algal bloom. After an eight-month recovery period, the salinity and chl *a* data indicated the sound had returned to pre-hurricane conditions, yet phytoplankton community compositional changes continued through the multi-year study period. This is an example of subtle, long-term aspects of estuarine recovery that should be considered in the context of a predicted 10-40 year period of elevated tropical storm activity in the western Atlantic Basin.

## **2.2 INTRODUCTION**

Tropical storms and hurricanes create large-scale, acute disturbances for coastal aquatic and terrestrial ecosystems (Valiela et al. 1998). In estuaries, extreme wind velocities, storm surges, and rainfall can cause intense mixing, alterations to circulation, and even changes to geomorphology (i.e., inlet formation or closure). An estuary is often classified by geomorphic type or water circulation patterns and both factors help control the ecological structure and function of these dynamic ecosystems (Day et al. 1989).

Therefore, when major storms make landfall on or near an estuary, their impacts can be considerable, at least in the short term. Often, storms produce floodwaters that reduce salinity and increase organic matter and nutrients as happened in the Chesapeake Bay after Tropical Storm Agnes (Chesapeake Research Consortium 1976), in the Herbert River after Cyclone Sadie (Mitchell et al. 1997), in Charleston Harbor after Hurricane Hugo (Van Dolah and Anderson 1991), and in the Cape Fear River after Hurricane Fran (Mallin et al. 1999). Similar impacts were observed in the Taiwan Strait after Typhoon Graff and Herb, although some of the nutrient increases were due to wind-driven upwelling (Shiah et al. 2000). Freshwater and nutrient loadings are not the only reported hurricane effects. Hurricane Donna had the opposite impact on Florida Bay when a massive storm surge temporarily increased salinity (Tabb and Jones 1962). Wind and storm surge from Hurricane Bob opened a new inlet into Waquoit Bay on Cape Cod (Valiela et al. 1998). Nor does every storm have the same effect on any one estuary; Mallin et al. (2002) documented variable responses by the Cape Fear River and its estuary to a series of hurricanes during latter half of the 1990s. Only a few studies have reported the longer-term impacts of major storms on estuaries.

In the fall of 1999, three sequential hurricanes passed through or near eastern North Carolina causing record flooding (Bales et al. 2000; Paerl et al. 2001). Hurricane Dennis bypassed the coast, meandered offshore, and then made landfall as a tropical storm on 4 September. Hurricane Floyd moved through the area as a category 2 hurricane September 15–16. Hurricane Irene never made landfall, but contributed additional rainfall and winds when it passed by North Carolina on 17 October. Our Pamlico Sound research cruises began in early October in response to the storms and extended ongoing long-term

monitoring and research on the Neuse River estuary, a sub-estuary of the sound (Luettich et al. 2000). The goals for the Pamlico Sound study were to monitor multi-annual water quality and phytoplankton community responses to and recovery from the fall 1999 storms.

There are surprisingly few reports on water quality in the Pamlico Sound, despite its critical role as a habitat resource for estuarine-dependent fisheries in the mid-Atlantic region (Epperly and Ross 1986; Steel 1991). Previous research on Pamlico Sound has focused mostly on hydrologic and hydrographic details (Williams et al. 1973; Giese et al. 1985; Pietrafesa et al. 1986). Woods (1967) briefly discussed nutrient concentrations and phytoplankton productivity in the sound. Aside from that report, most water quality research has concentrated on the major sub-estuaries, the Neuse and Pamlico Rivers (Steel 1991; Luettich et al. 2000). Therefore, the research presented here fills an informational void for this large and complex ecosystem.

Previous and ongoing reports indicate that substantial quantities of dissolved nutrients entered the Neuse River and its estuary from the hurricane-induced flooding (Bales et al. 2000; Paerl et al. 2001). Under normal hydrologic regimes, the sub-estuaries of Pamlico Sound remove nutrients prior to their entry into the sound (Christian et al. 1984; Rudek et al. 1991; Christian et al. 1991; Christian and Thomas 2000; Bales 2003). This removal, or filtering capacity, results largely from sedimentation, burial and denitrification. The ability of an estuary to cycle and remove nutrients is strongly influenced by its flushing or water residence time (Nixon et al. 1996; Eyre and Balls 1999; McKee et al. 2000). Nixon et al. (1996) found that for several North Atlantic estuaries, as residence time increased, the percent nitrogen (N) and phosphorus (P)

exported decreased and the percent N denitrified increased. In a comparison of Scottish coastal rivers, Balls (1994) noted that greater flushing times caused nutrients to deviate from conservative mixing behavior, presumably due to increased exposure to biological activity. Similar observations were made in sub-tropical (Eyre and Twigg 1997) and tropical systems (Eyre and Balls 1999), except with greater variation of discharge and flushing times compared to temperate estuaries. Network analysis of N cycling for the Neuse River estuary (Christian and Thomas 2000; Bales 2003) demonstrated that during periods of low discharge, low loading, and long residence time, biological processing removes considerable N before it can enter the sound. The opposite occurred when discharge and loading increased and residence time shortened. We hypothesize that, given the large nutrient inputs to and the short residence time in the sub-estuaries following the 1999 hurricanes, the nutrient loading to the sound was larger than usual and the response of the system was controlled in part by the excessive nutrient inputs.

The main objective of this paper is to describe the temporal and spatial patterns in the water quality and phytoplankton data since the hurricane disturbance. These patterns are used to quantify the time frame for recovery from the disturbance. We estimate the N loading to the sound from the hurricanes by extrapolating the network analysis results from earlier studies (Christian and Thomas 2000; Bales 2003; Christian and Thomas 2003). Finally, we examine the data for indications of long-term effects from the storms.

## **2.3 MATERIALS AND METHODS**

### **2.3.1 SYSTEM DESCRIPTION AND STUDY LOCATION**

The Pamlico Sound is a part of the Albemarle-Pamlico Estuarine System (APES). This system is the second largest estuarine ecosystem of any type in the United States

(Epperly and Ross 1986; Steel 1991). The APES drains an approximately 80,000 km<sup>2</sup> watershed that includes about one third of North Carolina and parts of Virginia (Giese et al. 1985; Steel 1991). Pamlico Sound is the largest component of the APES with a surface area of 5,335 km<sup>2</sup> (Giese et al. 1985), also making it the largest lagoonal estuary in the United States (Pietrafesa et al. 1986). The major tributaries of Pamlico Sound are the Neuse River, Pamlico River, and the Albemarle Sound (Giese et al. 1985). The average depth of Pamlico Sound is 4.9 m, but the bathymetry is distinguished by two major basins (maximum depth 7.3 m) separated by shoal regions (Giese et al. 1985). The circulation of the sound is dominated by wind tides and river flow, except near the 3 major inlets from the Atlantic Ocean (Giese et al. 1985; Pietrafesa et al. 1986).

A series of ten stations in southwestern Pamlico Sound (Figure 2.1), covering the sub-basin extending from the Neuse River, were visited at least monthly immediately following the hurricanes from early October 1999 until February 2000. Starting in March of 2000, the stations were relocated and reduced to nine (Figure 2.1). The new locations were chosen to overlap with other research group stations and the track of the NC Department of Transportation Cedar Island to Ocracoke ferry (Buzzelli et al. 2003). Trips continued at roughly monthly intervals through April 2002.

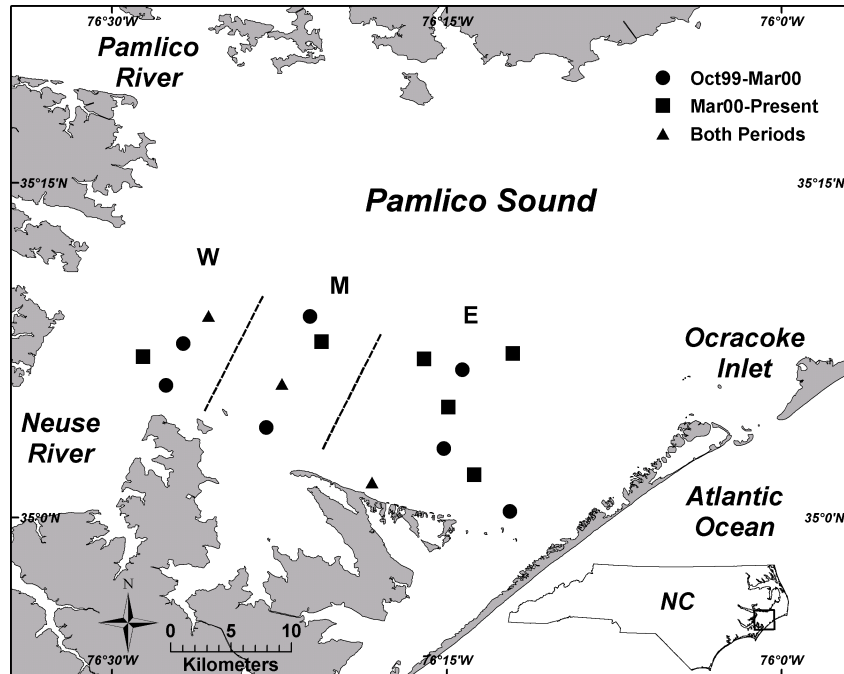


Figure 2.1. Map of study area including sampling stations and coverage dates. Station groups, identified by West (W), Middle (M), and East (E) are used for spatial comparisons.

### 2.3.2 FIELD SAMPLING

Vertical profiles of hydrographic and light data were collected at each station. A YSI 6600 sonde coupled to a 610 or 650 logger was used to measure temperature, salinity, pH, and dissolved oxygen. Conductivity (salinity) and pH sensors were calibrated with commercial standards and the dissolved oxygen sensor was calibrated using water-saturated air. In November 1999, the YSI sonde did not record complete profiles, so bottom values for that date are from duplicate profiles measured with a Hydrolab H20 sonde. The diffuse light attenuation coefficient,  $K_d$ , was determined from profiles of photosynthetically active radiation (PAR) using a LI-COR LI-193SA spherical quantum sensor. The slope of the linear regression between natural log-transformed PAR data and depth was used as the diffuse attenuation coefficient ( $K_d$ ).



Water samples were collected from the surface and near bottom layers and stored in acid-cleaned, high-density polyethylene (HDPE), 10 L containers. The bottom samples were collected near 0.5 m above the sediment with a horizontal plastic Van Dorn sampler, while the surface containers were either submerged just below the surface or filled from bucket casts. All containers were kept in dark coolers at ambient temperature until processed. All filtration was done within a few hours of collection and, when conditions permitted, on board the research vessel.

### **2.3.3 LABORATORY ANALYSES**

Dissolved nutrients were measured after vacuum filtration ( $< 25\text{kPa}$ ) of the collected samples through pre-combusted (3–4h at  $450\text{ }^{\circ}\text{C}$ ) Whatman GF/F glass fiber filters and frozen storage of the filtrate in acid-cleaned HDPE bottles. Nitrate plus nitrite, ammonium, and orthophosphate concentrations in  $\mu\text{mol L}^{-1}$  ( $\mu\text{M}$ ) were determined using a Lachat QuikChem 8000 flow injection analyzer and standard colorimetric methods. The limits of detection were approximately  $0.08\text{ }\mu\text{M}$ ,  $0.3\text{ }\mu\text{M}$ , and  $0.01\text{ }\mu\text{M}$  for  $\text{NO}_3+\text{NO}_2$ ,  $\text{NH}_4$ , and  $\text{PO}_4$ , respectively. Concentrations below these values were reported as one third of the method detection limits.

Additional aliquots of the GF/F filtrate were stored frozen in pre-combusted glass scintillation vials with Teflon-lined closures. These samples were used to measure dissolved organic carbon (DOC) concentrations using a Shimadzu TOC-5000A Analyzer. This instrument uses high temperature catalytic oxidation followed by non-dispersive infrared analysis of the  $\text{CO}_2$  produced. Samples were acidified to  $\text{pH} < 2$  and sparged with air before being analyzed for non-volatile organic carbon.

Particulate organic carbon (POC) and particulate nitrogen (PN) concentrations were determined by elemental analysis of material collected on pre-combusted GF/F filters. Carbonates were removed from the filters by vapor phase acidification (concentrated HCl). After drying at 60 °C, the filters were rolled in tin disks and injected into a PE 2400 Series II CHNS/O Analyzer calibrated with acetanilide. POC and PN concentrations were converted to molar C to N ratios (C:N).

Phytoplankton chlorophyll *a* (chl *a*) concentrations were measured using the modified in vitro fluorescent technique in EPA Method 445.0 (Arar et al. 1997). Samples (50–75 ml) were collected on 25 mm GF/F filters (vacuum filtration, < 25 kPa), blotted dry, and frozen immediately. Chl *a* was extracted from the filter using a tissue grinder and 90% aqueous acetone. The samples remained in the acetone overnight at –20 °C. The extracts were filter-clarified and analyzed on a TD700 fluorometer. The fluorometer was calibrated with chl *a* after determining the concentration using a Shimadzu UV160U Spectrophotometer and the extinction coefficients of Jeffrey and Humphrey (1975). The calibration was checked daily against a solid secondary standard (Turner Designs, proprietary formula).

Diagnostic phytoplankton photopigments were quantified using high-performance liquid chromatography (HPLC), coupled to photodiode array spectrophotometry (PDAS) separation and analysis (Jeffrey et al. 1997). Water samples (500–1000 ml) were gently vacuum filtered (< 25 kPa) onto 47-mm GF/F filters, blotted dry, then immediately frozen (–20 °C). The filters were placed in 100% acetone, sonicated, and extracted at –20 °C for 12–24 h. The HPLC configuration and other details used in the current study are described in Pinckney et al. (1996). The matrix factorization program CHEMTAX

(Mackey et al. 1996) was applied to chlorophyll and carotenoid (alloxanthin, antheraxanthin, chl *b*, total chl *a* [chl *a* + chlorophyllide *a*], fucoxanthin, lutein, peridinin, violaxanthin, and zeaxanthin) concentration data to determine the absolute contribution of five major phytoplankton divisions or classes (Cryptophyta, Cyanophyta, Bacillariophyta, Dinophyta, and Chlorophyceae) to total community biomass (Pinckney et al. 2001). The initial pigment matrix values came from Table 1 in Mackey et al. (1996) and the analyses were grouped by depth level and season.

We used photosynthetic rates to estimate phytoplankton N demand and compared that demand against N loading to the sound (see below). The rates were measured using an adaptation of Steemann Nielsen's (1952)  $^{14}\text{C}$  bicarbonate method (Paerl et al. 1998). Volumetric photosynthetic rates for each station and date were converted to areal carbon fixation by using a euphotic zone depth (1% of surface irradiance) calculated from  $K_d$  and assuming 8 hours of daylight. N demand for September to December 1999 was calculated using trapezoidal integration and stoichiometric conversion to N (Redfield C to N ratio of 6.6).

### **2.3.4 NETWORK ANALYSIS**

The network analyses of Christian and Thomas (2000; 2003) were used to determine N loading to the sound. Their analyses were on 16 seasonal networks of N cycling (Spring 1985 to Winter 1989) in the Neuse River estuary. The general network of the N cycle was divided into 7 compartments (as  $\text{mmol N m}^{-2}$ ) representing phytoplankton, aquatic heterotrophs, detritus, sediments and benthos, dissolved organic N (DON), nitrate plus nitrite, and ammonium. Fluxes (as  $\text{mmol N m}^{-2} \text{ season}^{-1}$ ) included import from loading, export into the sound, denitrification, nitrogen fixation, and 27

internal flows among compartments. Networks were constructed largely on results from spring 1985 through winter 1989 integrated over the entire estuary (Christian et al. 1991; Rizzo et al. 1992; Lackey 1992; Christian et al. 1992; Boyer et al. 1993; Boyer et al. 1994; Rizzo and Christian 1996). NETWRK4 (Ulanowicz 1987) was used to interpret the nature of N cycling in the networks and by inference in the field. Full explanations of model construction and analysis can be found in Christian et al. (1992) and Christian and Thomas (2000; 2003). Mass balance of the networks provided seasonal total N (TN) export fluxes for each seasonal TN import flux. The relationship between TN import (riverine loading) and export (to Pamlico Sound) for 1985 to 1989 was used to predict N export to Pamlico Sound during September-December 1999 using N data from Bales et al. (2000) and USGS records of flow.

### **2.3.5 STATISTICS**

Box and whisker plots (median, interquartile range, and extreme values) were used for basic data descriptions. Group comparisons were made with non-parametric methods as the data differed from the normal distribution (Kolmogorov goodness of fit test). The Kruskal-Wallis and Wilcoxon rank-sum tests were applied to group comparisons; significance was determined for these and all tests at  $\alpha = 0.05$ . Temporal and spatial comparisons were made using data pooled by flood period (October to March) or season (Fall = September, October, and November) and by station groups (Figure 2.1), respectively. Surface and bottom values for DOC, C:N, dissolved nutrients, chl *a*, and algal group biomass were combined for the group comparisons. For correlations, the Spearman rank correlation procedure was used. The TN loading/export relationship was

modeled with linear and polynomial least squares regression analysis. All statistical measures and tests were performed with S-Plus 6.0

## **2.4 RESULTS**

### **2.4.1 TEMPORAL PATTERNS**

The hurricanes of 1999 generated unprecedented rainfall in the watershed, record river flows, and record flooding (Figure 2.2; Bales et al. 2000; Paerl et al. 2001; Bales 2003). Peak stream flow in the Neuse River at Kinston reached over  $1000 \text{ m}^3 \text{ s}^{-1}$  in late September and returned to more typical levels by November. Salinity in southwestern Pamlico Sound rapidly responded to the flooding from the tributaries, although the response was lagged due to travel time from the watershed. Median surface salinity was less than 10 psu in early October 1999 after Hurricane Floyd and continued to drop until the beginning of November (Figure 2.2). Extreme low values of less than 2 psu were reported near the mouth of the Neuse River estuary (Paerl et al. 2001; Ramus et al. 2003). Salinity began to increase in the sound by the end of 1999. Summer 2000 brought a median surface salinity of about 22 psu, very close to the values for summer 1999 (Ramus et al. 2003) and 2001 (Figure 2.2). The next period of low salinity was in November 2000 through March 2001. This same early winter lag in salinity did not repeat in 2001, coincident with a very dry winter (Southeast Regional Climate Center, [www.dnr.state.sc.us/climate/sercc/](http://www.dnr.state.sc.us/climate/sercc/)).

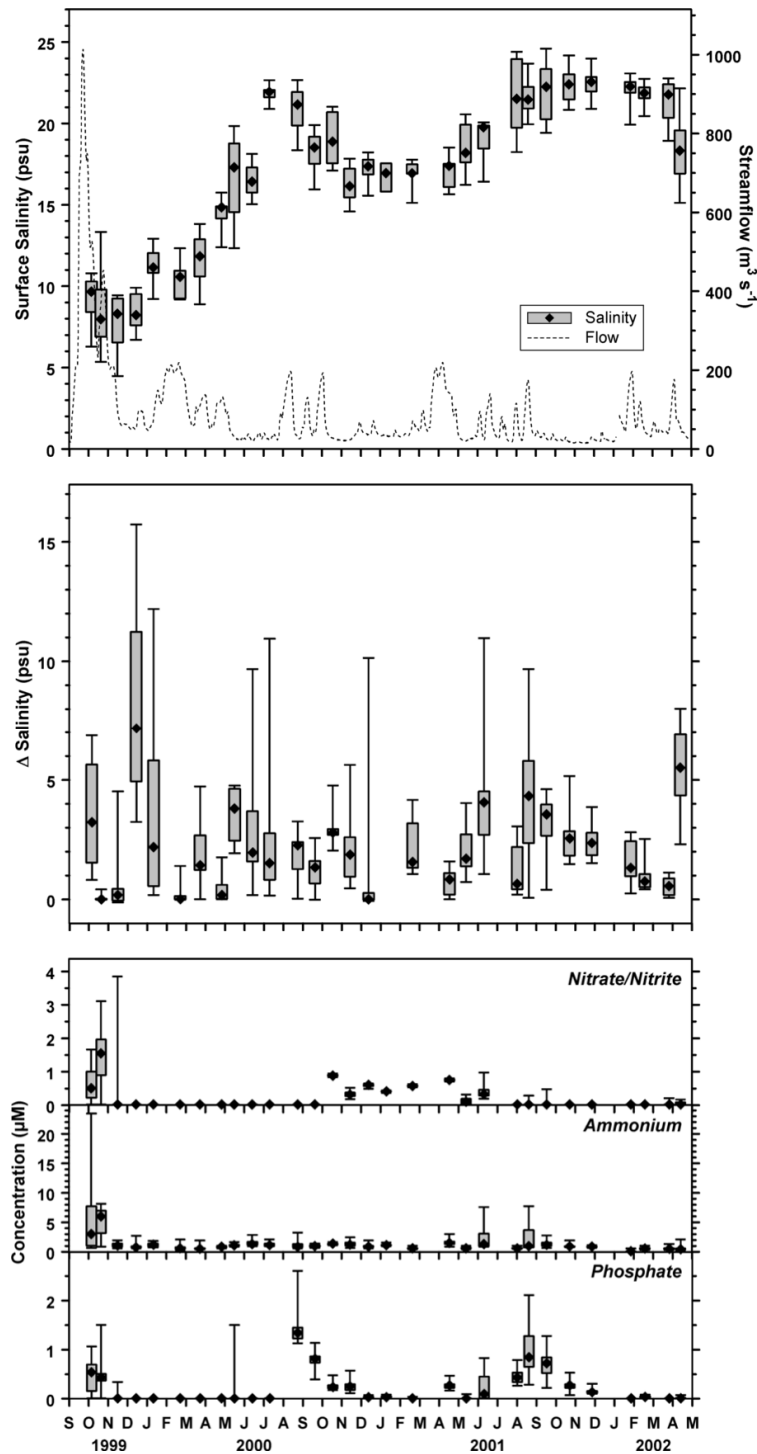


Figure 2.2 Box and whisker plots of surface salinity;  $\Delta S$  (difference between bottom and surface salinity); surface and bottom water nitrate plus nitrite (top), ammonium (middle), and orthophosphate (bottom); The diamond symbol is the median value, shaded boxes indicate interquartile range (25th to 75th percentile), and the whiskers are the minimum and maximum values ( $n = 9-10$  or  $18-20$ ). The flow data comes from the USGS gauging station at Kinston, North Carolina (station no. 02089500,  $N35^\circ 15' 29''$ ,  $W77^\circ 35' 09''$ ), and is daily mean stream flow in  $\text{m}^3 \text{s}^{-1}$ .

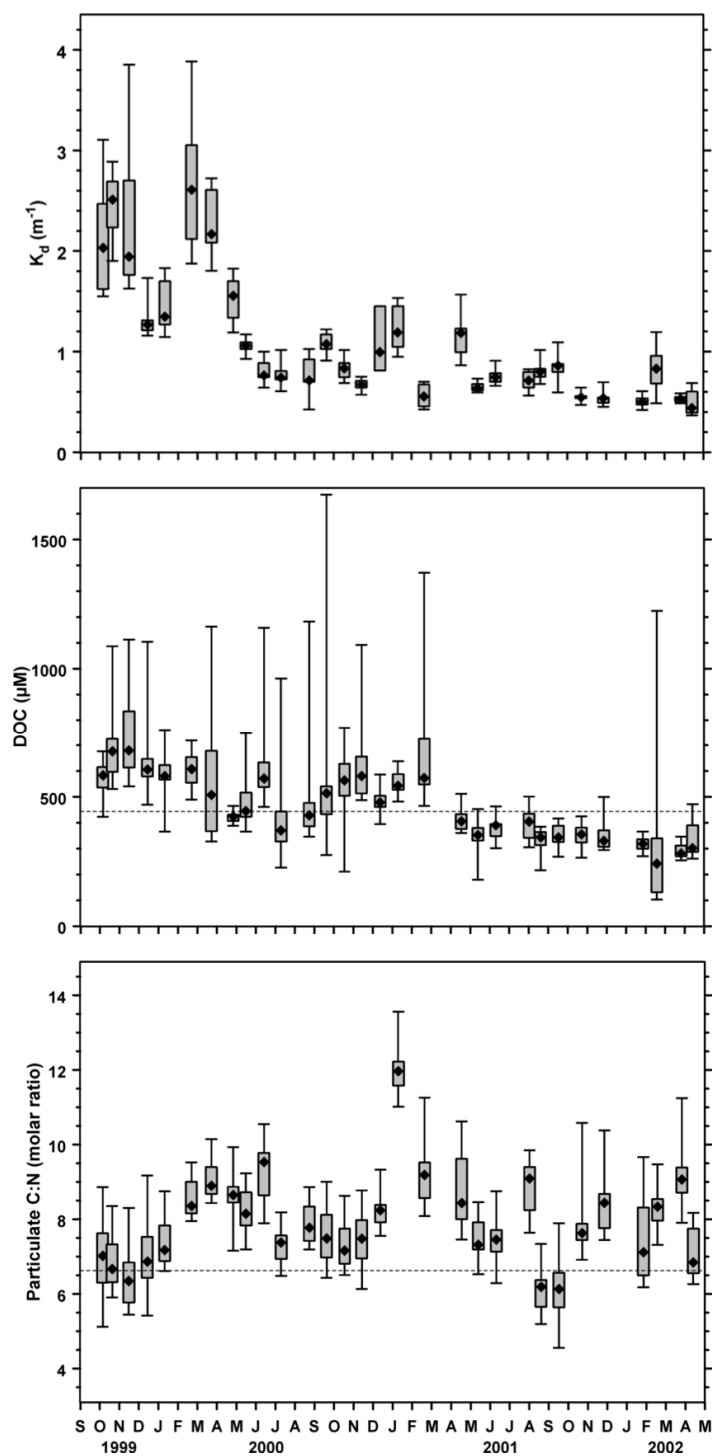


Figure 2.2 (Continued) Box and whisker plots of diffuse light attenuation coefficient,  $K_d \text{ (m}^{-1}\text{)}$ ; surface and bottom dissolved organic carbon (DOC) (dotted line represents the long-term median concentration for October 1999–April 2002); the molar ratio of POC to PN in surface and bottom water samples (the dotted line is the Redfield C:N ratio).

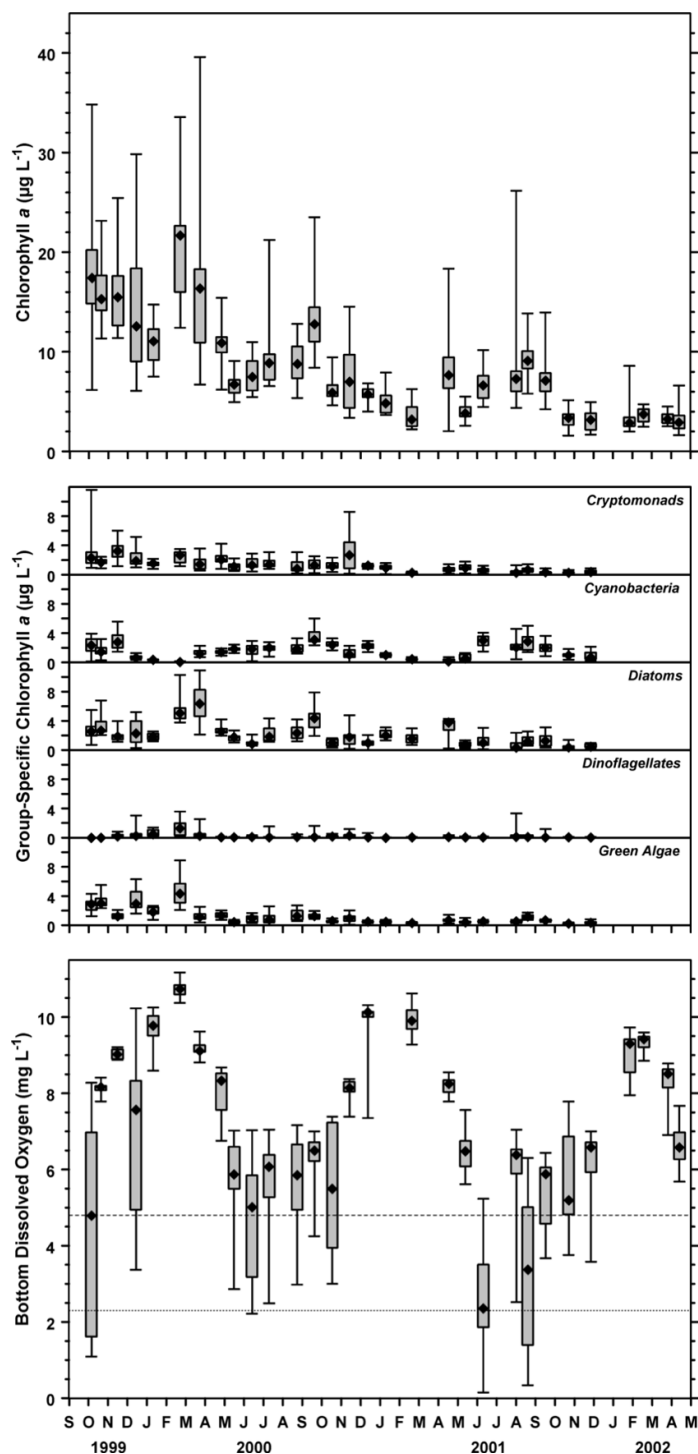


Figure 2.2 (Continued) Box and whisker plots of surface and bottom chl *a*; group-specific algal biomass; and bottom water DO in  $\text{mg L}^{-1}$  (upper dashed line is EPA criterion continuous concentration [ $4.8 \text{ mg L}^{-1}$ ] and the lower dotted line is the criterion minimum concentration [ $2.3 \text{ mg L}^{-1}$ ; USEPA 2000]. These limits signify critical hypoxic conditions) in Pamlico Sound over time.



We defined a flood period (October 1999 through March 2000) based on the period when salinities never overlapped median values for any other time (Figure 2.2). Comparing surface salinity from the flood period to the same months in the succeeding two years revealed significant differences between the years with a trend towards higher median salinity with time (Table 2.1). The same pattern appeared when the data were compared by the three fall seasons only (Table 2.1). Bottom salinities followed the same trends as the surface only with a greater range of values at each date (data not shown). Delta salinity ( $\Delta S$ , bottom minus surface) was used as a measure of water column stratification. During most sampling trips, the sound exhibited varying degrees of stratification with  $\Delta S$  at times exceeding 15 psu (Figure 2.2). A notable exception was immediately following the passage of Hurricane Irene in late October 1999, when the entire southwestern basin appeared to be well mixed.  $\Delta S$  did not differ significantly between the three years, except when comparing the fall seasons alone (Table 2.1). In that case, median  $\Delta S$  was lowest in fall 1999.

Table 2.1 Group comparisons for Pamlico Sound data pooled by time period. Flood period is October 1999–March 2000 compared against the same months in the succeeding two years. Fall is September, October, and November. Numbers are median values for each group. Significant difference between groups as determined by the Kruskal–Wallis rank-sum test is indicated by italics ( $p < 0.05$ ), italics + bold ( $p < 0.01$ ), and bold ( $p < 0.0001$ ). Salinity = surface salinity;  $\Delta$  Sal. = bottom salinity–surface salinity; DOC = dissolved organic carbon; C:N = molar carbon to nitrogen ratio;  $\text{NO}_3$  = nitrate + nitrite;  $\text{NH}_4$  = ammonium;  $\text{PO}_4$  = orthophosphate; DO = bottom dissolved oxygen; Chl  $a$  = fluorometrically determined chl  $a$ .

| Period or Season | Salinity (psu) | $\Delta S$ (psu) | $\text{NO}_3$ ( $\mu\text{M}$ ) | $\text{NH}_4$ ( $\mu\text{M}$ ) | $\text{PO}_4$ ( $\mu\text{M}$ ) | $K_d$ ( $\text{m}^{-1}$ ) | DOC ( $\mu\text{M}$ ) | C:N        | Chl $a$ ( $\mu\text{g L}^{-1}$ ) | DO ( $\text{mg L}^{-1}$ ) |
|------------------|----------------|------------------|---------------------------------|---------------------------------|---------------------------------|---------------------------|-----------------------|------------|----------------------------------|---------------------------|
| Flood            | <b>9.6</b>     | 1.3              | <b>0.03</b>                     | <b>0.9</b>                      | <i>0.004</i>                    | <b>2.0</b>                | <b>606.7</b>          | <b>7.3</b> | <b>15.3</b>                      | 9.0                       |
| Flood + 1 y      | <b>17.3</b>    | 1.9              | <b>0.6</b>                      | <b>1.1</b>                      | <i>0.05</i>                     | <b>0.8</b>                | <b>547.0</b>          | <b>8.3</b> | <b>5.5</b>                       | 8.4                       |
| Flood + 2 y      | <b>22.1</b>    | 1.5              | <b>0.03</b>                     | <b>0.7</b>                      | <i>0.04</i>                     | <b>0.5</b>                | <b>316.9</b>          | <b>8.1</b> | <b>3.2</b>                       | 8.3                       |
| Fall 1999        | <b>8.7</b>     | <i>0.4</i>       | <b>0.5</b>                      | <b>2.4</b>                      | 0.3                             | <b>2.2</b>                | <b>631.9</b>          | <b>6.6</b> | <b>15.9</b>                      | <b>8.2</b>                |
| Fall 2000        | <b>17.6</b>    | <b>2.0</b>       | <b>0.3</b>                      | <b>1.2</b>                      | 0.3                             | <b>0.8</b>                | <b>537.8</b>          | <b>7.4</b> | <b>8.6</b>                       | <b>6.9</b>                |
| Fall 2001        | <b>22.4</b>    | <b>2.6</b>       | <b>0.03</b>                     | <b>1.0</b>                      | 0.3                             | <b>0.6</b>                | <b>344.6</b>          | <b>7.6</b> | <b>3.8</b>                       | <b>5.9</b>                |

All nutrient concentrations in Pamlico Sound were elevated at the beginning of the study, but decreased to background levels within a month of the last storm (Figure 2.2).  $\text{NO}_3+\text{NO}_2$  reached levels as high as 3 to 4  $\mu\text{M}$  and then remained below detection limits except during October 2000–June 2001, when median concentrations hovered around 0.5  $\mu\text{M}$ .  $\text{NH}_4$  and  $\text{PO}_4$  rose immediately after the storms (median values of about 5 and 0.5  $\mu\text{M}$ , respectively) and were low or below detection shortly after. Elevated  $\text{NH}_4$  and  $\text{PO}_4$  conditions were observed in summer to fall periods. Nutrient concentrations pooled by flood period or season showed significant difference among all groupings, except for fall  $\text{PO}_4$ , which did not differ significantly between years (Table 2.1). Salinity was negatively correlated with  $\text{NO}_3+\text{NO}_2$  and  $\text{PO}_4$  for surface values during the two October 1999 cruises (N:  $r = -0.70$ ,  $p = 0.0023$ ; P:  $r = -0.52$ ,  $p = 0.022$ ;  $n = 20$ ).

Water clarity was determined by measuring the diffuse light attenuation coefficient  $K_d$ . The temporal pattern for  $K_d$  is shown in Figure 2.2. Large coefficients indicate that light is attenuated more rapidly with depth. Reduced light conditions characterized the flood period, as evidenced by median  $K_d$  values of about  $2 \text{ m}^{-1}$  or more. From May 2000 on, median  $K_d$  had decreased to about  $1 \text{ m}^{-1}$  or less; this corresponds to an approximate doubling of the euphotic zone depth. The  $K_d$  data grouped by flood period or fall season showed significant differences among years and lower median values in each succeeding year (Table 2.1).

The median dissolved organic carbon (DOC) concentration over the entire collection period was 444  $\mu\text{M}$  ( $n = 446$ ) with extreme concentrations ranging from about 100 to almost 1700  $\mu\text{M}$  (Figure 2.2). DOC concentrations appear to decline gradually

over the study period. Group medians for flood period and fall season declined with year, and the groups all differed significantly (Table 2.1). About 26% of the variability in  $K_d$  is explained by DOC ( $r = 0.51$ ,  $p < 0.0001$ ,  $n = 270$ ), but there was no significant correlation when using just the flood period data.

The pattern for particulate C and N resembles the chl *a* pattern (see below), and the box plots are not shown. Correlation coefficients for POC and PN versus chl *a* were 0.73 and 0.83, respectively ( $p < 0.0001$ ,  $n = 552$ ). The ratio of POC to PN (C:N) appears to follow a cyclical pattern with lower ratios in the summer and fall (Figure 2.2). At several time points, median C:N values were at or near the Redfield ratio for phytoplankton (6.6), especially during the flood period. Group comparisons of the C:N data show significant differences among both sets of groupings; the lowest median was in the first flood period or fall (Table 2.1).

Total phytoplankton community biomass was estimated using chl *a* concentrations (in vitro fluorescence technique). Chl *a* began the period relatively high, with median concentrations close to  $18 \mu\text{g L}^{-1}$  and peak concentrations of  $35 \mu\text{g L}^{-1}$  (Figure 2.2). A small drop in chl *a* was followed closely by a bloom in February and March 2000, with values of similar magnitude as in October 1999 (Figure 2.2). From then on, chl *a* decreased and median values stayed at  $10 \mu\text{g L}^{-1}$  or less with small peaks in August–September of each of the following years. This concentration level corresponds to pre-hurricane values for the system (Paerl et al. 2001). The three years were significantly different from each other ( $p < 0.0001$ ) when the chl *a* data was grouped by flood period or fall season and the group medians followed the observed

decrease (Table 2.1). Over the whole study period, chl *a* and  $K_d$  were strongly correlated ( $r = 0.78$ ,  $p < 0.0001$ ,  $n = 270$ ).

Diagnostic photopigments add to the phytoplankton community analysis by providing estimates of group-specific biomass. The CHEMTAX program converted pigment concentrations into cryptomonad (Cryptophyta), cyanobacteria (Cyanophyta), diatom (Bacillariophyta), dinoflagellate (Dinophyta), and green algae (Chlorophyceae) biomass, reported as chl *a*. It was evident that there were different temporal patterns in the group-specific biomass record (Figure 2.2). At the beginning of the study, the community was an approximately equal mixture of cryptomonads, cyanobacteria, diatoms, and green algae. Cryptomonads showed a gradual decrease from the beginning of the record except for a peak in November 2000. Diatoms and green algae became most dominant during the first winter and spring; dinoflagellates also reached maximum biomass during this period. Cyanobacteria declined to minimal levels after the storms, but maintained median biomass values of from  $2\text{--}3\ \mu\text{g L}^{-1}$  during the warm months. Diatom biomass peaked again in fall 2000 and spring 2001, but had only a small peak in fall 2001. After the flood period, dinoflagellates rarely contributed much to the total community biomass. Green algal biomass dropped off in April 2000, and median values rarely exceeded  $1.5\ \mu\text{g L}^{-1}$  for the rest of the study. All the phytoplankton groups had significant differences across the three years when pooled by time period (Table 2.2). Except for cyanobacteria, the median values declined from highest values in the first year. Cyanobacteria appeared to remain constant or increase; summer 2001 median biomass was higher than summer 2000 (data not shown) and the two seasonal groups were different at  $p < 0.0001$ .

Table 2.2 As in Table 2.1, but for algal taxonomic groups determined from diagnostic photopigments. All units are  $\mu\text{g chl } a \text{ L}^{-1}$ . BD = below detection.

| Period or Season | Cryptomonads | Cyanobacteria | Diatoms    | Dinoflagellates | Green Algae |
|------------------|--------------|---------------|------------|-----------------|-------------|
| Flood            | <b>1.9</b>   | <i>1.1</i>    | <b>2.6</b> | <i>0.2</i>      | <b>2.5</b>  |
| Flood+1 y        | <b>1.0</b>   | <i>1.2</i>    | <b>1.4</b> | <i>0.05</i>     | <b>0.5</b>  |
| Flood+2 y        | <b>0.3</b>   | <i>0.9</i>    | <b>0.4</b> | <i>0.03</i>     | <b>0.3</b>  |
| Fall 1999        | <b>2.3</b>   | <b>2.2</b>    | <b>2.5</b> | <b>BD</b>       | <b>2.4</b>  |
| Fall 2000        | <b>1.3</b>   | <b>2.4</b>    | <b>1.8</b> | <b>0.1</b>      | <b>0.9</b>  |
| Fall 2001        | <b>0.3</b>   | <b>1.1</b>    | <b>0.5</b> | <b>0.03</b>     | <b>0.4</b>  |

Bottom water dissolved oxygen (DO) followed a seasonal pattern with highest values during the coldest periods (Figure 2.2). The first occurrence of hypoxia was after the first two storms in early October 1999, but the bottom layer was rapidly re-saturated after the mixing effect of Hurricane Irene (Figure 2.2). During the warmer periods, DO concentrations ranged from supersaturated to values that were at or below the criteria set by EPA for hypoxia (i.e., 2.3–4.8  $\text{mg L}^{-1}$ ; U.S. Environmental Protection Agency 2000). The periods of lowest DO coincided with periods of significant salinity stratification (Figure 2.2); summertime bottom DO and  $\Delta S$  were significantly correlated ( $r = -0.68$ ,  $p < 0.0001$ ). Hypoxia was evident in the 2000 summer and fall season, but median DO concentrations were above the upper hypoxia limit. In the summer of 2001, however, extreme hypoxia and even anoxia prevailed on two sampling dates. While there were differences between years, the most significant difference was when comparing fall periods (Table 2.1). Median DO concentrations decreased with each succeeding fall season.

### **2.4.2 SPATIAL PATTERNS**

The sampling stations covered an approximately 450 km<sup>2</sup> portion of the southwest basin of Pamlico Sound. Some of the variables showed large variation over this spatial scale during the flood period. We evaluated spatial differences in stratification, hypoxia and phytoplankton by comparing three sampling areas (west, middle, and east; Figure 2.1), pooling results from stations within each. In early October 1999, the greatest stratification was evident in the western and northern portions of the sampling area (Figure 2.3). The most stratified area moved to the eastern stations during December and January 2000. The winter season was the only season of the three that the station groups exhibited significant differences in  $\Delta S$  (Table 2.3). When considering all of the data, stratification was different among the station groups with eastern stations having a higher median. Hypoxia varied over space as well. On October 6, low bottom DO water concentrations were found in the western and northern stations, parallel to the maximum stratification pattern (Figure 2.3). Low DO appeared in December 15 at a few stations, but overall, there were no significant differences among station groups in any of the seasons or when considering all of the data (Table 2.3).

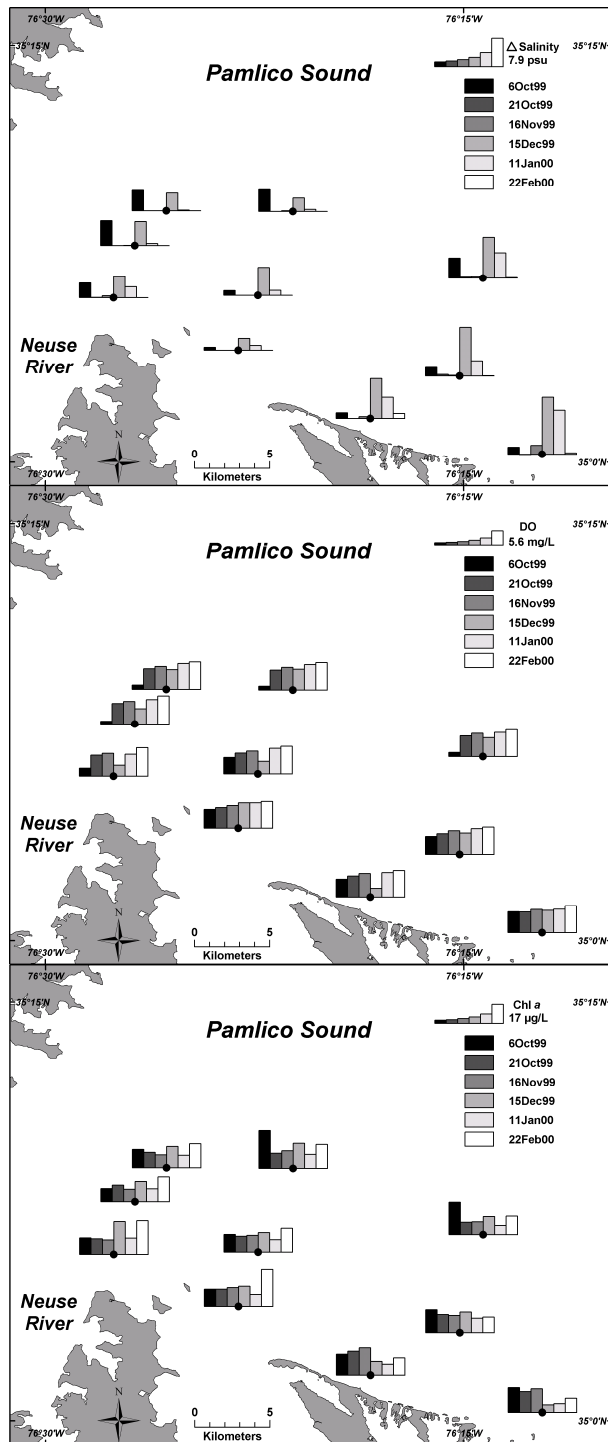


Figure 2.3 Spatial distribution of  $\Delta S$  (psu), bottom DO (mg L<sup>-1</sup>), and surface chl *a* (μg L<sup>-1</sup>) from October 6, 1999–February 22, 2000. Closed circles indicate actual station locations and each bar indicates the value for a specific date at that station. A scale bar is in the upper right corner.

Table 2.3 As in Table 2.1 and Table 2.2, but for data pooled by station groups. Spatial comparisons were conducted for three different seasons during 1999 and 2000 and for all available data.

| Season/<br>Year | Station<br>Group | $\Delta$ Sal.<br>(psu) | DO<br>(mg L <sup>-1</sup> ) | Chl <i>a</i><br>( $\mu$ g L <sup>-1</sup> ) | Crypto-<br>monads | Cyano-<br>bacteria | Diatoms    | Dino-<br>flagellate<br>s | Green<br>Algae |
|-----------------|------------------|------------------------|-----------------------------|---|-------------------|--------------------|------------|--------------------------|----------------|
| Fall 1999       | East             | 0.4                    | 8.2                         | <b>19.7</b>                                 | 2.2               | 3.1                | <b>3.6</b> | BD                       | 2.8            |
|                 | Middle           | 0.0                    | 8.2                         | <b>16.2</b>                                 | 2.4               | 2.1                | <b>2.4</b> | BD                       | 2.5            |
|                 | West             | 0.03                   | 8.1                         | <b>14.0</b>                                 | 1.9               | 1.7                | <b>2.0</b> | BD                       | 2.1            |
| Winter 1999     | East             | 6.4                    | 9.5                         | 12.5  | 1.7               | 0.3                | 2.5        | <b>0.2</b>               | 2.7            |
|                 | Middle           | 1.3                    | 10.2                        | 15.4  | 1.6               | 0.4                | 2.3        | <b>0.8</b>               | 2.8            |
|                 | West             | 0.6                    | 9.6                         | 17.6  | 2.3               | 0.4                | 3.0        | <b>1.0</b>               | 3.9            |
| Spring 2000     | East             | 1.9                    | 8.3                         | <b>9.0</b>                                  | <b>1.2</b>        | 1.4                | 2.5        | <b>0.05</b>              | <b>0.8</b>     |
|                 | Middle           | 0.4                    | 8.5                         | <b>11.0</b>                                 | <b>2.0</b>        | 1.4                | 2.9        | <b>0.07</b>              | <b>1.2</b>     |
|                 | West             | 1.4                    | 8.1                         | <b>13.4</b>                                 | <b>2.2</b>        | 1.8                | 2.6        | <b>0.1</b>               | <b>1.6</b>     |
| All data        | East             | 2.1                    | 7.1                         | <b>6.4</b>                                  | <b>0.9</b>        | 1.5                | 1.7        | <b>0.05</b>              | <b>0.7</b>     |
|                 | Middle           | 1.0                    | 7.7                         | <b>7.8</b>                                  | <b>1.4</b>        | 1.5                | 1.9        | <b>0.08</b>              | <b>1.0</b>     |
|                 | West             | 1.6                    | 7.0                         | <b>8.3</b>                                  | <b>1.4</b>        | 1.5                | 1.7        | <b>0.09</b>              | <b>0.9</b>     |

Chl *a*, however, did display significant variation in space for the fall and spring period (Table 2.3). Wintertime station groups were only just outside of the significance level ( $p = 0.056$ ). The highest median chl *a* was in the east group in fall 1999, shifting to the west group by spring; Figure 2.3 illustrates some of this heterogeneity. The pattern of higher biomass in the west was still detectable when considering all of the data (Table 2.3). Given that the lowest salinity levels tended to be near the river mouth, the spatial trend was also evident in the negative correlation between surface chl *a* and salinity ( $r = -0.69$ ,  $p < 0.0001$ ,  $n=270$ ). When the phytoplankton groups were analyzed separately, not all the groups showed spatial differences. Diatoms and cyanobacteria had significant spatial differences (higher medians in the east stations) in fall 1999, while only dinoflagellates had wintertime differences (Table 2.3). By spring, cryptomonads, cyanobacteria, dinoflagellates, and green algae differed among station groups (higher



medians in the west). Over the entire study, cryptomonads, dinoflagellates, and green algae showed a significant spatial difference.

### **2.4.3 N LOADING**

Significant regressions were found between seasonal TN loading to the Neuse River estuary and TN export to Pamlico Sound for the 16 seasonal networks (Figure 2.4). Explained variance in export ( $r^2$ ) was 0.94 for a linear relationship and 0.98 for a second order polynomial relationship. We estimated TN loading to the estuary from mid-September to mid-December as  $1000 \text{ mmol N m}^{-2} \text{ season}^{-1}$ . This was nearly twice the highest estimated loading during the four-year study. Extrapolating to this loading value using the regressions, the amount of export to Pamlico Sound ranges from approximately  $750 \text{ mmol N m}^{-2} \text{ season}^{-1}$  (linear regression) to the entire loading amount (second order polynomial regression). This corresponds to a filtering capacity of 0 to 25%. Calculations of phytoplankton N demand from photosynthetic rates resulted in an estimate of  $874 \text{ mmol N m}^{-2}$  for the same period. This is comparable to the range of total nitrogen export to the sound extrapolated from the regressions.

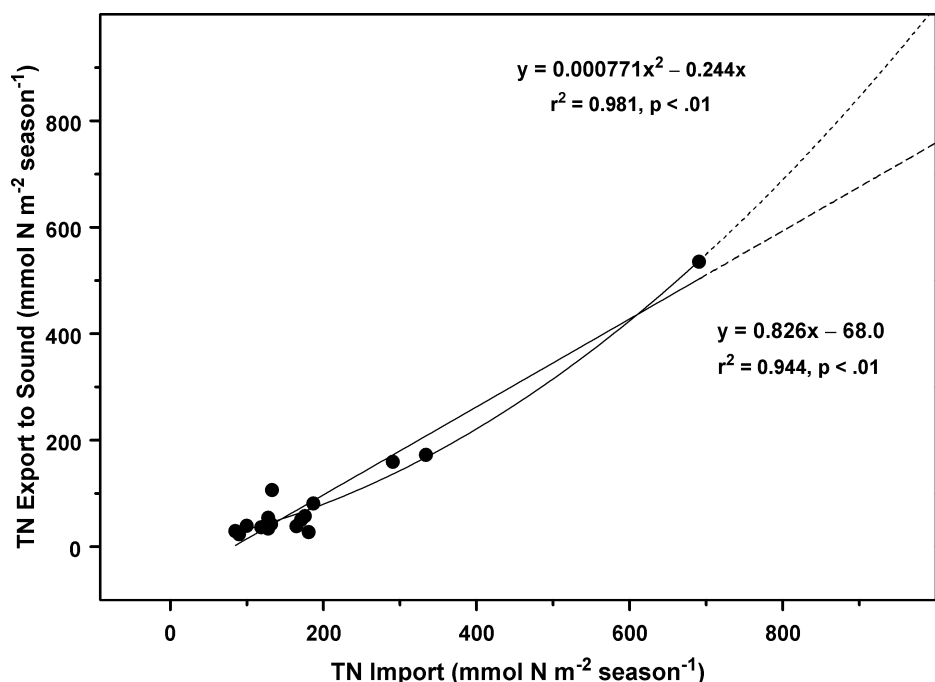


Figure 2.4 Relationship of total N (TN, in  $\text{mmol m}^{-2} \text{ season}^{-1}$ ) exported to Pamlico Sound as a function of TN loaded to the Neuse River estuary as determined by network analysis. Each point represents one season from the 16 consecutive seasonal networks for the period 1985–1989. The most extreme import and export values occurred as a result of major storms in winter 1987. Lines are least squares linear and non-linear (2nd order polynomial) regression. Dotted sections of lines indicate extrapolation beyond the data.

## 2.5 DISCUSSION

Hurricanes and other large storms can directly affect the water column of estuaries in several ways. Substantial rainfall reduces local salinity, increases stratification, and washes in dissolved and particulate material from connected watersheds (Chesapeake Research Consortium 1976; Van Dolah and Anderson 1991; Mallin et al. 1999). Increased freshwater input also reduces estuarine water residence time as seen in the seasonal patterns of temperate (Balls 1994), subtropical (Eyre and Twigg 1997), and tropical (Eyre and Balls 1999) estuaries. In the case of the 1999 hurricanes, the sound's residence time decreased from approximately 1 year to less than 2 months (Paerl et al. 2001). High wind velocity disrupts water column stratification and

mixes bottom sediments into the water column (Tabb and Jones 1962; Valiela et al. 1998). Storm surges can increase salinity and change circulation patterns by modifying geomorphology (e.g., opening a new inlet) (Tabb and Jones 1962; Valiela et al. 1998). Not all of these storm effects occurred for Pamlico Sound in 1999. Since the sound is isolated from the Atlantic Ocean by barrier islands, direct storm surge effects on the sound water column were minimal. The basic morphology of the sound stayed intact despite severe erosion and overwash on the barrier islands. Heavy rainfall and powerful winds did have impacts on the entire APES. The combined rains from Hurricane/Tropical Storm Dennis and Hurricane Floyd brought significant freshwater, particulate and dissolved organic matter, and nutrients into the Neuse and Pamlico Rivers (Bales et al. 2000; Paerl et al. 2001), while the winds from Hurricane Irene mixed the entire water column and resuspended sediments.

The impact of the freshwater flood was obvious in the surface salinity time course for Pamlico Sound (Figure 2.2 and Table 2.1). Beyond May 2000, the salinity returned to pre-hurricane conditions (Paerl et al. 2001; Ramus et al. 2003) and the record shows seasonal variability, probably related to local climate. Except for the extreme flood from the storms, the salinity record in the southern portion of the sound did not show significant response to the river discharge peaks at Kinston, over 120 km upstream. This suggests that other factors such as direct rainfall, evaporation, and seawater intrusion play a role in controlling the sound's salinity. Furthermore, modulation of freshwater pulses occurs in the Neuse River, as the water may take weeks to months to pass through the sub-estuary under average flow rates (Christian et al. 1991). The flux of freshwater from the storms decreased water residence time in the sub-estuary and promoted intervals of

density stratification in the sound. In December 1999, the combination of low salinity river water and seawater from the ocean inlets produced salinity differences much greater than typically reported (1 to 6 psu; Pietrafesa et al. 1986). Aside from that extreme, stratification during the flooding was either lower or not different than in later years (Table 2.1), although the  $\Delta S$  record could be biased due to the tendency to sample on relatively calm days. Spatial differences in salinity and stratification were expected based on previous hydrologic research (Giese et al. 1985; Pietrafesa et al. 1986). During the flood period, highest  $\Delta S$  shifted east from near the Neuse River estuary mouth to near the ocean inlet, as seawater returned underneath the fresher storm water (Figure 2.3).

Inorganic nutrients showed a clear short-term increase from the flood (Figure 2.2 and Table 2.1).  $\text{NO}_3 + \text{NO}_2$  was transported with the freshwater as demonstrated by the negative correlation with salinity. The lack of correlation between salinity and  $\text{NH}_4$  was evidence that the  $\text{NH}_4$  came from remineralized particulate and dissolved organic matter flushed to the sound.  $\text{PO}_4$  correlated with salinity, also suggesting dilution of a riverine source, although elevated  $\text{PO}_4$  may have come from internal sources given the similar peaks during the next two summer/fall seasons. All nutrients rapidly decreased after reaching the sound in fall 1999, presumably to support the growing algal community. Under non-storm conditions, the nutrient patterns, particularly of  $\text{NH}_4$  and  $\text{PO}_4$ , were likely dominated by sediment remineralization and planktonic uptake rather than loading from the sub-estuary (Day et al. 1989). From October 2000 to June 2001,  $\text{NO}_3 + \text{NO}_2$  unexpectedly remained above detection, ranging from about 0.5 to  $1\mu\text{M}$  (Figure 2.2). This  $\text{NO}_3 + \text{NO}_2$  could have been produced through nitrification of remineralized N in the flood-derived organic matter. There is not strong evidence to support this, but oxygen

levels were high, algal biomass (N demand) was lower, and  $\text{NH}_4$  increased after this period suggesting the process had abated. We cannot rule out external supply (i.e., from runoff; see reduced salinity during same period, Figure 2.2) or some other process that might account for the  $\text{NO}_3+\text{NO}_2$  temporal pattern. Except for the immediate spatial pattern driven by floodwater dilution and some occasional bottom water hotspots, the sound remained relatively homogenous and oligotrophic with respect to nutrients.

Light attenuation increased in direct response to the storms and continued to be elevated during the algal bloom in winter/spring 2000 (Figure 2.2). By May 2000,  $K_d$  appeared to be at stable, perhaps typical, levels, although we have no pre-storm data to support this. Dissolved and particulate organic matter control much of light attenuation variability in estuaries (Day et al. 1989).  $K_d$  did correlate with DOC, but the relationship was not as strong as the correlation with chl *a* (see results). Also, the sound DOC data never exhibited the large pulse that accompanied the floodwater discharge in the upper Neuse River estuary (Paerl et al. 2001), although our sampling effort may have missed some of the initial concentration increase. This comparison of DOC and  $K_d$  is limited in that only the colored components of the DOC pool (colored dissolved organic matter or CDOM) affect light attenuation (Tester et al. 2003). The other major control of light attenuation is particulate matter, usually a mixture of allochthonous material, resuspended sediments, and planktonic organisms. We did not attempt to separate these particulate sources, but the C:N during the flood period (Figure 2.2, near Redfield ratio) suggests a seston dominated by phytoplankton. Chl *a* and  $K_d$  were significantly correlated over the whole study period, suggesting that overall, even during the flood, phytoplankton were the main particulate component of light attenuation. While sediment can change light

penetration through wind-driven resuspension, we have observed this turbidity to decrease rapidly with reduced wind stress.

Phytoplankton community biomass was enhanced during the flood period (Figure 2.2), beginning with a rapid increase from pre-storm chl *a* levels of 5 to 10  $\mu\text{g L}^{-1}$  (Paerl et al. 2001; Ramus et al. 2003). While many variables regulate estuarine phytoplankton (Day et al. 1989), N inputs were the most probable controlling factor for the biomass increase (Paerl 1988; Nixon 1995; Pinckney et al. 1998). Light may have limited production early in the study (euphotic zone ranged from 1 to 2.8 m deep), but after May 2000, light was sufficient throughout the water column. Another river discharge peak in January and February probably supplied enough N to maintain high biomass levels in the winter/spring period, although N concentrations remained low, perhaps because uptake was rapid. After spring 2000, chl *a* decreased and then cycled seasonally. Nutrient limitation could explain the drop in algal biomass, but it is also possible that the grazer community re-established itself and began to strongly influence chl *a* levels. This is supported by observations of large populations of gelatinous and crustacean zooplankton that appeared in net hauls from spring 2000 onward (Kleppel personal communication). The initial phytoplankton bloom was unevenly distributed across the sound. Peak chl *a* concentrations were found at northern and eastern stations, away from the river mouth, perhaps a result of advection in the flood waters (Tester et al. 2003). As discharge decreased, the phytoplankton biomass maximum shifted towards the western stations and the river mouth. After the flood period, the sound became more homogeneous with respect to chl *a*, but a trend towards higher biomass near the Neuse remained. This

pattern may be related to higher nutrient supply or biomass dilution from upstream maxima; the negative correlation between chl *a* and salinity supports the latter possibility.

While chl *a* (total phytoplankton biomass) re-established itself to pre-hurricane levels within about 8 months (Paerl et al. 2001; Ramus et al. 2003)), the phytoplankton community composition proved far more dynamic and changed both spatially and temporally over the study period (Figure 2.2). Phytoplankton community composition is controlled by a complex interaction of environmental factors, physiological preferences, competition, and herbivory (Day et al. 1989; Cloern 1996; Pinckney et al. 1998). The mechanisms driving the observed pattern of community structure are difficult to distinguish, but it is clear that the N loading and lowering of salinity by the floodwaters had a profound effect on the phytoplankton community. The initial post-hurricane community was a mixture of all the taxonomic groups except dinoflagellates. Previous bioassay work using Neuse River phytoplankton assemblages revealed a similar community composition under N enriched conditions (Pinckney et al. 2001). In the sound, green algae and diatoms responded to the floodwaters with dramatic biomass increases, although green algae became a minor component of the community after February 2000. This loss of green algae may have resulted from increased salinity, decreased nutrients, or increased selective grazing. Diatoms maintained biomass dominance throughout the following year. Peak diatom biomass coincided with river discharge peaks, pointing to rapid utilization of external N (Collos 1986; Pinckney et al. 1999). Dinoflagellates, which are a seasonally-dominant component of local estuarine communities (Pinckney et al. 1998; Litaker et al. 2002), had only a modest bloom in the first winter/spring period and were otherwise rare. Either this group could not meet its

resource requirements after the flood, or an efficient grazer community kept dinoflagellate biomass low. As a group, cyanobacteria have relatively slow growth rates (i.e., long doubling times) and show a strong preference for relatively warm conditions (> 15 °C; Paerl 1999). This is reflected in both their lack of immediate response to the floodwaters and relatively large growth responses throughout the sound during the following two summers (2000 and 2001). It is unclear why cryptomonads maintained a significant presence in the first year, yet were much lower in 2001. Not all the taxonomic groups showed spatial differentiation at all times (Table 2.3), but for those that did, the pattern found for the whole community applied.

Evaluating the phytoplankton group-specific responses with the concurrent hydrologic and water quality data indicates that physical-chemical drivers are largely responsible for community composition shifts following large climatic perturbations. The combination of salinity, water residence time (flushing), and nutrient availability appears to exert a strong control on the spatial-temporal response of each taxonomic group . Other researchers have also suggested this mechanism to explain phytoplankton community changes in, for example, a Norwegian fjord after an extreme flooding event (Kristiansen 1998) and a seasonal Australian estuary (Chan and Hamilton 2001). When considered in the context of a predicted 10-40 year increase in Atlantic tropical storm and hurricane activity (Goldenberg et al. 2001), our observations indicate that the higher and more long-lasting incidences of freshening associated with such a scenario may have profound short- and long-term effects on the phytoplankton community supporting the base of these estuarine food webs. Changes in primary producers could produce changes in grazer communities and higher trophic levels (finfish and shellfish), critical elements



of Pamlico Sound's ecology and economy. Both finfish and shellfish catches in the sound were depressed in the 2 yr following the storms (Crowder, personal communication). Whether the observed changes at the phytoplankton group level have precipitated these changes (via differences in phytoplankton palatability or toxicity) remains to be investigated. If however, the sound continues to be impacted by more frequent and elevated floodwater discharge due to increased storm frequency, this system may further experience phytoplankton community shifts while it is still recovering from previous freshening events. Such climatically driven ecological instability should be investigated with long-term monitoring, food web and fisheries management-oriented research.

The hypoxia created by the floodwaters caused concern for its potential impact on fisheries (Paerl et al. 2001). After a short period of patchy, low DO, the system seemed to return to a seasonal pattern controlled by temperature and water stability (Buzzelli et al. 2002), apparently unrelated to the storms (Figure 2.2). Hypoxic events still occurred in the following two summers and some of the lowest DO readings occurred in June and August 2001. These events correlated with high stratification and may have been enhanced by the residual sediment organic matter deposited during and after the storms. Low DO concentrations appeared where stratification was pronounced (e.g. west/north in October and middle/south in December 1999; Figure 2.3), but the lowest DO concentration did not always coincide with the highest salinity difference, especially at the east stations where sediments were sandy and organic-poor (Giese et al. 1985). Given that sediment organic matter content varies across the sound (Giese et al. 1985) and there are frequent wind mixing events, hypoxia in Pamlico Sound is probably local and ephemeral as was observed by Woods (1967) in the mid-1960s. The main effect of the

storms on DO, therefore, was to add organic matter to the sediment pool and increase biological oxygen demand.

The nutrient filtering capacity of the Neuse River estuary was significantly reduced during the hurricane period. We estimate that 75 to 100% of TN loaded from the Neuse River passed through into the sound during September–December 1999 (Figure 2.4). This would be equivalent to 2–3 years of normal loading as calculated for the 4 years of study used for the network analysis. In contrast, for the same 4-mo period, the Neuse River estuary received less than 1.5 years of TN loading based on the years 1985–1989. Paerl et al. (2001) estimated that dissolved inorganic N loading to the Neuse River estuary from September to October 1999 was 71% of annual loading, based on the years 1994–1997. The N loading to the sound is potentially much greater than what would be predicted from calculations of loading to the sub-estuaries and assumptions that the sub-estuaries were functioning as nutrient filters.

The mechanism for reduced filtering capacity appears to be the balance between the time scales of physical transport and biological processing (Christian et al. 1991; Balls 1994; McKee et al. 2000). Nixon et al. (1996) found that among several estuaries, those with longer residence times have higher fractions of N denitrified and lower fractions of N exported. Other studies have documented similar control of N export within individual estuaries, especially tropical and sub-tropical systems dominated by episodic flooding (Eyre and Balls 1999; Eyre 2000). At the extremes of low discharge, low loading, and high residence time during the 1985–1989 study, less than 25% of TN entering the Neuse River estuary was estimated to export into the sound (Christian and Thomas 2000; Christian and Thomas 2003). Recycling, as indexed through network

analysis, was extensive during these times; the average N atom entering the sub-estuary as nitrate was estimated to cycle through phytoplankton over 20 times within the sub-estuary (Christian and Thomas 2000; Christian and Thomas 2003). When discharge and loading increase and residence time shortens because of major storms, less cycling and removal occurs. If the storm is strong enough, we predict that potentially all N entering the sub-estuary can pass through. This prediction is based on extrapolation from network analysis of a data set that did not include such high flow conditions and from a power curve relationship (Figure 2.4). We used both a power curve and linear relationship of TN import and export to bracket possible results in the extrapolation. Both curves gave  $r^2$  values greater than 0.9. Thus, the results should be considered indicative of what occurred, but within the limitations of extrapolation and curve fitting.

Once passed the sub-estuaries, the exported N could have been assimilated and cycled within the sound or transported, unprocessed out of the system to coastal waters. The freshwater replacement time for the sound (normally about 11 mo) dropped to less than 2 mo during the storm period (Bales et al. 2000), but this still would have provided plenty of time for the alternate possibility of biochemical filtration (Sharp et al. 1984). We tested this by calculating phytoplankton N demand, and found a value very similar to the extrapolated estimates of N exported to the sound, suggesting that the biochemical filter could have converted most of the loaded N to particulate matter. Assuming the N was immediately transformed to particulate matter, the fate of that N could be transfer to higher trophic levels, remineralization and recycling, storage in sediments, denitrification, export to the coastal ocean, or some combination thereof (Day et al.

1989). We hope that continued work in this system will provide more insight into these processes.

In comparison to other estuarine flooding events, the hurricane flooding in Pamlico Sound produced similar responses. The increase in algal biomass due to N loading is a typical flood response seen in a range of systems (Kristiansen 1998; Eyre 2000; Chan and Hamilton 2001). The highly episodic nature of the flood resembled the hydrology of tropical estuaries (Eyre and Balls 1999), although the sound was never completely freshened. The sound has limited connection with coastal shelf waters, so most of the nutrient and organic matter processing proceeds within the basin. In this way, the mass of floodwater in the sound resembles shelf waters which receive plumes from well-flushed estuaries (Balls 1994; Eyre and Balls 1999). The sound is much more shallow and enclosed than shelf waters and is probably more sensitive to excess nutrient and organic inputs. The future frequency of this type of extreme event may control the sound's resilience to potential eutrophication.

This study has provided critical baseline information on the Pamlico Sound ecosystem and extends our understanding of the sound's sub-estuaries (Christian et al. 1991; Rudek et al. 1991; Boyer et al. 1993; Paerl et al. 1998; Luettich et al. 2000). The water quality data collected for over 2 yr after the hurricanes revealed a range in recovery times to more normal conditions from 1 to 2 mo for dissolved nutrients to about an 8-mo recovery for particulate matter and salinity. We acknowledge that normal is difficult to define, particularly since we have limited pre- and post-hurricane data and cannot fully evaluate interannual variability. Most of the other reports on estuaries impacted by hurricanes also indicated rapid recovery, but this usually meant 3 mo or less (Chesapeake

Research Consortium 1976; Van Dolah and Anderson 1991; Valiela et al. 1998). While total phytoplankton biomass (chl *a*) returned to pre-hurricane levels within a year, the community composition appeared to be still changing more than two years later. Costanza et al. (1993) suggest that the lack of structure and prevalence of highly mobile and generalist species in estuaries creates resilience to disturbance. The Pamlico Sound water quality record after the hurricanes supports this notion of resilience in estuaries. The observed phytoplankton community structure, however, was less resilient and took longer to recover, if at all. The community shifts may be further affected by a predicted increase in tropical storm frequency. The biogeochemical and trophic implications of these climatic and ecological changes may be significant, and still need to be evaluated, especially at higher trophic levels (i.e., fish). Continued long-term monitoring will certainly add to an understanding of this system as it responds to additional storm events and more chronic, anthropogenic disturbances.

## **2.6 ACKNOWLEDGEMENTS**

We are grateful for the use of the R/V Capricorn and for the invaluable help of her crew, Joe Purifoy and Stacy Davis. We also are indebted to efforts of many technicians and students, including Tom Gallo, Malia Go, Nathan Hall, Brad Hendrickson, Laura Hill, Karin Howe, Lois Kelly, David Kimbro, Jessi O'Neal, Courtney Stephenson, Christina Tallent, and Pam Wyrick. Tammi Richardson and Luke Twomey contributed to project management and helpful discussions. Lexia Weaver provided CHEMTAX analyses and invaluable data management. We appreciate the critical comments from Amy Waggener and two anonymous reviewers. This work was supported by the National Science Foundation (DEB 9815495), U.S. Dept. of Agriculture NRI Project 9600509,

U.S. EPA STAR Project R82-5243-010, NOAA/North Carolina Sea Grant Program  
R/MER-43, and the North Carolina Dept. of Natural Resources and Community  
Development, Div. of Air Quality and Division of Water Quality/UNC Water Resources  
Research Institute (Neuse River Estuary Monitoring and Modeling Project-ModMon).

## **CHAPTER 3**

### **TEMPORAL PATTERNS AND CONTROLS OF BACTERIOPLANKTON**

#### **3.1 INTRODUCTION**

Heterotrophic bacterioplankton and phytoplankton dominate the microbial community at the base of most pelagic food webs. These microorganisms control much of the planktonic carbon and nutrient cycling in aquatic ecosystems through their metabolic processes. Resolving the temporal dynamics of these processes and the biomass driving the metabolism is essential to the overall understanding of ecosystem function.

Over the past three decades, bacterioplankton productivity (BP) determinations have become routine in the study of pelagic microbial communities, despite lingering methodological limitations (Gasol et al. 2008). This measurement, along with respiration when available, can be used as an indicator of microbial loop activity and overall carbon cycling. Estuarine BP has been relatively well studied compared to other marine ecosystems (Ducklow and Shiah 1993), but much of the research has been limited in time and space. Individual estuaries are unique systems based on their geomorphic, hydrologic, climatic, and watershed characteristics, and it remains a challenge to make generalizations about the patterns and controls of estuarine BP (Wright and Coffin 1983; McManus et al. 2004). Estuaries are some of the most fertile and functionally significant aquatic ecosystems on Earth and yet are often the most anthropogenically stressed (Day

et al. 1989), making an understanding of microbial processes and carbon cycling in these systems critically important in the face of regional and global change.

Many studies of bacterioplankton productivity (BP) in estuaries and other aquatic systems have noted temperature and the supply of dissolved organic carbon and dissolved inorganic nutrients as important controlling factors (Hoch and Kirchman 1993; Shiah and Ducklow 1994a; Goosen et al. 1997; Revilla et al. 2000; Pomeroy and Wiebe 2001). Of these, temperature seems to dominate as a driver of productivity, especially in estuarine systems where organic matter supply is plentiful.

Previous research examined aspects of the bacterioplankton community in the Neuse River and Pamlico Sound (NRPS) estuarine system (Christian et al. 1984), but that study was limited to the summer of one year. This study examines the temporal variability of BP in the NRPS system over a four year period. Temporal variation of co-occurring environmental and biological variables will be considered also, with a special focus on the effects of temperature and event scale alterations to the system. A major goal is to establish what bottom-up processes best determine overall bacterioplankton activity.

## **3.2 METHODS AND ANALYSIS**

### **3.2.1 STATIONS AND COLLECTION**

Most of the sampling for bacterioplankton was done in parallel with the field measurements and water collection for a long term water quality monitoring program (ModMon, [www.unc.edu/ims/neuse/modmon/](http://www.unc.edu/ims/neuse/modmon/)). During the years 2002 through 2005, biweekly to monthly visits were made to the estuary, depending on the region. Selected stations included four in the Neuse River and four in the Pamlico Sound, chosen to span the known salinity and trophic gradient (Figure 3.1).



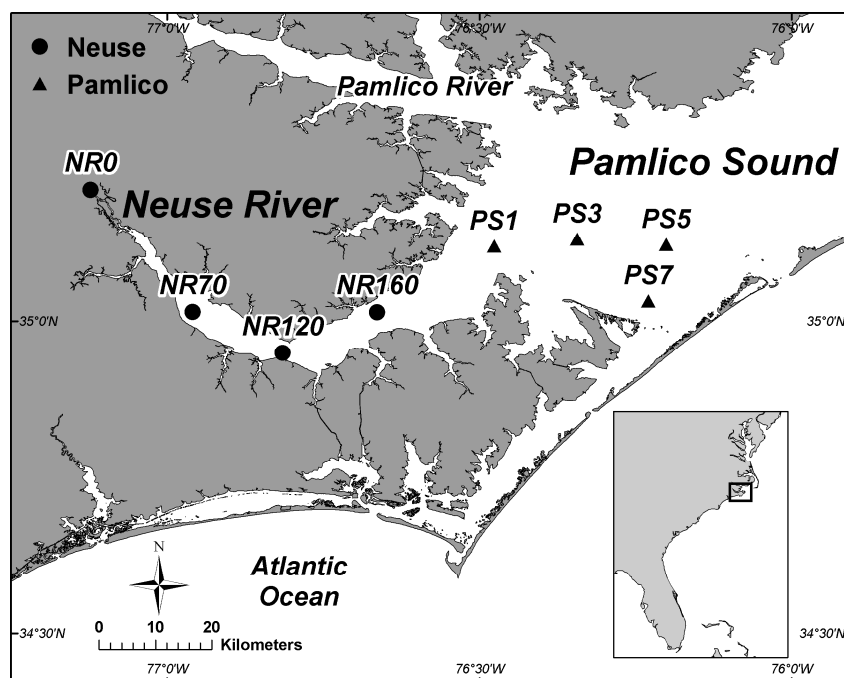


Figure 3.1 Map of study area showing station locations. Station labels are prefixed with the station group indicator NR (Neuse River) or PS (Pamlico Sound). Inset shows the extent of the map in context with the southeastern U.S.

Profiles of basic water quality characteristics were collected at each station using a YSI 6600 sonde (Yellow Springs, OH) configured to measure temperature and salinity (reported as parts per thousand, ppt, as recorded by the sonde). Sensors were calibrated prior to the sampling date. Readings were collected at 0.5 m intervals starting at the surface and continuing until just off the bottom. River discharge data came from USGS Gage No. 02091814 near Ft. Barnwell, NC ([waterdata.usgs.gov/nc/nwis](http://waterdata.usgs.gov/nc/nwis)). At each station, water was collected from the surface by submerging cleaned (dilute acid and deionized water) and sample-rinsed polyethylene containers 10 to 20 cm below the water surface. All samples were kept covered during transport to the laboratory.

### **3.2.2 CHEMISTRY AND PHYTOPLANKTON**

Much of the methods for organic matter, nutrients, phytoplankton variables are described in detail in Chapter 2 (Peierls et al. 2003), so only a brief summary will be given. Dissolved organic carbon (DOC) was measured on glass fiber (GF/F) filtrate using high temperature catalyzed oxidation coupled with infrared analysis. Dissolved organic nitrogen (DON) was the difference between total dissolved N (TDN) and dissolved inorganic N (DIN; sum of nitrate and ammonium), both measured by flow injection analysis (after inline digestion for TDN). Dissolved phosphate was measure with the same flow injection analysis system. Particulate organic carbon (POC) and nitrogen (PON) concentrations were determined using seston collected on GF/F filters and a CHN elemental analyzer. Chlorophyll *a* was extracted from filtered material using a tissue grinder and acetone and measured on a fluorometer configured with narrow band pass excitation and emission filters. Phytoplankton productivity (PP) was determined using <sup>14</sup>C-bicarbonate uptake in light and dark bottles under a variable irradiance system.

### **3.2.3 BACTERIOPLANKTON**

Bacterioplankton abundance (BA) was determined using direct enumeration and the SYBR Green I nucleic acid stain (Noble and Fuhrman 1998). Briefly, small volumes of formalin preserved (1 to 2 % final) samples were filtered onto aluminum oxide (Anodisc) filters and stained on drops of SYBR Green I in a petri dish. An antifade solution was added and the filter was mounted to a slide. Bacterial cells were identified separately from viral particles and counted using blue excitation on a Nikon E800 compound microscope configured for epifluorescence. Cell counts were made using a set fraction of 10 random fields to get a total of at least 200 cells.

Productivity was measured by  $^3\text{H}$ -leucine uptake (Kirchman et al. 1985) using an adaptation of the microcentrifuge-based method of Smith and Azam (1992). Sample aliquots (1.8 mL) were dispensed into 2 mL, screw top microcentrifuge tubes that were preloaded with  $^3\text{H}$ -L-leucine (4,5- $^3\text{H}$ , ICN or MP Biomedicals). The brand and style of tube remained the same throughout the study (Pace et al. 2004). Specific activities of the stock ranged throughout the study period from 40 to 116 Ci mmol $^{-1}$ . Stock isotope was diluted 10-fold to get an activity of 100  $\mu\text{Ci mL}^{-1}$ . A stock of non-radioactive L-leucine (2  $\mu\text{mol L}^{-1}$ ) was used to make up final leucine concentrations as needed; leucine uptake rates were corrected for this known dilution (Kirchman 1993). Incubations were done in the dark at *in situ* temperatures for one hour, which was tested to assure linear incorporation.

After ending incubation with TCA (5% final), samples were centrifuged at 16,110 x g for 15 minutes, rinsed once with 5% TCA, and counted on a Beckman scintillation counter using Cytoscint scintillation cocktail (ICN or MP Biomedicals). Counts were corrected for quench by the H-number technique. Samples collected after September 2004 received a base addition step to facilitate protein solubilization and incorporation into the cocktail. For these samples, 100  $\mu\text{L}$  0.5 N NaOH was added after the rinse step and mixed. After 30 minutes, 50  $\mu\text{L}$  of 0.5 N HCl was added to prevent the Cytoscint from gelling. This technique produced counts that were 21 % higher on average, and samples without the base addition were corrected by that average difference.

Initial studies determined that leucine uptake was saturated at leucine concentrations of about 20 nmol L $^{-1}$ . A series of 44 experiments measuring leucine uptake kinetics showed this concentration did not always produce saturated uptake as has

been shown elsewhere (Riemann and Azam 1992). Maximum uptake rates ( $V_{\max}$ ) were calculated by non-linear regression fits of the data to the Michaelis Menten model (Riemann and Azam 1992). The ratio of  $V_{\max}$  to measured uptake rate was assumed to be the isotope dilution factor (ID). The non-linear fit of ID versus leucine concentration from all the experimental replicates was used to calculate  $V_{\max}$  for the estuary data set (see Appendix). *In situ* BP was calculated using the estimated  $V_{\max}$  following Kirchman (2001).

### **3.2.4 STATISTICS AND ANALYSIS**

Correlations were done using the non-parametric Spearman's rank correlation test ( $\rho$  = coefficient reported). The non-parametric Kruskal-Wallis rank sum test was used for one-way grouped data comparisons. Simple and multiple linear regression were used to test relationships between BP and environmental factors. All variables, except temperature were natural log transformed before regression analysis to meet the assumption of normality and homoscedasticity. A significance level of  $\alpha = 0.05$  was chosen for all tests. All analysis and plotting was done using S-Plus version 7.0 (Insightful Corp.).

## **3.3 RESULTS**

### **3.3.1 SUMMARY**

A total of 109 visits were made to the NRPS system during the years of 2002 to 2005. Data for surface water samples collected are summarized in Table 3.1. Salinity ranged from fresh water to almost full sea water reflecting the geographical span of station locations. Dissolved organic matter (DOM) was abundant and carbon rich when compared to the Redfield C to N ratio (6.6) or reported bacterial C to N ratios (5.9-6.8,

Fukuda et al. 1998). For inorganic nutrients, DIN was highly variable due to nitrate variability and the median value was slightly greater than  $1 \mu\text{mol L}^{-1}$ . Phosphate was less variable than DIN and typically less than  $1 \mu\text{mol L}^{-1}$ . Median inorganic N to P ratio was less than the Redfield ratio (16), but because of high variability, measured ratios were often higher than 16. Concentrations of POC were lower and less variable than DOC concentrations, while PON concentrations were of similar magnitude and variability to DON concentrations. This produced particulate C to N ratios that were often close to Redfield ratio. When considering total organic matter, the summarized DOC to POC ratio indicates that the dominant form was the dissolved fraction.

Table 3.1 Summary of surface physical, chemical, and biological variables measured during 2002–2005 in the NRPS. IQR is interquartile range (third quartile minus first quartile) and N is the number of samples. BD = below detection (reported as method detection limit/3, DIN: 0.14, Phos.: 0.004).

| Variable                                      | Median | IQR   | Min.–Max.    | N   |
|---|--------|-------|--------------|-----|
| Temperature ( $^{\circ}\text{C}$ )            | 20.8   | 12.6  | 3.4–33.6     | 426 |
| Salinity (ppt)                                | 7.7    | 13.5  | 0.0–29.2     | 428 |
| DOC ( $\mu\text{mol L}^{-1}$ )                | 519.3  | 207.5 | 224.9–1368.2 | 422 |
| DON ( $\mu\text{mol L}^{-1}$ )                | 21.9   | 7.6   | 6.1–73.4     | 421 |
| DOC:DON                                       | 23.9   | 7.8   | 7.2–91.5     | 417 |
| DIN ( $\mu\text{mol L}^{-1}$ )                | 1.3    | 17.6  | BD–60.4      | 426 |
| Phosphate ( $\mu\text{mol L}^{-1}$ )          | 0.4    | 0.8   | BD–4.4       | 422 |
| DIN:DIP                                       | 8.9    | 30.6  | 0.1–529.9    | 422 |
| POC ( $\mu\text{mol L}^{-1}$ )                | 111.7  | 80.6  | 13.2–1025.9  | 426 |
| PON ( $\mu\text{mol L}^{-1}$ )                | 16.7   | 11.8  | 1.4–173.2    | 420 |
| POC:PON                                       | 7.2    | 1.8   | 2.0–32.4     | 420 |
| DOC:POC                                       | 4.4    | 3.5   | 0.5–40.5     | 422 |
| Chlorophyll <i>a</i> ( $\mu\text{g L}^{-1}$ ) | 12.8   | 15.8  | 0.3–419.4    | 426 |
| PP ( $\mu\text{g C L}^{-1} \text{ h}^{-1}$ )  | 23.1   | 35.4  | 0.3–255.7    | 425 |
| BA ( $\times 10^6$ cells $\text{mL}^{-1}$ )   | 7.5    | 6.7   | 0.66–79      | 102 |
| BP ( $\mu\text{g C L}^{-1} \text{ h}^{-1}$ )  | 2.3    | 2.8   | 0.2–24.6     | 428 |

Considering the planktonic microbial community, overall median chlorophyll *a* concentration, a proxy for autotrophic biomass, was almost  $13 \mu\text{g L}^{-1}$  with a peak of over  $400 \mu\text{g L}^{-1}$  (Table 3.1). About nine percent of the samples had concentrations greater than  $40 \mu\text{g L}^{-1}$ , which is the water quality standard used by the North Carolina Department of Environment and Natural Resources, Division of Water Quality for establishing the total maximum daily load (TMDL) for total N ([h2o.enr.state.nc.us/tmdl/Docs\\_TMDL/Neuse TN TMDL II.pdf](http://h2o.enr.state.nc.us/tmdl/Docs_TMDL/Neuse_TN_TMDL_II.pdf)). The median rate of phytoplankton productivity (PP) was about  $23 \mu\text{g C L}^{-1} \text{ h}^{-1}$  with a peak greater than  $250 \mu\text{g C L}^{-1} \text{ h}^{-1}$ . The variables for heterotrophic microbes included BA, which ranged from under  $1 \times 10^6$  to almost  $80 \times 10^6$  cells  $\text{mL}^{-1}$  and had a median of  $7.5 \times 10^6$  cells  $\text{mL}^{-1}$ . Note that the number of samples analyzed for BA was about one quarter of the other factors. Heterotrophic productivity (BP) was about 10% of median PP and ranged from 0.2 to almost  $25 \mu\text{g C L}^{-1} \text{ h}^{-1}$ .

### **3.3.2 INTERANNUAL PATTERNS**

The differences in climate during the four years of the study produced marked changes in one of the main driving factors affecting system variability. Daily mean discharge for the Neuse River varied significantly by year ( $p < 0.0001$ ; Figure 3.2). The lowest median discharge by year occurred during the very dry 2002, while 2003, which was wetter than normal, had the highest median discharge. The result of this interannual variation in discharge produced the inverse pattern in surface salinity (significantly different by year,  $p < 0.0001$ ).

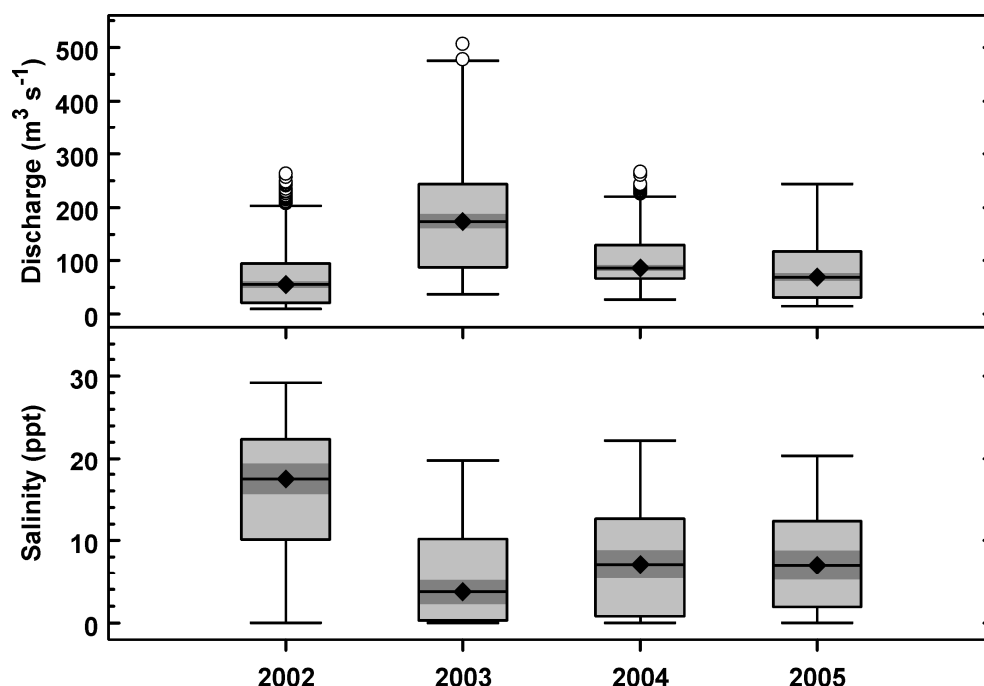


Figure 3.2 Daily mean Neuse River discharge (top) and surface salinity in NRPS (bottom) by year. Discharge data came from the USGS gage at Fort Barnwell (# 02091814). Solid diamond is the median, light grey box is the interquartile range (IQR), and whiskers are drawn to the last value within the span from the quartiles ( $1.5 \times \text{IQR}$ ). Values outside of the span are considered outliers and are indicated by open circles. The dark grey box indicates 95% confidence intervals around the median.

The interannual variation in discharge also caused differences in the other variables. Values for DOC concentration showed a pattern similar to discharge and the variation by year was significant ( $p < 0.0001$ ; Figure 3.3). A similar pattern and significance was found for DON and the dissolved C to N ratio. For inorganic nutrients, nitrogen was significantly different by year ( $p < 0.0001$ ), but this had more to do with differences in the spread of the data; the median concentrations were similar across years (Figure 3.4). Phosphate did not show a significant difference by year ( $p = 0.084$ ). Particulate C and N also did not show any difference across years ( $p = 0.35$  and  $0.22$  respectively), but the particulate C to N ratio did ( $p < 0.001$ ).

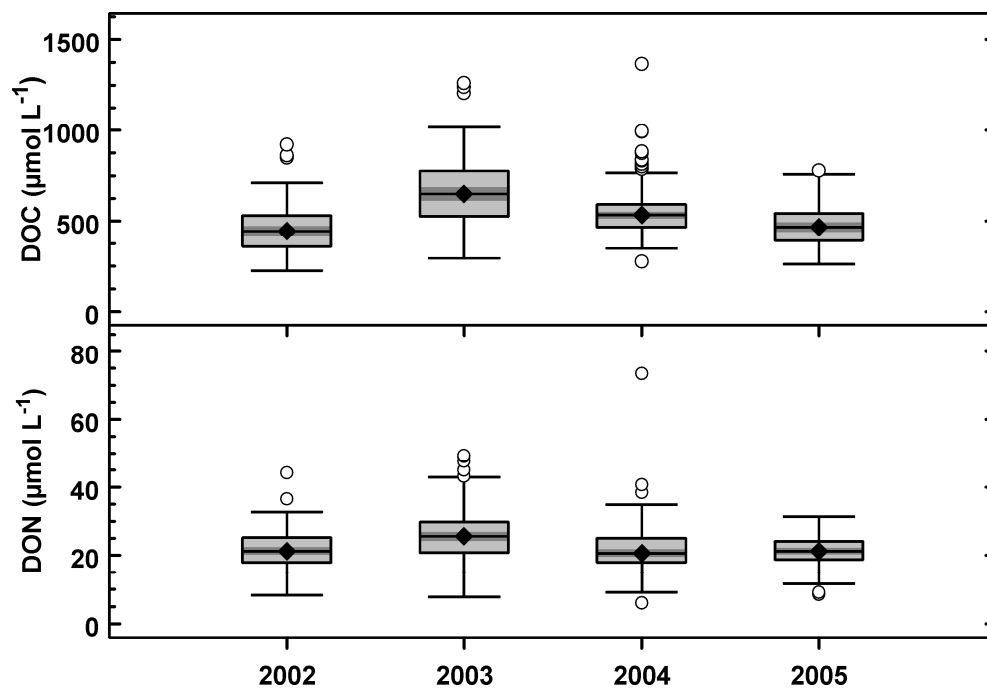


Figure 3.3 Surface DOC (top) and DON (bottom) in NRPS by year. Symbols as in Figure 3.2.

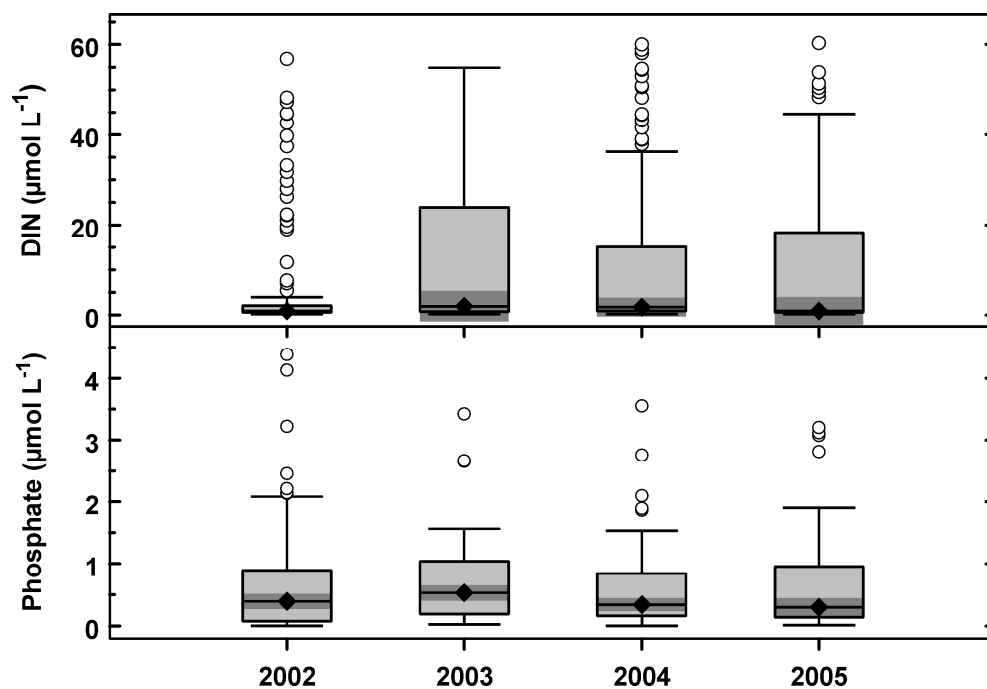


Figure 3.4 Surface DIN (top) and phosphate (bottom) in NRPS by year. Symbols as in Figure 3.2.



The biological variables were also affected by the differences between years. Chlorophyll *a* varied significantly by year ( $p = 0.014$ ) and the median concentrations were different between 2002 and 2003 (by non-overlapping confidence intervals; Figure 3.5). On the other hand, PP did not show a difference by year ( $p = 0.27$ ), although the within-year variability (IQR and span) was greatest in 2003. Interannual variation for BA was not determined because of unbalanced collection and analysis during the study period. The pattern for BP showed significant difference between years ( $p < 0.0001$ ), but the trend in median rates was different from the other parameters (Figure 3.7). Median BP decreased continuously across the four years from 3.2 in 2002 to 1.4 in 2005; the IQR and spans decreased as well.

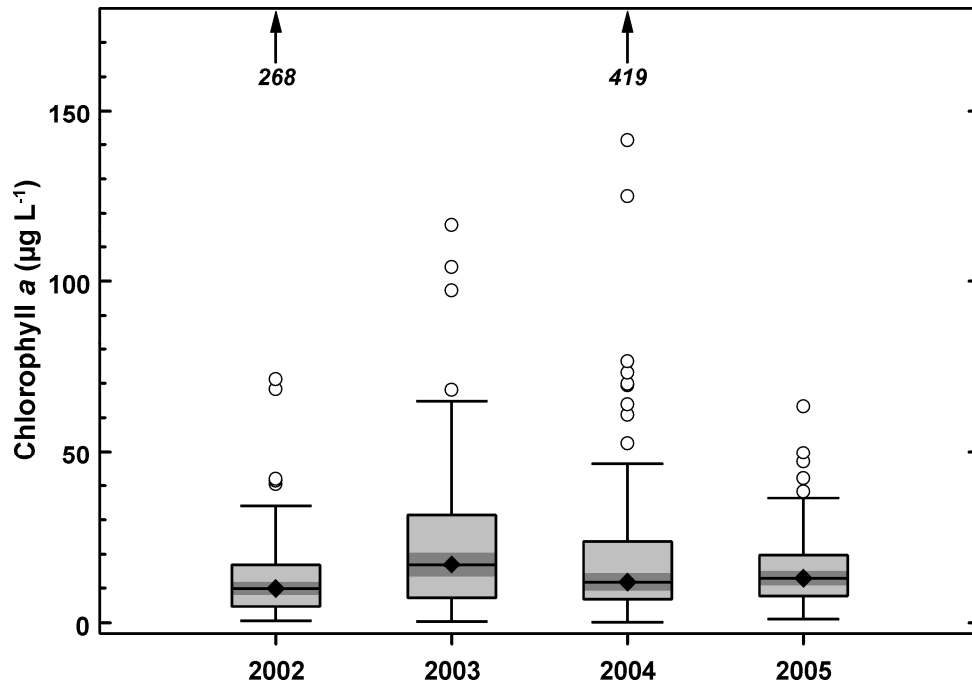


Figure 3.5 Surface chlorophyll *a* in NRPS by year. Symbols as in Figure 3.2. Outliers outside of the axis scale are indicated by the number and an arrow.

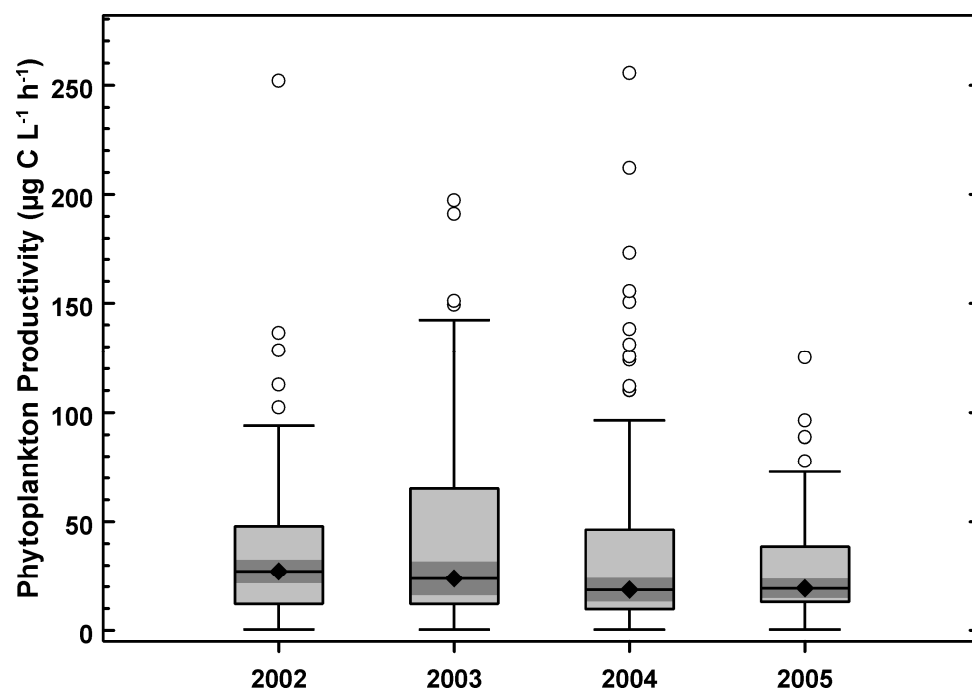


Figure 3.6 Surface phytoplankton productivity in NRPS by year. Symbols as in Figure 3.2.

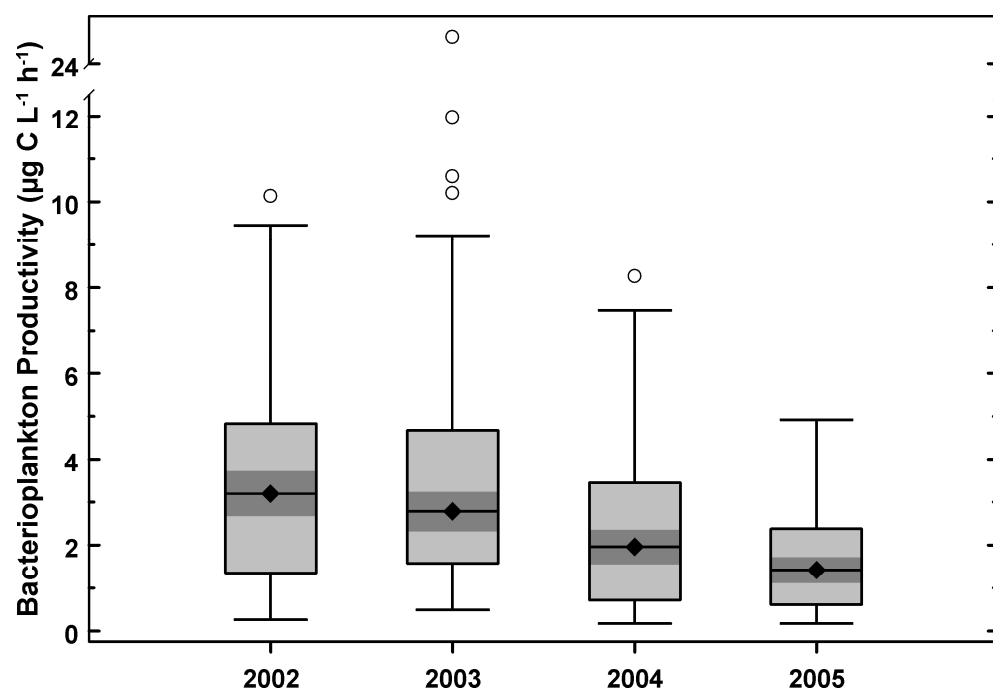


Figure 3.7 Surface bacterioplankton productivity in NRPS by year. Symbols as in Figure 3.2.

### 3.3.3 MONTHLY PATTERNS

Surface water temperature during the study period showed a predictable seasonal pattern, with lowest monthly median in February (although the lowest temperature was in January) and the highest in July (Figure 3.8). The range in monthly values represents interannual variability, since station to station variability was generally low. Daily mean river discharge at the Fort Barnwell USGS gage (about 25 km upstream from station NR0) showed a different seasonal trend during the study period (Figure 3.9). The highest monthly median values were noted in spring and winter months, while the lowest monthly median discharge occurred in July. Some months were more variable than others and the large range of values by month indicated high interannual variability.

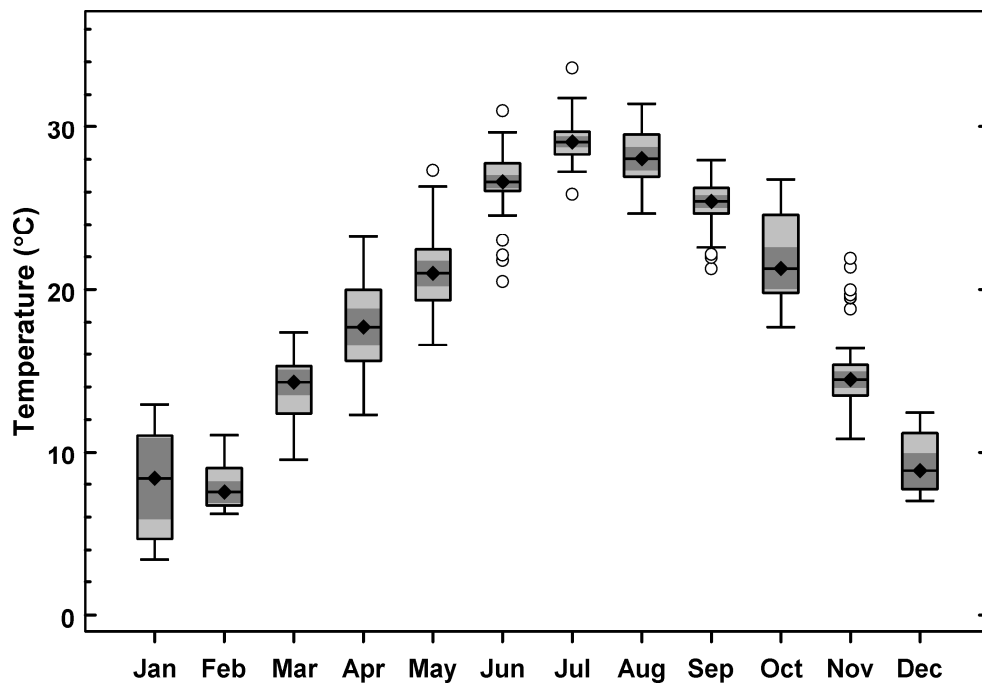


Figure 3.8 Surface water temperature in NRPS by month for the period 2002 through 2005. Symbols as in Figure 3.2.

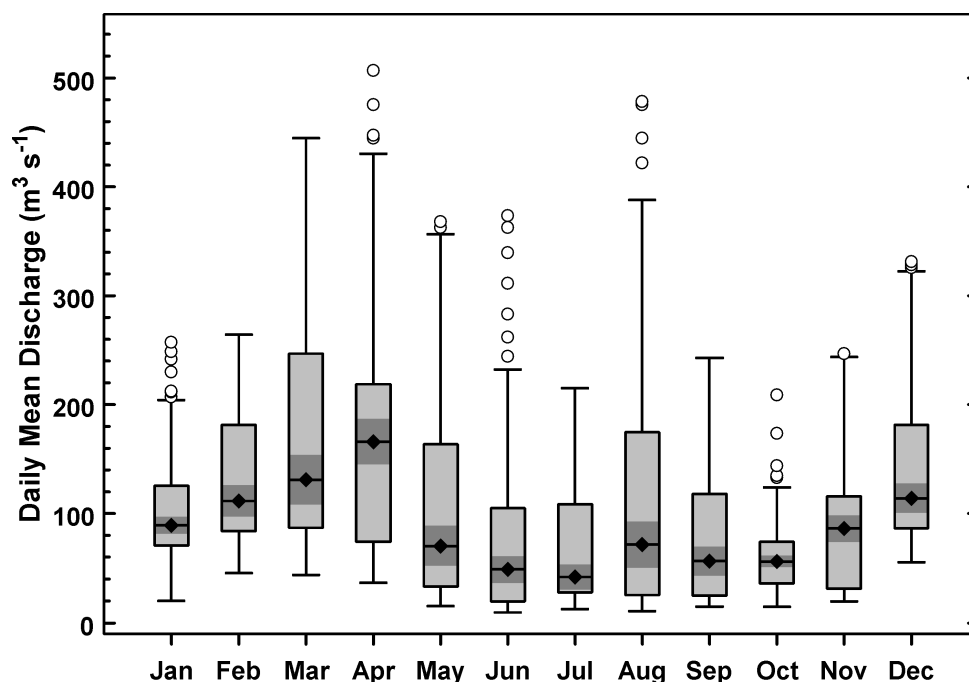


Figure 3.9 Daily mean Neuse River discharge for the period 2002 through 2005. Data from the USGS gage near Fort Barnwell, NC. Symbols as in Figure 3.2.

Dissolved constituents were examined in a similar fashion. Surface organic matter, as measured by DOC and DON concentrations, showed less obvious seasonality (Figure 3.10), although there were significant differences by month ( $p = 0.0014$  and  $p < 0.0001$ , respectively). Monthly median concentrations for both DOC and DON ranged from 12 to 18 % of the overall medians (Table 3.1). Surface DIN concentrations did not differ by month ( $p = 0.39$ ) and the monthly medians were all near the overall median of  $1.4 \mu\text{mol L}^{-1}$  except for December (Figure 3.11). What did vary by month was the DIN variability; summer and early fall had small IQR and spans compared to the other seasons. Surface phosphate concentrations varied by month ( $p < 0.0001$ ) and had peak median concentrations occurring in July and August. Phosphate concentration and temperature were significantly correlated when considering all of the data ( $\rho = 0.43$ ,  $p < 0.001$ ,  $n = 422$ ).

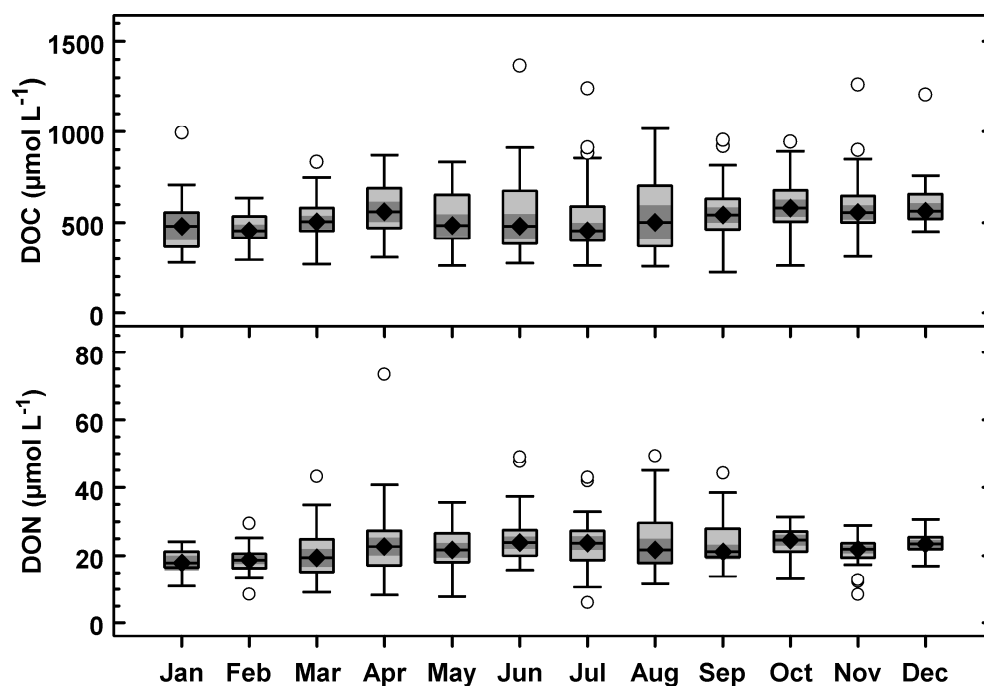


Figure 3.10 Surface DOC (top) and DON (bottom) concentration in NRPS by month for the period 2002 through 2005. Symbols as in Figure 3.2.

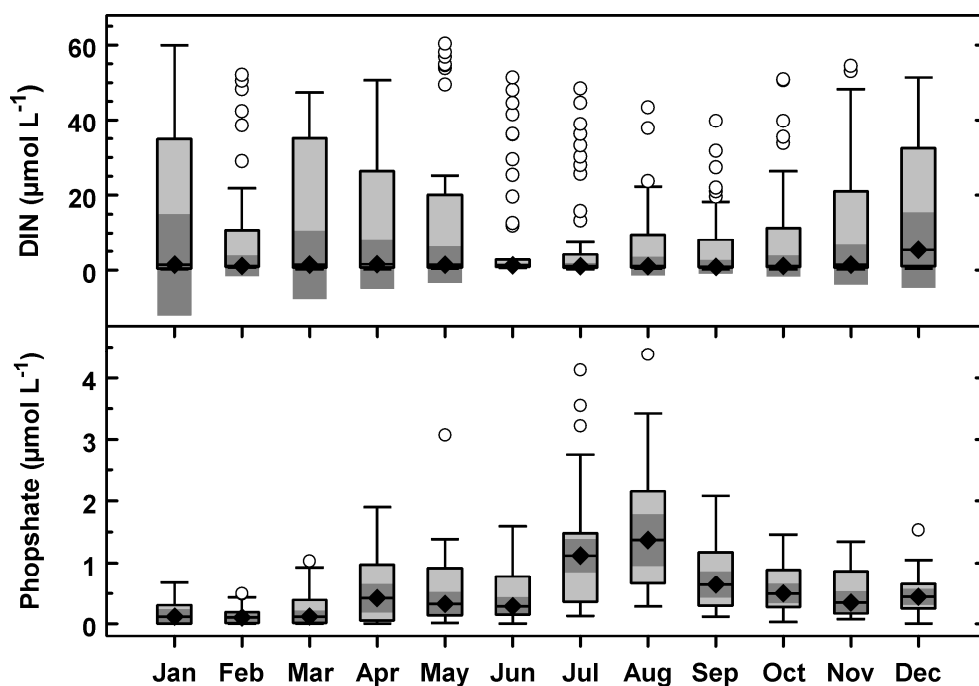


Figure 3.11 Surface DIN (top) and phosphate (bottom) in NRPS by month for the period 2002 through 2005. DIN is the sum of nitrate/nitrite and ammonium concentrations. Symbols as in Figure 3.2.

Phytoplankton biomass and productivity showed little or no seasonal patterns. Chlorophyll *a* concentrations were not different by month ( $p = 0.48$ ) and the monthly median concentrations were all within 50 % of the overall median (Figure 3.12). There is a similarity of the chlorophyll *a* monthly pattern to that of DIN, but the two parameters were in fact negatively correlated ( $\rho = -0.15$ ,  $p < 0.002$ ,  $n = 426$ ). Phytoplankton productivity was similarly lacking in differences by month (Figure 3.13), although the  $p$  value (0.07) was close to the chosen limit. Primary productivity and biomass were well correlated ( $\rho = 0.83$ ,  $p < 0.0001$ ,  $n = 425$ ) and this was obvious when the monthly median values were plotted together on a smaller scale (Figure 3.14). The comparison of POC and PON by month (not shown) was similar to the phytoplankton pattern and was not significant ( $p = 0.07$  and  $0.40$ , respectively), although this was not surprising as POC and PON correlate strongly with chlorophyll *a* ( $\rho = 0.85$ ,  $p < 0.0001$ ,  $n = 426$  and  $420$  respectively).

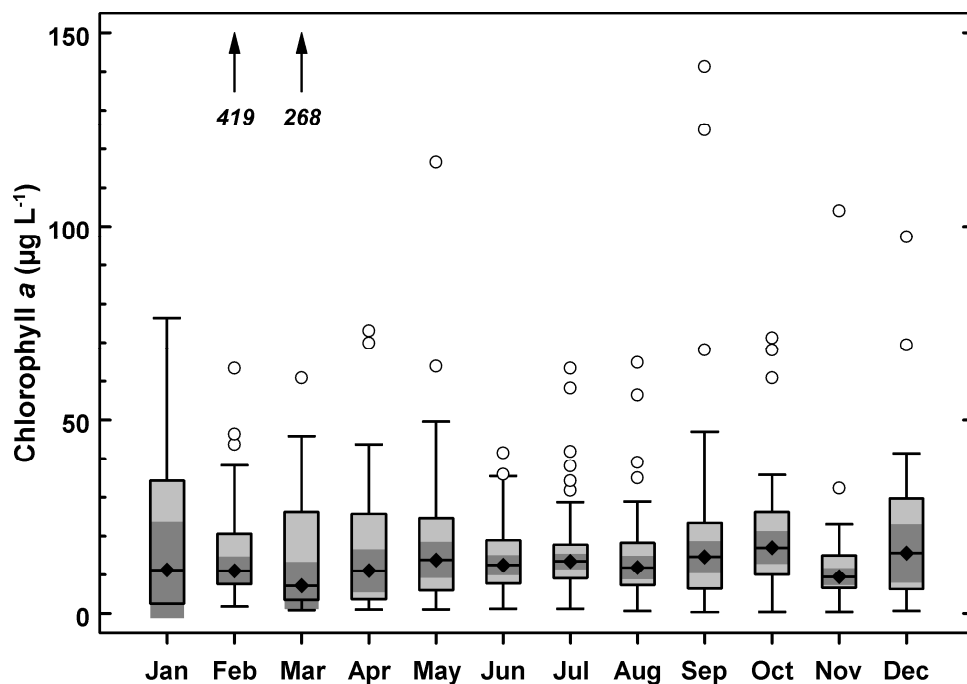


Figure 3.12 Surface chlorophyll *a* concentrations in NRPS by month for the period 2002 through 2005. Symbols as in Figure 3.2. Outliers outside of the axis scale are indicated by the number and an arrow.

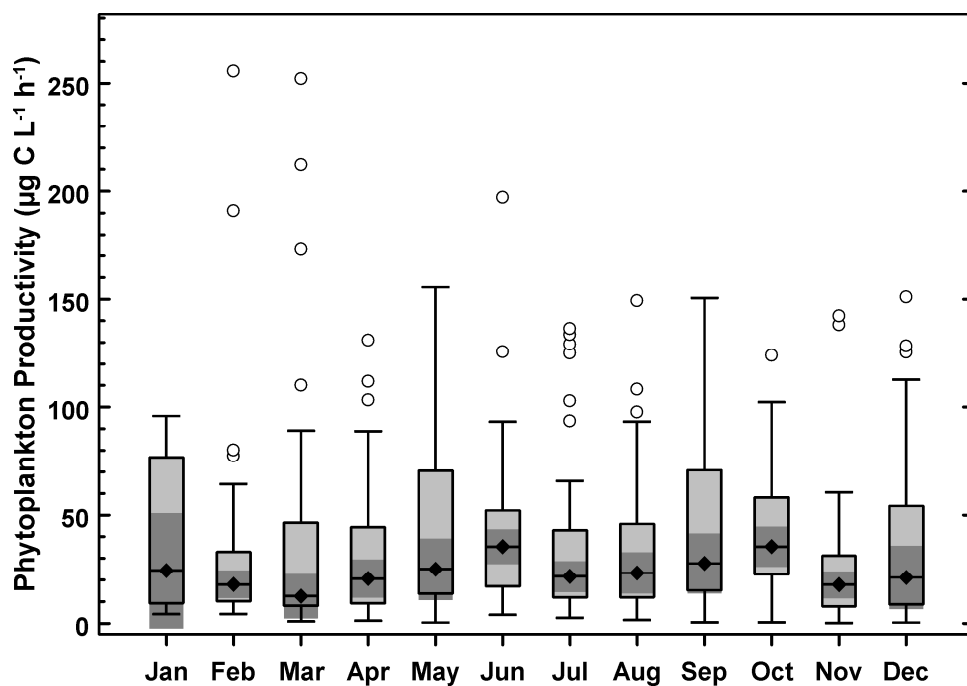


Figure 3.13 Surface primary productivity in NRPS by month for the period 2002 through 2005. Symbols as in Figure 3.2.

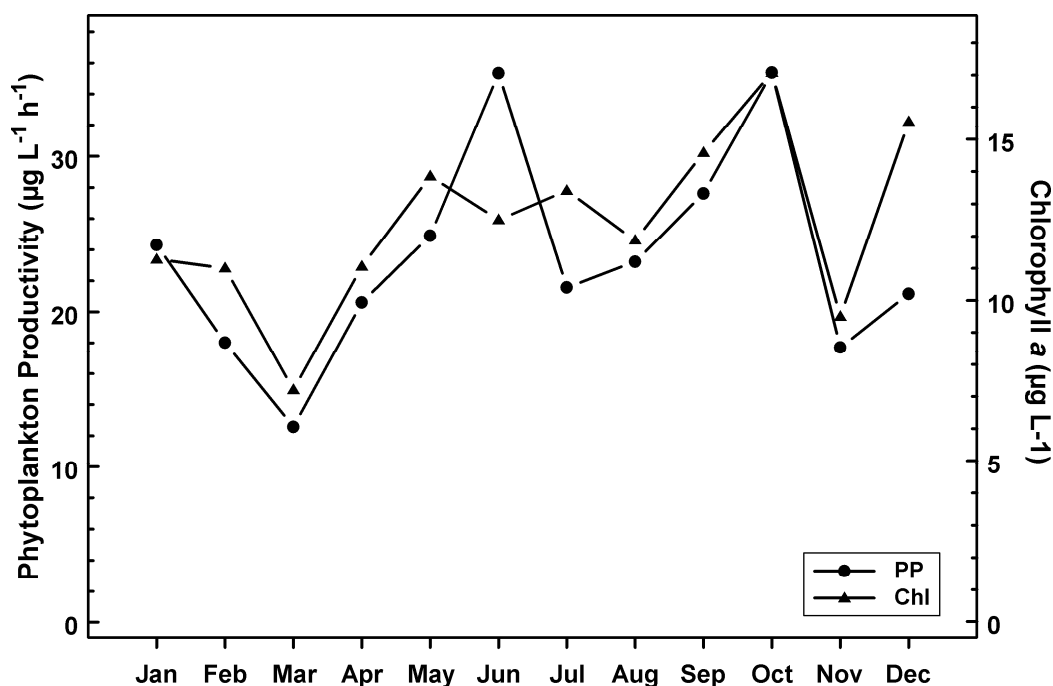


Figure 3.14 Median surface phytoplankton productivity and chlorophyll *a* concentration by month in NRPS.

A similarly lack of strong seasonality was found for BA (Figure 3.15). Higher monthly median cell counts were noted for July, August, and October, although the small and uneven sample sizes ( $n = 2$  to 21 per month) and overlapping confidence intervals made it difficult to differentiate between months ( $p = 0.42$ ). The pattern for BP was strongly seasonal, with maximum and minimum values occurring mostly during the warmest and coldest months respectively (Figure 3.16). The difference in BP by month was significant ( $p < 0.0001$ ). Variability, as represented by the monthly IQR and span, also increased with temperature. Seasonality in BP was repeated across the four years of the study (Figure 3.17). The end result was that temperature and BP were highly correlated ( $\rho = 0.69$ ,  $p < 0.001$ ,  $n = 426$ ).



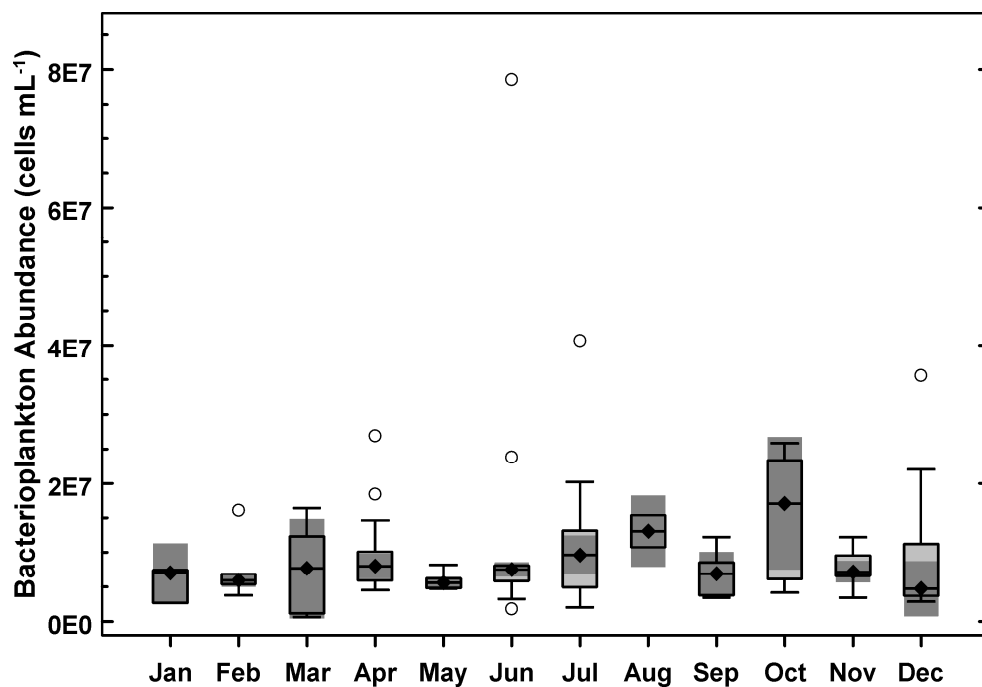


Figure 3.15 Surface bacterioplankton abundance in NRPS by month for the period 2002 through 2005. Symbols as in Figure 3.2.

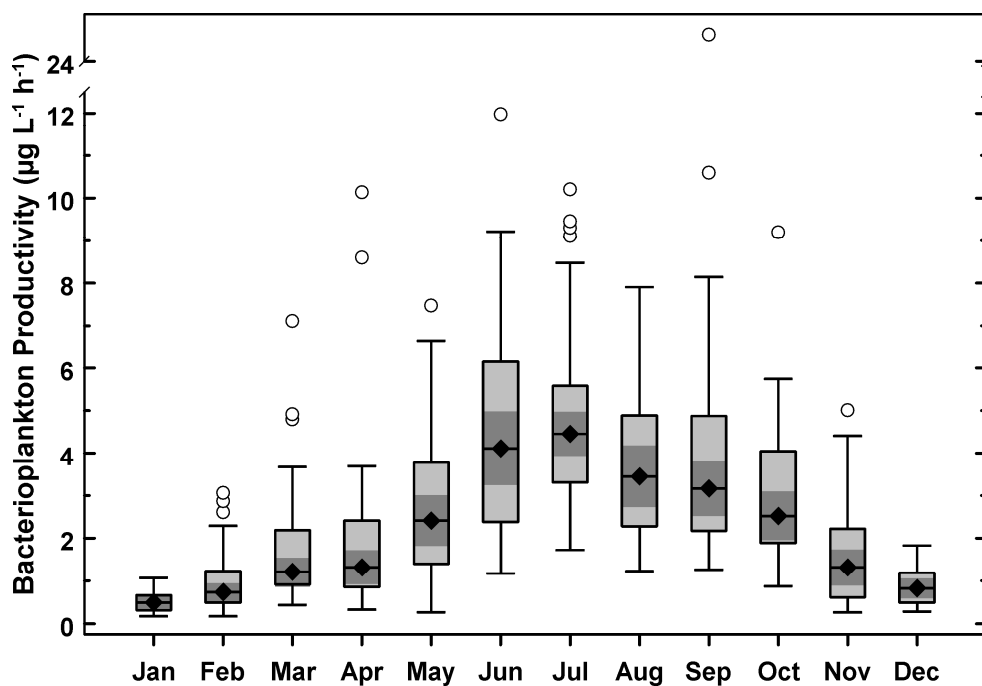


Figure 3.16 Surface bacterioplankton productivity in NRPS by month for the period 2002 through 2005. Symbols as in Figure 3.2.

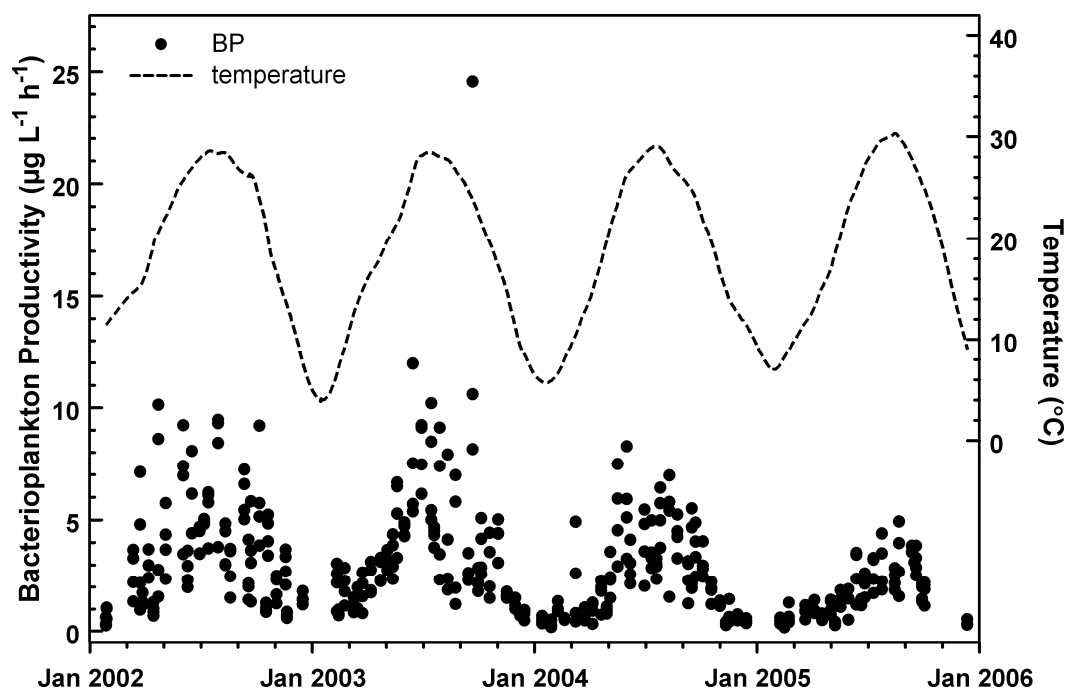


Figure 3.17 Surface bacterioplankton productivity (BP) and water temperature in NRPS versus date. Filled circles are BP measured at individual stations. Dotted line is a smoothed line through the temperature data using a LOESS (locally weighted regression) smoothing function.

### 3.3.4 EFFECT OF TEMPERATURE

Given that BP and temperature were highly correlated, BP was regressed against temperature (Figure 3.18). Many biological processes respond exponentially to temperature, so the linear form of the exponential equation was used for the fit. The regression was significant ( $p < 0.0001$ ) and temperature explained 50 % of the variation in BP. The slope of the regression line can be used to estimate the ecological temperature coefficient,  $Q_{10}$ , by the relation  $Q_{10} = e^{(\text{slope} \times 10)}$ . For the temperature range encompassed by this data set,  $Q_{10}$  was 2.35 (95% confidence interval: 2.17–2.56). A third order polynomial fit of  $\ln(\text{BP})$  versus temperature (not shown) indicated a decreasing slope starting at about 25 °C. When the rates of BP were divided into two groups by this temperature, the regression slope was lower for temperatures greater than 25 °C, but it

was a non-significant regression and the slope did not differ significantly from the slope for temperatures  $\leq 25$  °C (Figure 3.19).

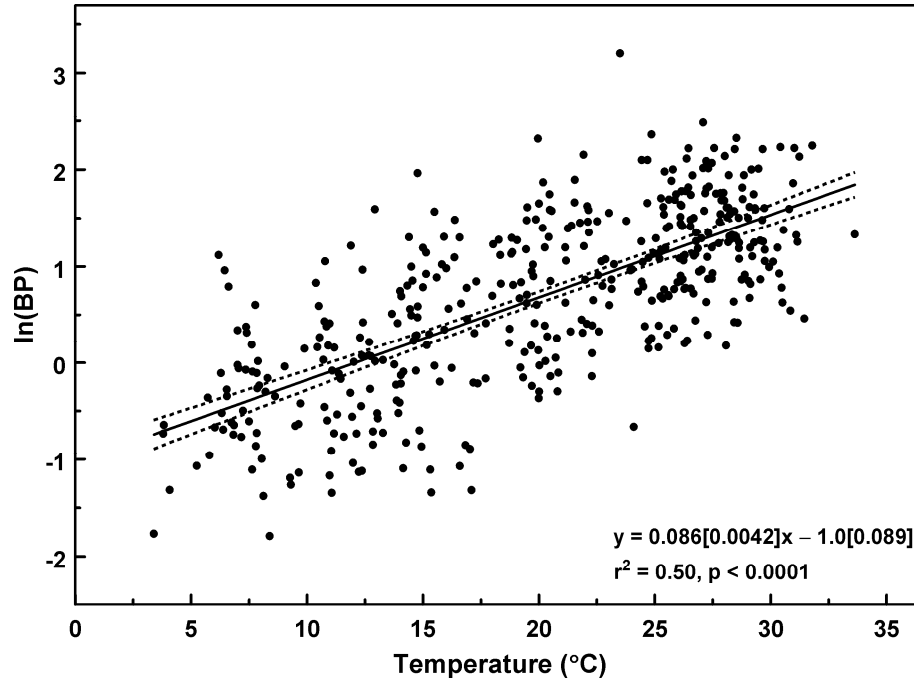


Figure 3.18 Linear regression of natural log-transformed surface BP versus temperature. The solid line is the least squared regression and the dashed lines are the 95 % confidence limits for the regression. Bracketed numbers in equation are coefficient standard errors.

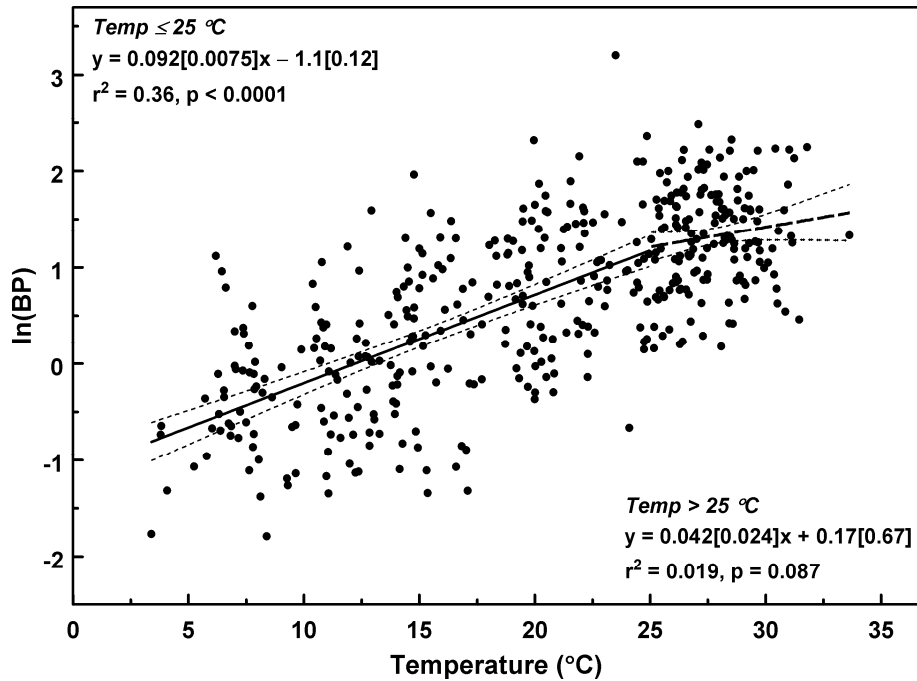


Figure 3.19 Linear regressions of natural log-transformed surface BP versus temperature, for temperature  $\leq 25$  °C (solid line) and  $> 25$  °C (long dashed line). The short dashed lines are the 95 % confidence limits for the regression. Bracketed numbers in equations are coefficient standard errors.

A similar way to represent the effect of temperature on metabolic rate is using the Boltzmann factor,  $e^{(-E/kT)}$ , where  $E$  is the activation energy (eV),  $k$  is the Boltzmann constant ( $8.617343 \times 10^{-5}$  eV/K), and  $T$  is the absolute temperature (Brown et al. 2004). Theory predicts that natural log-transformed, mass-corrected metabolic rates will be a linear function of the inverse of temperature times the Boltzmann constant and will yield a slope that is the activation energy of the process (Gillooly et al. 2001). Using the data from this study and assuming that the volumetric BP and PP are mass corrected, the activation energy was 0.63 eV (95 % CI: 0.57–0.69) for BP and 0.16 eV (95 % CI: 0.05–0.27) for PP (Figure 3.20). Gillooly et al. (2001) reported a mean activation energy of 0.62 eV for a wide variety of organisms ranging from microbes to mammals.

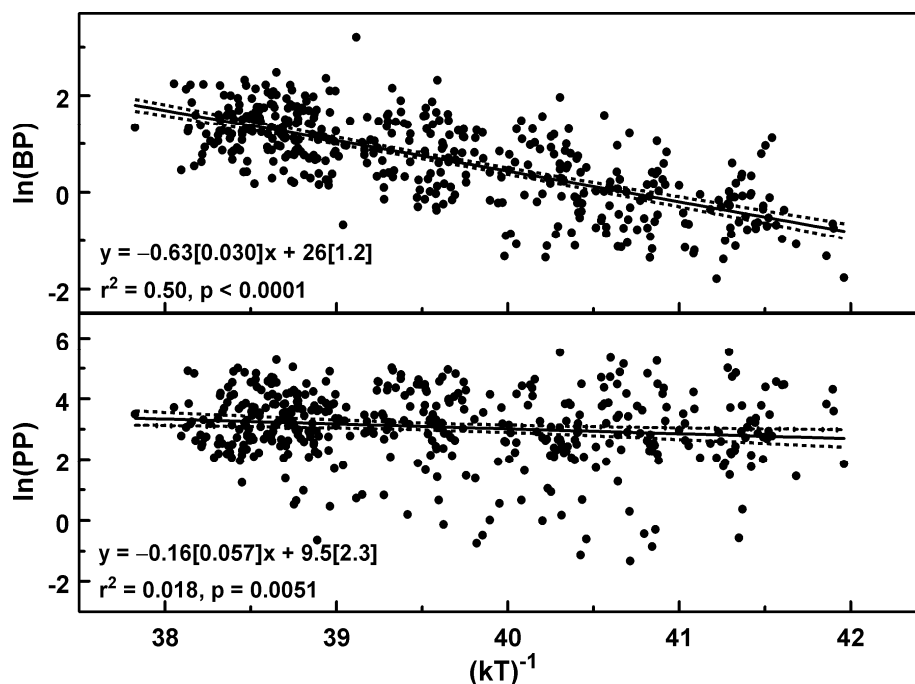


Figure 3.20 Linear regression of natural log-transformed surface BP (top) and PP (bottom) versus the inverse of absolute temperature ( $T$ ) times the Boltzmann constant ( $k$ ). Lines and equations as in Figure 3.18.

### 3.3.5 MULTIPLE REGRESSION ANALYSES

Multiple regression analysis was used to determine what variables might improve on the BP versus temperature relationship. The variables selected were those that might be considered resources for bacterioplankton (phytoplankton, DOM, POM, and nutrients) and that showed positive correlation with BP (Table 3.2). The analysis used a stepwise technique that minimized AIC (Akaike Information Criterion) with the addition or deletion of terms. Using the largest data set possible, the best fit of  $\ln(\text{BP})$  was:

$$[0.085 \times T] + [0.70 \times \ln(\text{DOC})] + [0.49 \times \ln(\text{PON})] + [-0.15 \times \ln(\text{Chl } a)] - 6.4$$

$$(r^2 = 0.61, p < 0.0001, n = 417)$$

where  $T$  is temperature. Removing chlorophyll  $a$  from the model produced an alternate model that explained almost the same amount of variation in BP:

$$b) [0.084 \times T] + [0.69 \times \ln(\text{DOC})] + [0.28 \times \ln(\text{PON})] - 6.1$$

$$(r^2 = 0.60, p < 0.0001, n = 417).$$

Data records that had BA values were used in a second stepwise regression analysis. The most likely model using this subset was:

$$[0.10 \times T] + [0.56 \times \ln(\text{POC})] + [-0.23 \times \ln(\text{BA})] + [-0.15 \times \ln(\text{Chl } a)]$$

$$(r^2 = 0.83, p < 0.0001, n = 102)$$

The intercept term was not significantly different from zero and was therefore removed.

Dropping the chlorophyll *a* term again led to a simpler model with similar predictive power

$$[0.10 \times T] + [0.34 \times \ln(\text{POC})] + [-0.19 \times \ln(\text{BA})]$$

$$(r^2 = 0.82, p < 0.0001, n = 102).$$

Table 3.2 Correlation coefficients for selected parameters versus BP. The coefficient was determined using the Spearman rank correlation test.

| Parameter            | Coefficient ( $\rho$ ) | p        | N   |
|----------------------|------------------------|----------|-----|
| DOC                  | 0.24                   | < 0.0001 | 422 |
| DON                  | 0.32                   | < 0.0001 | 421 |
| DIN                  | -0.04                  | 0.39     | 426 |
| Phosphate            | 0.34                   | < 0.0001 | 422 |
| POC                  | 0.30                   | < 0.0001 | 426 |
| PON                  | 0.32                   | < 0.0001 | 420 |
| Chlorophyll <i>a</i> | 0.25                   | < 0.0001 | 426 |
| PP                   | 0.26                   | < 0.0001 | 425 |
| BA                   | 0.08                   | 0.43     | 102 |

### 3.3.6 IMPACT OF EVENTS

During the period of this study, four tropical cyclones crossed through or passed near the area (Paerl et al. 2006a) (Figure 3.21). Hurricane Isabel made landfall 18

September 2003 as a category 2 storm and crossed directly over the junction of the Neuse River and Pamlico Sound. A storm surge as high as 10 feet above normal was recorded along the Neuse River shoreline causing severe flooding in low lying areas. Hurricane Alex grazed the Outer Banks as a category 2 storm on 3 August 2004. The Ocracoke Island-Cape Hatteras area sustained most of the storm's impact, although the lower Neuse River and Pamlico Sound experienced tropical storm force winds, one to four feet of storm surge, and one to five inches of rain. Hurricane Charley passed through the Neuse River watershed on 14 August 2004 at tropical storm strength. The main impact of this storm was flash flooding from the four to six inches of precipitation along the storm track; storm surge was minimal. During 14 to 15 September 2005, Hurricane Ophelia crawled along the southern Outer Banks as a category 1 storm. Because of its slow passage, the main impact on the NRPS was storm surges of from four to nine feet above normal.

The data collected during this study provided before and after conditions for the four storms. No parameter showed an obvious change after storms except BP (Figure 3.22), and this was only after Hurricane Isabel in 2003. Four days after Isabel, BP increased from 1.2 to almost 20 times the rates at the same stations the month before. The BP data collected three days before Isabel were from the Pamlico Sound stations and BP at those stations showed a slight decrease when sampled on 1 October. The only other apparent change was in PP after Hurricane Ophelia (data not shown). Median PP increased from  $15 \mu\text{g C L}^{-1} \text{ h}^{-1}$  on 22 August to  $79 \mu\text{g C L}^{-1} \text{ h}^{-1}$  on 19 September 2005, the difference being significant ( $H_a: \mu > 0$ ,  $p = 0.014$ ). Samples from the study stations on 8 September 2005 (not included in the summarized data since no BP measurements

were made) had a median PP of  $34 \mu\text{g C L}^{-1} \text{ h}^{-1}$ , but this was not significantly different from the post-storm value.

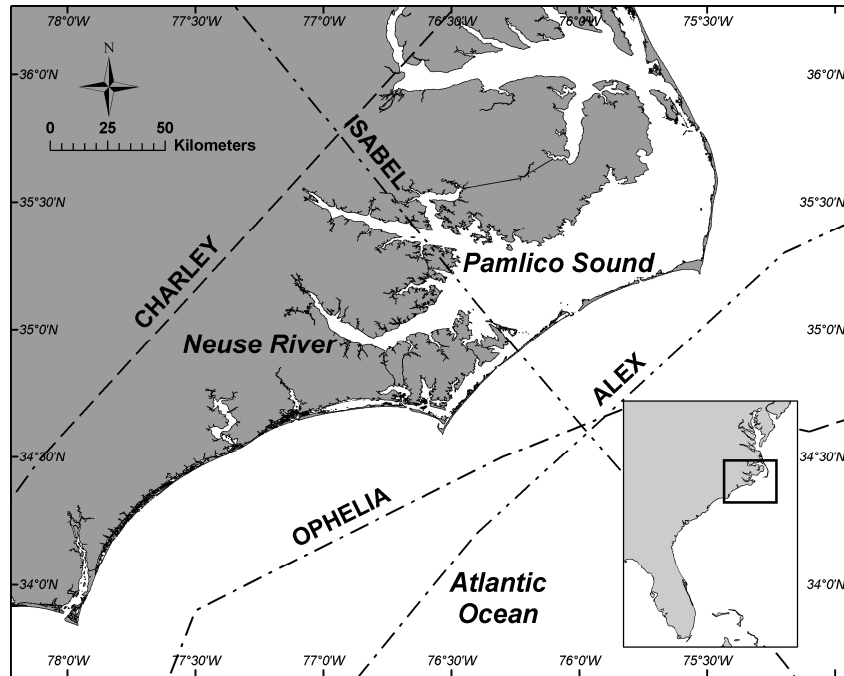


Figure 3.21 Map of study area showing tracks of storms that impacted during the period of study. Line type indicates category of storm: dashed = tropical storm; dash-1 dot = cat. 1 hurricane, dash-2 dots = cat. 2 hurricane. Inset shows the extent of the map in context with the southeastern U.S. Storm tracks courtesy of NOAA Coastal Services Center ([maps.csc.noaa.gov/hurricanes/](http://maps.csc.noaa.gov/hurricanes/)).



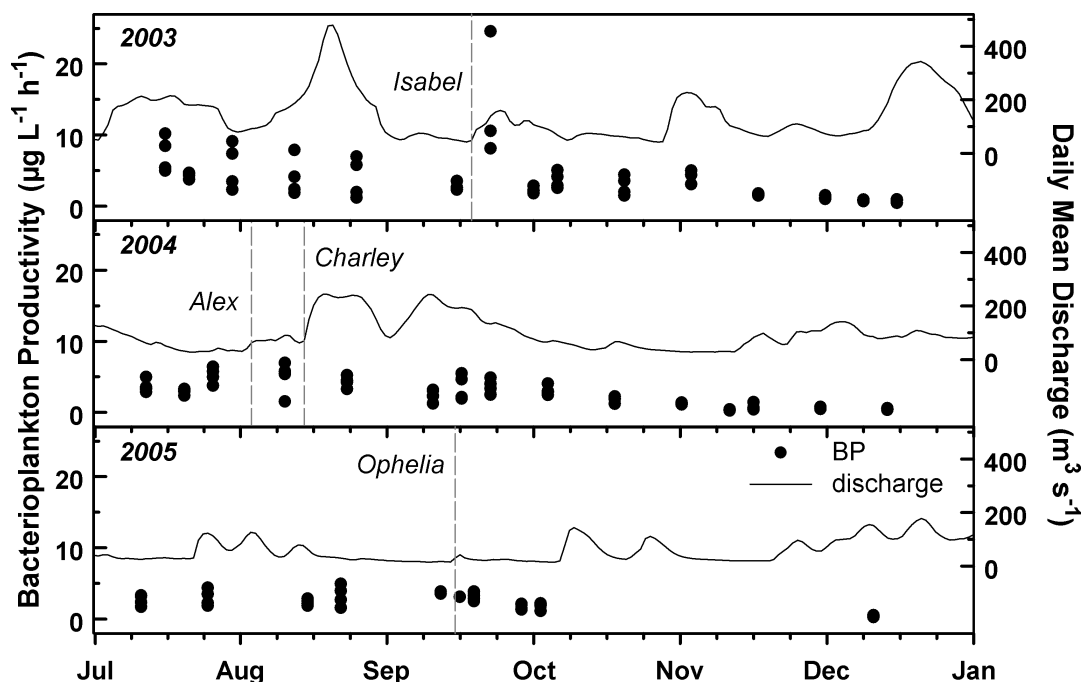


Figure 3.22 Surface bacterioplankton productivity (BP) in NRPS and daily mean Neuse River discharge at Fort Barnwell versus date. Filled circles are BP measured at individual stations and solid line is the discharge data.

The annual summaries of river discharge revealed significant differences between the years, especially the drought of 2002 and the very wet 2003 (Figure 3.2). These hydrologic variations were examined for any impact on BP (Figure 3.23). During the almost record discharge in the spring of 2003, the variability of BP seemed reduced compared to 2002 and 2004, both years with below normal spring discharge. The coefficient of variation (CV) for BP on each date during spring months (March through May) was used as a measure of variability. Considering the Neuse River stations only, mean CV for Spring 2002 was greater than that for 2003 or 2005 (t-test  $H_a: \mu > 0$ ,  $p = 0.038$  and  $0.045$ ,  $n = 11$ ). The same was found for 2004, a year with below normal spring discharge; mean spring CV was greater than that for 2003 or 2005 ( $p = 0.028$  and  $0.034$ ,  $n = 12$ ).

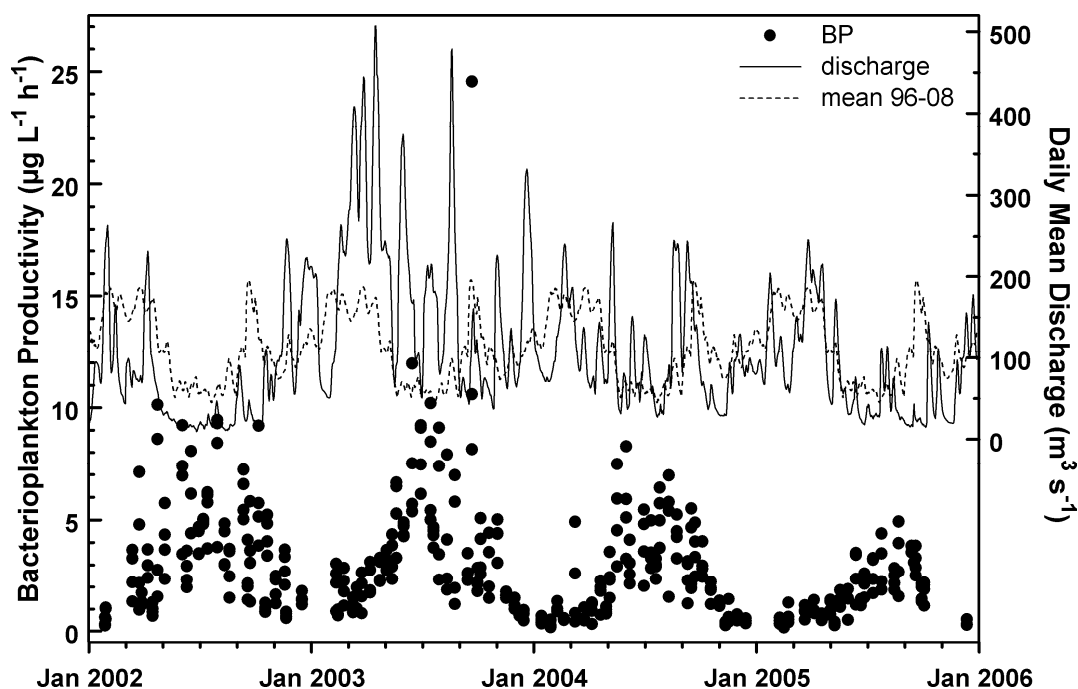


Figure 3.23 Surface bacterioplankton productivity (BP) in NRPS and daily mean Neuse River discharge at Fort Barnwell versus date. Filled circles are BP measured at individual stations, solid line is the discharge data, and the dashed line is the 12 year mean discharge by day.

### 3.4 DISCUSSION

Environmental conditions in the NRPS represent its global location and its geomorphic and hydrologic characteristics. The temperature median and range (Table 3.1) is typical for a temperate mid-Atlantic estuary. The major energy driving the system is from wind and river discharge due to the lagoonal nature of the system (Giese et al. 1985) and the large salinity range reflects the input of river water mixing with the limited input of ocean water through a few restricted inlets. The system is enriched in organic matter and nutrients supplied by drainage of the river's watershed. Measurements of phytoplankton production, when extrapolated to an annual scale (Mallin et al. 1993; Boyer et al. 1993), put the system in the meso- to eutrophic category (Nixon 1995).

Bacterial parameters measured in the NRPS were comparable to measurements in other estuaries around the world. The range of BA measurements for this system (Table

3.1) was similar if not greater than for several estuarine systems reviewed by Ducklow and Shiah (1993). Methodology differences may explain the higher values from this study; the SYBR Green I stain is brighter and more specific than other nucleic acid stains typically used for direct count techniques (Noble and Fuhrman 1998). Ducklow and Shiah (1993) also reviewed BP measurements in estuaries. The median and range of BP rates in NRPS spans the average range of BP in both global and temperate estuaries reported in this review. It is interesting to note that few of the studies in the Ducklow and Shiah review used leucine uptake for BP measurement. An earlier review (White et al. 1991) and more recent estuarine BP measurements (Revilla et al. 2000; Apple et al. 2004; Barrera-Alba et al. 2008) confirm that the results from this study are within the normal range for estuaries.

This study spanned four years that differed by at least precipitation patterns and amounts, particularly between 2002 and 2003. This led to large differences in discharge between those years, which in turn led to differences in nutrient and organic matter loading. Concentrations, and by extension loading, of DOC and DON were greater in 2003 than the other years. DIN differed by year, but in spread rather than central tendency. Since loading is a function of concentration and discharge, more DIN entered the estuary in 2003 than the other years. Phytoplankton biomass, but not productivity, mirrored the pattern of discharge with peak median chlorophyll *a* concentration in 2003. As N tends to be the limiting nutrient (Paerl et al. 1998; Paerl 2006), the biomass response was presumed to be due to the greater inorganic and organic N loading, but the lack of difference in primary productivity by year puts that in question. Another

hypothesis is that the high discharge in 2003 may have had some negative influence on grazer populations leading to greater phytoplankton biomass.

The rates of BP also differed by year, but the pattern was different from the discharge pattern in that the medians and span decreased with time. This did not match the patterns for discharge or any of the other parameters that could be considered bacterial resources. This suggests that BP is not strongly influenced by discharge or those factors. There is the possibility that methodological changes may have caused this decrease. The discovery that the leucine uptake kinetics were not constant led to the use of increased leucine concentration over time in order to achieve saturation. Higher leucine incubation concentrations could cause uptake by phytoplankton (Hietanen et al. 2002), but this would only lead to greater BP rates, not the observed decrease. Another change was that a base addition step was added to the processing to increase counting efficiency. Earlier samples were corrected (increased) for the lack of that step. Even without any corrections for processing or isotope dilution, the BP pattern remained the same and significant.

When examined by month, many of the environmental parameters, such as DOM, DIN, and phytoplankton biomass and productivity did not match the seasonal pattern seen in the temperature data. While there were differences between months, the lack of seasonality suggests that these factors were not controlled by temperature. Phosphate concentrations varied seasonally by month and were positively correlated with temperature. Phosphate concentrations are known to peak in summer due to a direct temperature effect on sediment remineralization rates or a change in sediment redox conditions (Day et al. 1989). Summer conditions in the NRPS are often characterized by

intermittent periods of water column stratification producing hypoxic or anoxic bottom waters, which in turn could affect sediment phosphate release.

Rates of BP by month matched the seasonality of the temperature pattern, providing strong evidence for the control of bacterial metabolism by temperature. The lack of correspondence between BP and most of the other parameters suggests that BP is not strongly controlled by potential resources such as phytoplankton, DOM, and nutrients, at least at the interannual and seasonal scale. This despite weak correlation between all those resource parameters and BP (Table 3.2). The correlation between BP and phosphate, however, could be simply a function of both being correlated with temperature. The lack of interannual and seasonal correspondence between BP and phytoplankton has been seen for some estuarine systems (Findlay et al. 1991; Ducklow and Shiah 1993; Staroscik and Smith 2004; Alonso-Sáez et al. 2008), while others report close coupling between BP and phytoplankton parameters (Cole et al. 1988; Hoch and Kirchman 1993; Goosen et al. 1997), but the number of studies with multi-year coverage is limited. It is clear that the relationship between BP and bacterial resources is complex and not discernible at interannual and seasonal scales.

The relationship between BP and temperature, however, is somewhat less complicated. It has long been known that biochemical processes are sensitive to changes in temperature and can be at times a limiting factor (Pomeroy and Wiebe 2001). Microbial metabolism and growth typically show a response represented by  $Q_{10}$  values of from two to three at optimum temperatures (Pomeroy and Wiebe 2001); a range which has become almost canonical. The apparent  $Q_{10}$  (Hoch and Kirchman 1993) determined for BP in the NRPS (2.35, 3–34 °C) was right in the middle of that range and temperature

explained about half of the variance in BP rates. This was similar to the relationships found in Narragansett Bay (Staroscik and Smith 2004), Chesapeake Bay (Shiah and Ducklow 1994a), Massachusetts salt marsh estuaries (Wright and Coffin 1983), and enrichment mesocosms (Hobbie and Cole 1984). Using the alternate Boltzmann formulation, the calculated activation energy of 0.63 eV for BP was remarkably similar to the predicted 0.62 eV from Gillooly et al. (2001) and the average of 0.63 eV reported by Brown et al. (2004). The activation energy for PP ( $0.16 \pm 0.11$  eV) did not match the 0.33 eV reported for terrestrial net primary productivity (Brown et al. 2004).

The microbial metabolism–temperature relationship in aquatic ecosystems is not always constant over a range of temperatures. Hoch and Kirchman (1993) found that for the Delaware Bay there was a distinct break and lowered slope in the plot of log-transformed specific growth against temperature at 12 °C. In the Chesapeake Bay, there is evidence that bacterial growth and production is limited only by temperature when temperatures are below 20 °C (Shiah and Ducklow 1994a). Apple et al. (2006) found a non-linear relationship between log-transformed BP and temperature, both for their study site in Monie Bay, MD and for a meta-analysis of nine different estuaries. Their results showed that temperature was a strong controlling factor of BP at lower temperatures, but beyond about 22 °C, BP ceased to change or even decreased with temperature. The possibility that a similarly variable BP–temperature relationship exists in the NRPS was tested by breaking the regression into two parts. While the high temperature slope was smaller, it was not significant, supporting the conclusion of a constant BP and temperature relationship over the range of temperatures studied. Staroscik and Smith (2004) also failed to find a break in the BP–temperature relationship, concluding that

Delaware Bay was not substrate limited in the summer. The same conclusion probably holds true for BP in the NRPS.

The evidence for the lack of a constant temperature relationship leads to the idea of a complex interaction between the control of bacterial metabolism by temperature and substrates (Pomeroy and Wiebe 2001; Apple et al. 2006). The search for this interaction in the NRPS began with multiple regression models that included temperature and several resource variables. The most parsimonious model using all the data identified DOC and PON concentrations as important factors in addition to temperature. Concentrations of DOC might correlate with bioavailable organic substrates, while PON might relate to substrates such as phytoplankton exudates or hydrolysates from abiotic particles. A significant proportion of BP was found associated with particles based on preliminary centrifugation experiments (data not shown). These kinds of substrates should control production in the absence of other limiting factors.

The positive regression coefficients for the DOC and PON indicate that at fixed levels of the other factors, BP varies positively with the substrates as would be expected. Despite the ecologically relevant parameters, the model explained only about 10 % more of BP variability than temperature alone. In the original model that included phytoplankton biomass, the coefficient for chlorophyll *a* was negative, which is a relationship not expected if autotrophic biomass is providing substrates for bacterioplankton. Since chlorophyll *a* and PON are strongly correlated, the biomass term was considered redundant. Using a subset (about 25 %) of the data that had cell abundance estimates, another model was identified using BA, POC, and chlorophyll *a* in addition to temperature. As before, chlorophyll *a* could be dropped from the model

without much loss in predictive power. Another indicator of particulate substrates, POC, was again important as was BA, but with a negative coefficient. Unlike other systems where BA correlates with BP (e.g. Staroscik and Smith 2004), BA was not correlated with BP in the NRPS, so the regression coefficient may reflect some indirect relationship. Also, the proportion of active cells may not be a constant through time or space (del Giorgio and Scarborough 1995). This last model did explain more than 80 % of the variation in BP, but the data used for the regression did not cover the same range of space and time as the full data set. The remaining unexplained variation in BP might be explained by top-down factors such as grazing or viral lysis (Noble and Fuhrman 2000), but those were beyond the scope of this study.

The data used to generate these models were collected over a long period with varying environmental conditions including several acute events. Tropical storms have increasingly impacted the study area since about 1996 (Paerl et al. 2006a) and this higher frequency of storms may continue in the future (Goldenberg et al. 2001). The storms that occurred during the study period had different characteristics that influenced their effect on the system. The only storm that had a noticeable impact on bacterioplankton was Hurricane Isabel. The highest BP value during the four years of study came a few days after Isabel. The high storm surge during this storm caused severe flooding along the banks of the Neuse River. The return of these flood waters to the river probably brought in enough particulate and dissolved organic matter to stimulate productivity. Sediment resuspension and increased discharge from storms have been documented as being responsible for BP increases (Cotner et al. 2000; Williams et al. 2008). Alternatively, the flood waters may have washed in an allochthonous population of bacteria that responded



well to the storm impacted estuary. Either way, the effect was short-lived and BP rates were back to normal within two weeks. The other storms in 2004 and 2005 did not seem to have any impact on the microbial community, save for a possible increase in PP after Hurricane Ophelia; it is not clear why this occurred with this low rainfall storm. Hurricane Charley did bring rains and some flooding, so it is possible there was some impact on the microbial community, but the post-storm sampling (about a week later) may have missed it.

Aside from the acute impact of tropical storms, yearly extremes in precipitation were another kind of event that affected the system. The drought of 2002 caused severely reduced river discharge, while the extensive precipitation during spring 2003 brought discharge to almost record levels. The result was less inter-station variability for BP in the wet year compared with the more dry 2002 and 2004. This could be a case of the extreme spring discharge reducing the salinity gradient over the same range of stations, thereby producing similar environmental conditions and less biological variability over the same spatial scale. An extreme case of this was seen in the 1999 floods from Hurricane Dennis and Floyd, when flood waters extended into Pamlico Sound (Peierls et al. 2003).

### **3.5 CONCLUSIONS**

A four-year, spatially extensive study of the NRPS system was used to evaluate the patterns and bottom-up controls of the resident bacterioplankton community. This rich and productive estuarine system was found to have high concentrations of bulk dissolved and particulate organic matter. The dissolved fraction varied with discharge, but showed little variation with temperature. A large part of the particulate fraction was

the planktonic microbial community itself and it showed little variation over seasonal or annual time scales. The dissolved nutrients showed some variation with time, with DIN variation probably related to discharge. Phosphate concentrations correlated with temperature and showed little variation across years. The phytoplankton community showed some change across years (chlorophyll *a*), but the seasonal patterns did not point to control by temperature.

The patterns for bacterioplankton were different from all of the resource parameters and it is unclear what parameters control interannual variations in BP. However, the productivity data were best matched with temperature, as has been seen elsewhere. Half of the variation in BP could be explained by temperature. Proxies for bacterial substrates improved the predictive power of multiple regression models, but much of the variation in productivity remains unexplained. Some of the variation could be just a function of the inherently complex nature of estuaries, including the impact of stochastic events such as storms. It is difficult to measure bacterial substrates *in situ*, so it is possible that this study was not able to tease out the complex interactions of temperature and substrates on microbial activity. Other sources for the unexplained variation could be top-down effects such as grazing and bacterial mortality. Further research that includes those top-down impacts as well as experimental studies on bottom-up controls will help refine the understanding of the planktonic microbial community in this estuarine system.

## **CHAPTER 4**

### **SPATIAL PATTERNS AND CONTROLS OF BACTERIOPLANKTON**

#### **4.1 INTRODUCTION**

An essential part of understanding microbial activity in any system is to determine the patterns of variation through space and time. Estuaries can be considered ecotonal ecosystems (Odum and Barrett 2005), forming the transition between inland and oceanic waters, and are typically characterized by great spatiotemporal variability. In particular, the mixing of water masses form strong chemical (i.e., salinity and nutrients), and biological gradients. Resident bacterioplankton exposed to these gradients will form varying patterns of activity and abundance through a combination of physical forces (e.g. tides, flushing, mixing), resource availability, and grazing or viral pressure.

Given that estuaries are considered some of the world's most productive ecosystems, there usually exists a trophic gradient that decreases as salinity increases from estuarine to oceanic systems (Day et al. 1989). Rates of bacterioplankton productivity (BP) have been shown to correlate positively with rates of primary productivity across many systems (Cole et al. 1988). Therefore, BP and bacterioplankton abundance (BA) would be predicted to show a decrease along the increasing salinity gradient in estuaries, either because of conservative mixing and loss of cells, or because of a parallel decrease in autochthonous or allochthonous resources along the salinity gradient.

Indeed, that is what many authors studying a range of systems have found. Palumbo and Fergusen (1978) found a linear decrease in BA with increasing salinity in the shallow, tidal Newport River estuary. This was also seen in the Fraser River (Bell and Albright 1981), and for both BA and bacterial activity in the St. Lawrence River (Painchaud et al. 1987; Painchaud et al. 1996). A decrease in BP and BA along a seaward transect was also reported for the Schelde (Goosen et al. 1997), Urdaibai (Revilla et al. 2000), Rhone (Troussellier et al. 2002), and Roskilde Fjord (Jensen et al. 1990) estuaries. In the York River, BP showed the same pattern, but BA increased with increasing salinity (Schultz et al. 2003).

Another spatial pattern that researchers have frequently reported is a mid-estuarine peak of abundance and/or activity. Systems including the Essex River (Wright and Coffin 1983), Chesapeake Bay (Ducklow et al. 2000), Delaware Bay (Kirchman and Hoch 1988), and Ria de Aveiro (Cunha et al. 2000) estuaries and the Mississippi River plume (Chin-Leo and Benner 1992) had peaks of BA and BP or activity at intermediate salinities relative to the estuarine gradient. Other systems have a positive correlation between bacterial measurements and salinity. This trend appeared in the lower Hudson River (Sañudo-Wilhelmy and Taylor 1999) and in Mobile Bay on occasion (McManus et al. 2004).

Christian et al. (1984) examined the Neuse River estuary, a shallow, microtidal, meso- to eutrophic coastal plain estuary, and found a similar increase in BP and BA with increasing salinity, although they did not cover the full salinity gradient. The Neuse River has been the subject of much research over the past several decades, in part because of a well-documented history of nuisance algal bloom, hypoxia/anoxia, and fish kill events

thought to be symptoms of eutrophication driven by human activities in the watershed (Paerl et al. 1998; Paerl 2006). Most of this research has focused on phytoplankton and water quality issues. The long-term monitoring program already in place in this estuary (ModMon; Luetlich et al. 2000; Paerl 2006) provided the opportunity to focus on the less-studied bacterioplankton community. Here, the results from a 4-year study of bacterioplankton in the Neuse River and Pamlico Sound (NRPS) estuarine system are used to describe and discuss the spatial patterns and potential controlling factors of BP and BA along the full salinity gradient and across depth. In particular, the question of bacterioplankton and phytoplankton coupling will be addressed.

## **4.2 METHODS**

Most of the methods used for this section were the same as for Chapter 3 and will not be repeated except where there are differences or additions. Station names and locations are indicated in Figure 3.1.

### **4.2.1 FIELD MEASUREMENTS AND WATER COLLECTION**

Profiles of basic water quality characteristics were collected at each station visit using a YSI 6600 sonde (Yellow Springs, OH) configured to measure temperature, salinity, dissolved oxygen (DO), pH, and chlorophyll fluorescence. Sensors were calibrated prior to the sampling date, except DO, which was calibrated in the field and checked throughout the run. Readings were collected at 0.5 m intervals starting at the surface and continuing until just off the bottom. River discharge data came from USGS Gage No. 02091814 near Ft. Barnwell, NC ([waterdata.usgs.gov/nc/nwis](http://waterdata.usgs.gov/nc/nwis)) and annual averages were based on calendar year.

At each station, water was collected from the surface and near bottom levels. Surface samples were collected by submerging cleaned (dilute acid and deionized water) and sample-rinsed polyethylene containers 10 to 20 cm below the water surface. Subsurface samples were collected with a horizontal Van Dorn collector. The device was lowered to approximately 0.5 m above the sediment surface and, when required, to the approximate depth of the pycnocline determined from salinity profiles. Samples were transferred to cleaned and sample-rinsed polyethylene containers. All samples were kept covered during transport to the laboratory. In addition to the long term sampling, the Neuse River between stations NR0 and NR120 (Figure 3.1) was sampled four times over two weeks in June 2005 as part of an exercise to track estuarine algal biomass at a smaller scale. The locations were chosen so that the station group at each time point was centered on the local surface chlorophyll *a* maximum (Paerl et al. 2007), with the upstream and downstream locations spaced between 5 and 10 km from the center.

#### **4.2.2 LAB AND DATA ANALYSES**

Chromophoric dissolved organic matter (CDOM) was determined fluorometrically on glass fiber (Whatman GF/F) filtrate stored at 4 °C. Samples were analyzed using a Turner Designs TD700 fluorometer configured with a near-UV mercury vapor lamp, a 350 nm excitation filter, and a 410-600nm emission filter. The fluorometer was calibrated with solutions of quinine sulfate made up in 2N sulfuric acid.

Correlations were done using the non-parametric Spearman's rank correlation test. Paired group comparisons were done using the non-parametric Wilcoxon rank sum test. Comparisons of more than two groups were made using the non-parametric Kruskal-Wallis rank sum test. Analysis of covariance (ANCOVA) was used to examine the effect

of a factor on regression models of continuous variables. Fits of the data with and without the interaction term were analyzed for differences by ANOVA. For all tests the significance level was  $\alpha = 0.05$ . Rates of BP were normalized (Goosen et al. 1997) to 20 °C using a  $Q_{10}$  of 2.35, calculated from the exponent in an exponential fit of BP against temperature (Chapter 3). Spatial coherence was determined by comparing the trend pattern along the property–salinity plot for each sampling date. The trend pattern was specified by slope (positive, negative, or no change) for each of the three segments on each transect; a non-zero slope was scored when there was no overlap in adjacent 95 % confidence intervals. Daily volumetric productivity rates were calculated by assuming a constant rate throughout the day and day length of 24 and 10 hours for bacterioplankton and phytoplankton productivity, respectively. All analysis and plotting was done using S-Plus version 7.0 (Insightful Corp.).

## **4.3 RESULTS**

### **4.3.1 SUMMARIES BY STATION**

Surface temperature in the Neuse River and Pamlico Sound followed a typical seasonal pattern, but did not vary by station ( $p > 0.99$ ). Surface salinity consistently showed a strong increasing gradient along the length of the river and into the sound (Figure 4.1). The steepness of the gradient decreased at the last two sound stations, which had very similar salinity characteristics. Stratification, as measured by  $\Delta$  salinity, did not show a monotonic trend and mid-estuarine station NR120 showed the highest median value, although the ranges from the adjacent stations overlapped. Both DO and pH showed a similar pattern across stations, namely NR0 having noticeably lower DO and pH than all the other stations (Figure 4.2). The next two downstream stations had median

DO greater than 100 % saturation and median pH greater than 8. Median DO and pH decreased slightly moving further downstream.

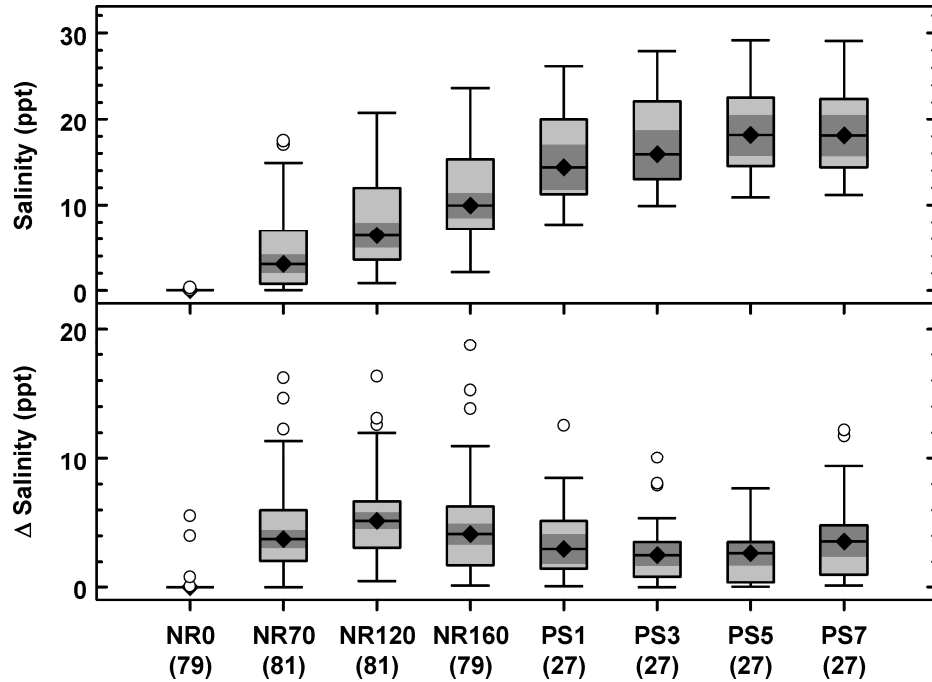


Figure 4.1 Surface salinity and  $\Delta$ salinity by station in NRPS during 2002-2005.  $\Delta$ salinity is the difference between near bottom and surface salinity. Value below station label is number of samples. Solid diamond is the median, light grey box is the interquartile range (IQR), and whiskers are drawn to the last value within the span from the quartiles ( $1.5 \times \text{IQR}$ ). Values outside of the span are considered outliers and are indicated by open circles. The dark grey box indicates 95% confidence intervals around the median.



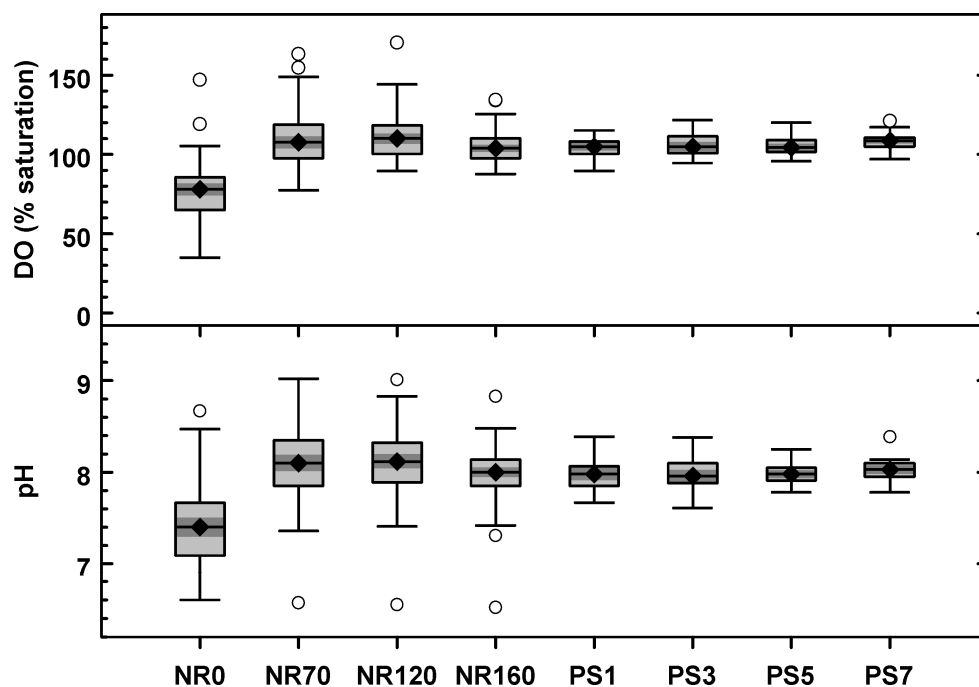


Figure 4.2 Surface dissolved oxygen percent saturation (DO, top) and pH (bottom) by station in NRPS during 2002-2005. Symbols as in Figure 4.1

Dissolved organic carbon (DOC) concentrations differed by station ( $p < 0.0001$ ) and generally decreased with increasing salinity, except between the first two stations (Figure 4.3). Median DOC concentrations ranged from 363 to 622  $\mu\text{mol L}^{-1}$  with the peak at station NR70, although the adjacent station medians were not different based on confidence limits. Dissolved organic nitrogen (DON) concentrations exhibited the same pattern except for the lack of a peak at NR70. Both DOC and DON showed less variability (indicated by the interquartile range and span) in the sound than in the river stations. The ratio of DOC to DON, a measure of dissolved organic matter quality, did differ by station ( $p < 0.0001$ ), but it was within a fairly small range (median ratio 20 to 25; Figure 4.4). Chromophoric dissolved organic matter (CDOM), the optically active fraction of organic matter, showed a trend similar to the decrease in DOC with increasing salinity, at least for the stations at which measurements were made.

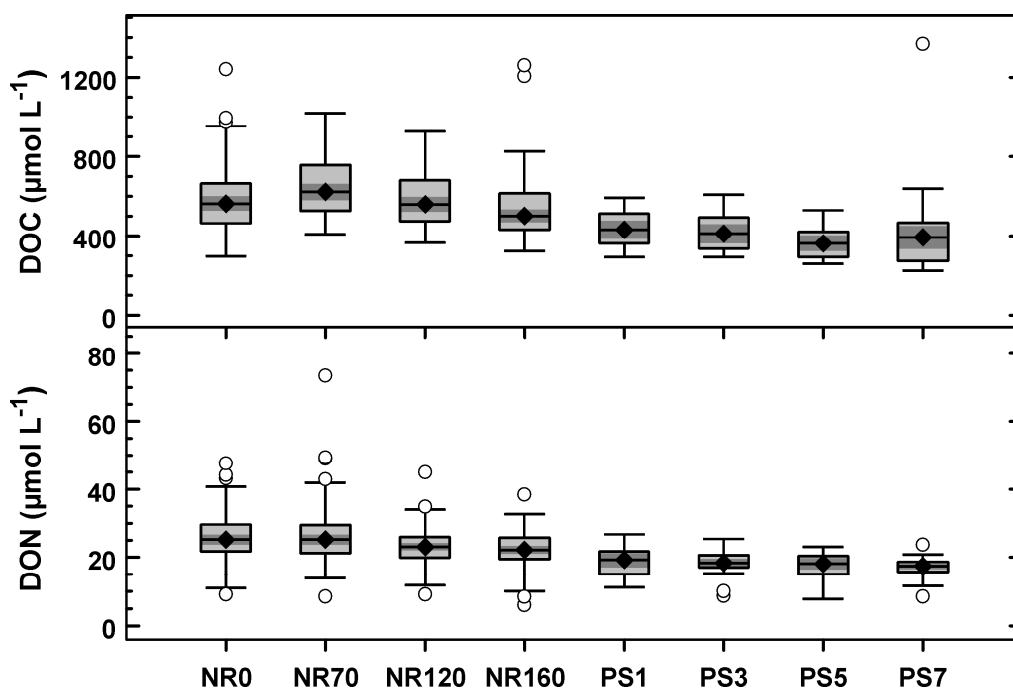


Figure 4.3 Surface dissolved organic carbon (DOC, top) and dissolved organic nitrogen (DON, bottom) in  $\mu\text{mol L}^{-1}$  by station in NRPS during 2002–2005. Symbols as in Figure 4.1.

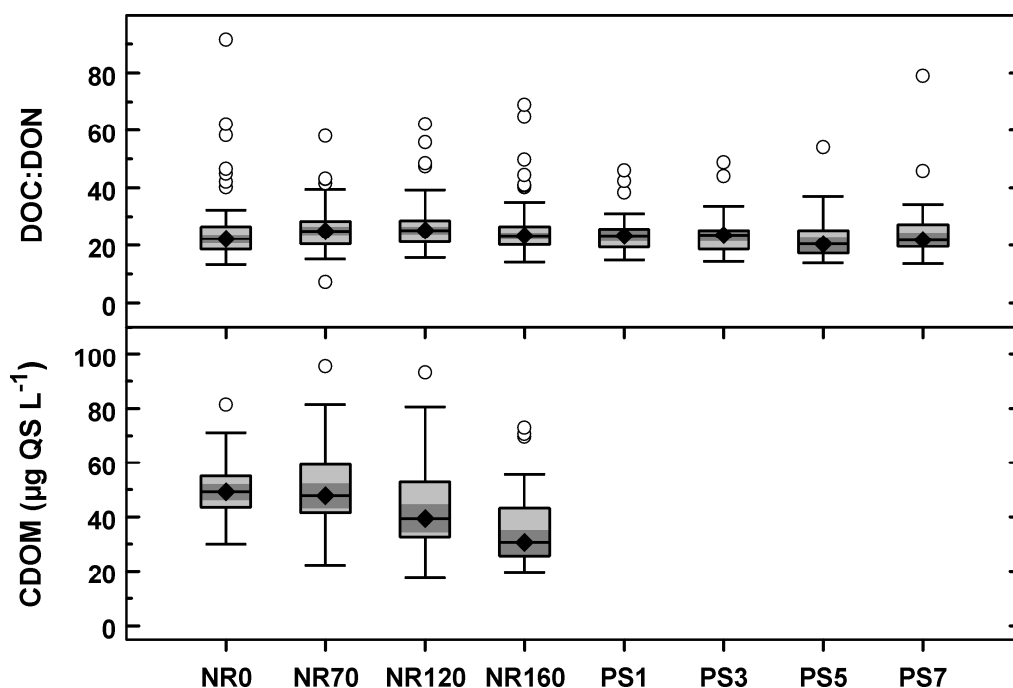


Figure 4.4 Surface DOC to DON ratio (molar, top) and chromophoric dissolved organic matter (CDOM) in  $\mu\text{g quinine sulfate L}^{-1}$  (QS, bottom) by station in NRPS during 2002–2005. Symbols as in Figure 4.1.

The overall spatial pattern for surface water dissolved inorganic nitrogen (DIN) concentration was one of rapid decrease, going from a median value of about 40  $\mu\text{mol L}^{-1}$  to about 1  $\mu\text{mol L}^{-1}$  throughout the lower river and sound stations (Figure 4.5). Variability was high at the two upstream stations, and became dramatically less variable starting at station NR120. Inorganic phosphorus (P), measured as phosphate, showed a more moderate decline in median values from about 1  $\mu\text{mol L}^{-1}$  at the freshwater end to less than 0.2  $\mu\text{mol L}^{-1}$  in the sound stations. Phosphate variability was more constant over the stations, although the Pamlico Sound stations were less variable than the Neuse River stations. Inorganic N to P ratios were greater than 16:1 at station NR0 and were mostly below that throughout the rest of the system.

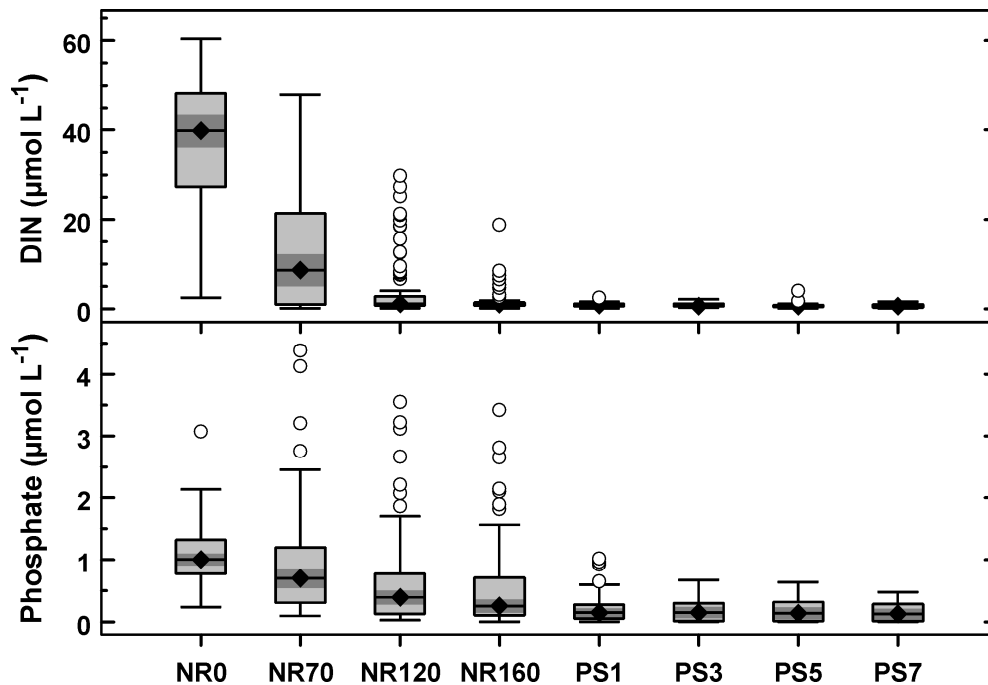
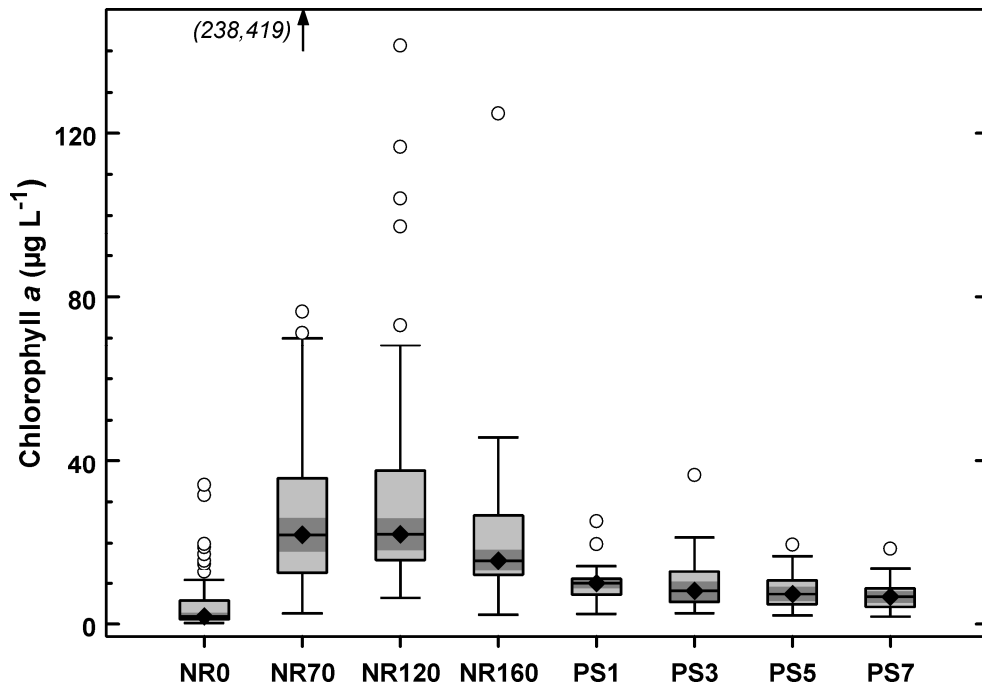


Figure 4.5 Surface dissolved inorganic nitrogen (DIN, top) and phosphate (bottom) in  $\mu\text{mol L}^{-1}$  by station in NRPS during 2002-2005. Symbols as in Figure 4.1

Phytoplankton biomass, estimated by chlorophyll *a* concentrations, exhibited a nonlinear pattern when the data was grouped by station (Figure 4.6). Concentrations and variability peaked in the region of stations NR70 and 120 and decreased downstream. Concentrations at NR0 were typically lower than at all other stations. The spatial pattern for the biomass data was closely matched by the pattern for particulate organic carbon and nitrogen (POC & PON; Figure 4.7) and phytoplankton productivity (PP, Figure 4.8); this reinforced the finding of strong correlations between those variables (Chapter 3). As was found for chlorophyll *a*, variability tended to be greatest at the stations with largest medians, NR70 and 120. The ratio of POC to PON (not shown) was different by station ( $p = 0.0002$ ), but not when NR0 was left out of the comparison ( $p = 0.10$ ). Median POC to PON ratio was higher at NR0 and this was significant in a two-group comparison ( $p < 0.0001$ ).



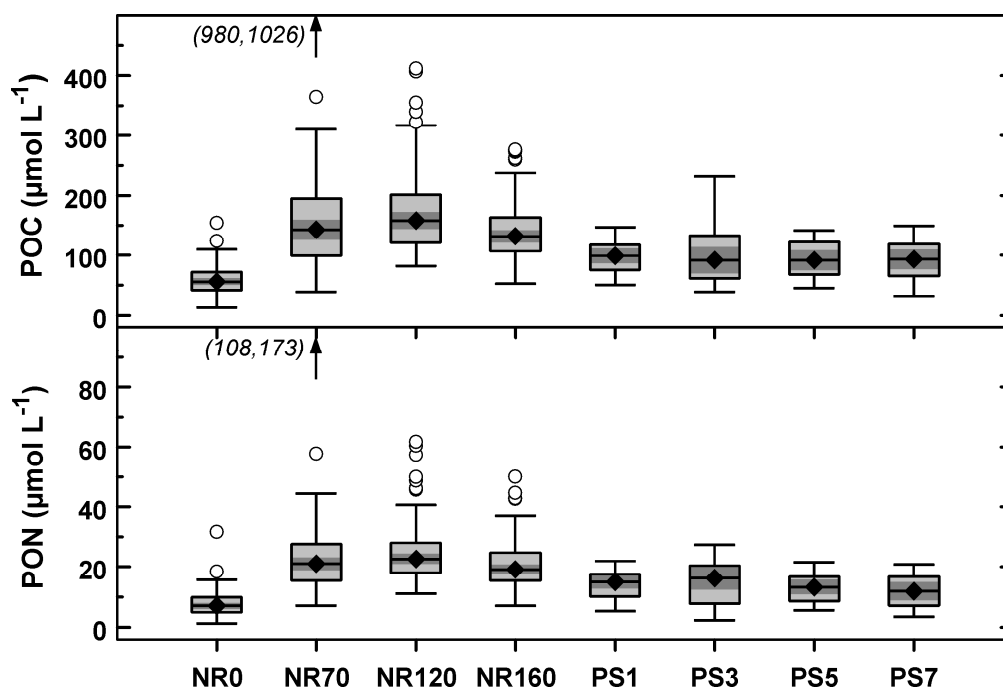


Figure 4.7 Surface particulate organic carbon (POC, top) and nitrogen (PON, bottom) in  $\mu\text{mol L}^{-1}$  by station in NRPS during 2002-2005. Outliers at station NR70 indicated by values next to arrows. Symbols as in Figure 4.1.

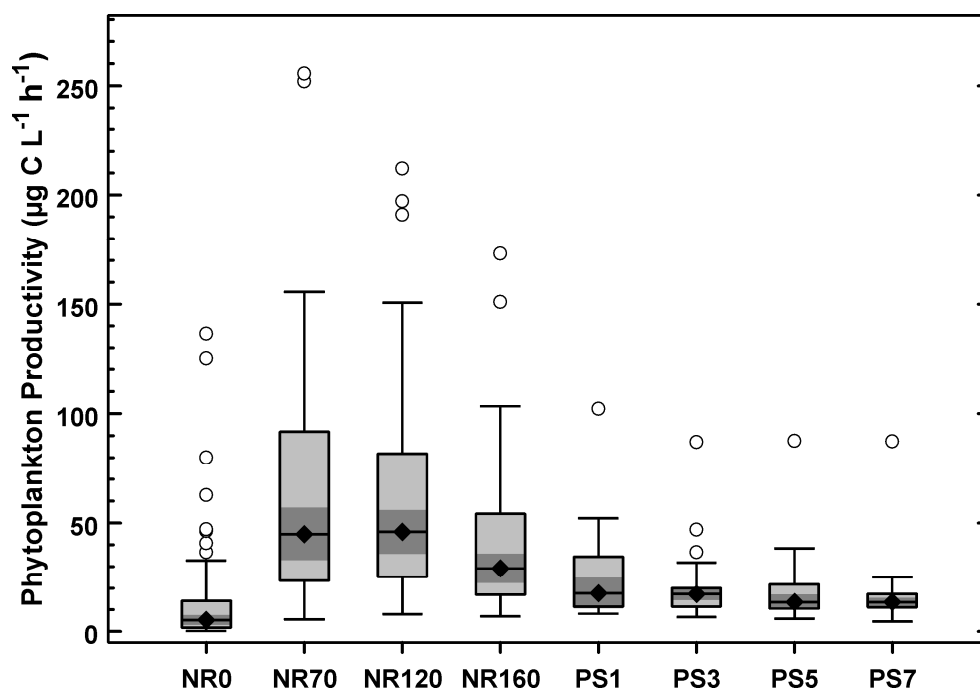


Figure 4.8 Surface phytoplankton productivity in  $\mu\text{g C L}^{-1} \text{ h}^{-1}$  by station in NRPS during 2002-2005. Symbols as in Figure 4.1.

The spatial pattern for BA appeared to be curvilinear with a peak in the lower river, but the Pamlico Sound stations did not have enough values to make the pattern clear or significant ( $p = 0.14$ ; Figure 4.9). Considering only the Neuse River stations, the difference by station becomes more clear ( $p = 0.055$ ). The pattern for BP was also curvilinear across space with a peak in median values at NR120 (Figure 4.10), although the large confidence limits around the medians prevent clear distinction of adjacent values. Within-station variation for BP was high (station spans were as much as  $10 \mu\text{g C L}^{-1} \text{ h}^{-1}$ ), but this was not constant over the system and Pamlico Sound sites exhibited lower within-station variation. When BP was normalized to  $20^\circ\text{C}$  ( $\text{BP}_{20}$ ) in order to eliminate variability due to temperature, the distribution of data by station looked quite similar to the uncorrected distribution, except the within-station variability was lower (Figure 4.11). Both patterns for BP resembled those for phytoplankton and particulate organic matter (POM); BP showed weak, but significant correlations with particulate variables ( $\rho = 0.23$  to  $0.34$ ,  $p < 0.0001$ ).

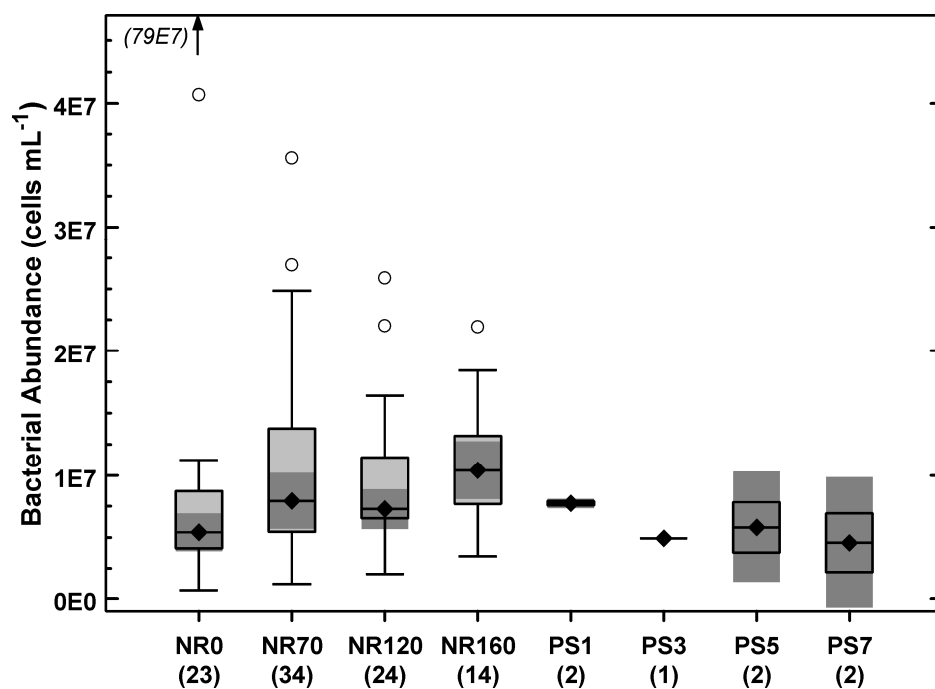


Figure 4.9 Surface bacterioplankton abundance in cells mL<sup>-1</sup> by station in NRPS during 2002-2005. Outlier at station NR0 indicated by arrow. Symbols as in Figure 4.1. Note that Pamlico Sound stations are based on only one or two data points.

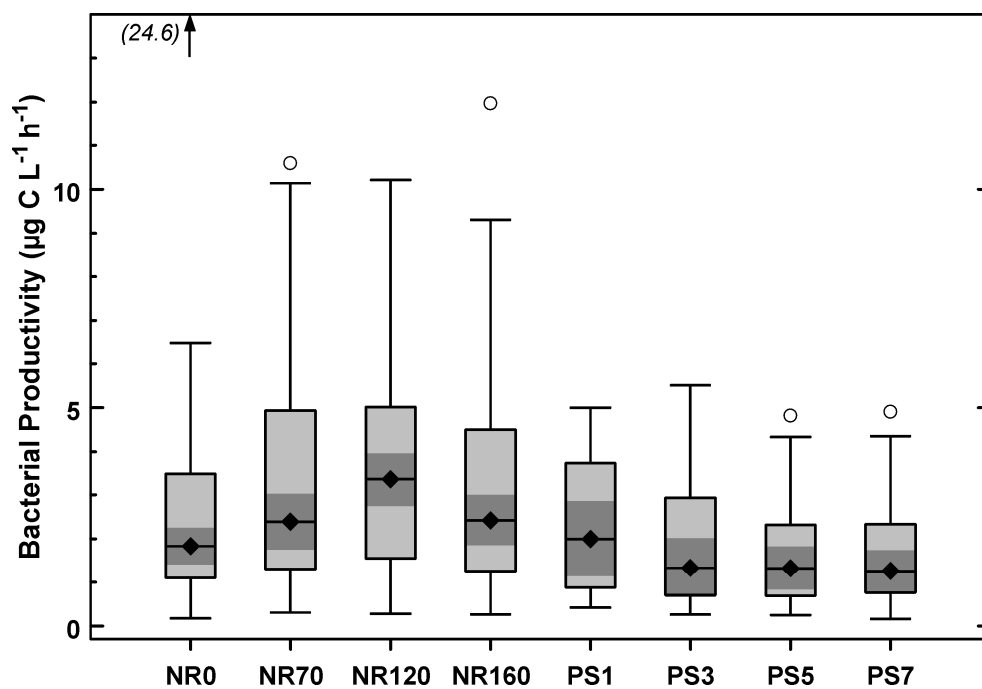


Figure 4.10 Surface bacterioplankton productivity in µg C L<sup>-1</sup> h<sup>-1</sup> by station in NRPS during 2002-2005. Outlier at station NR0 indicated by arrow. Symbols as in Figure 4.1.

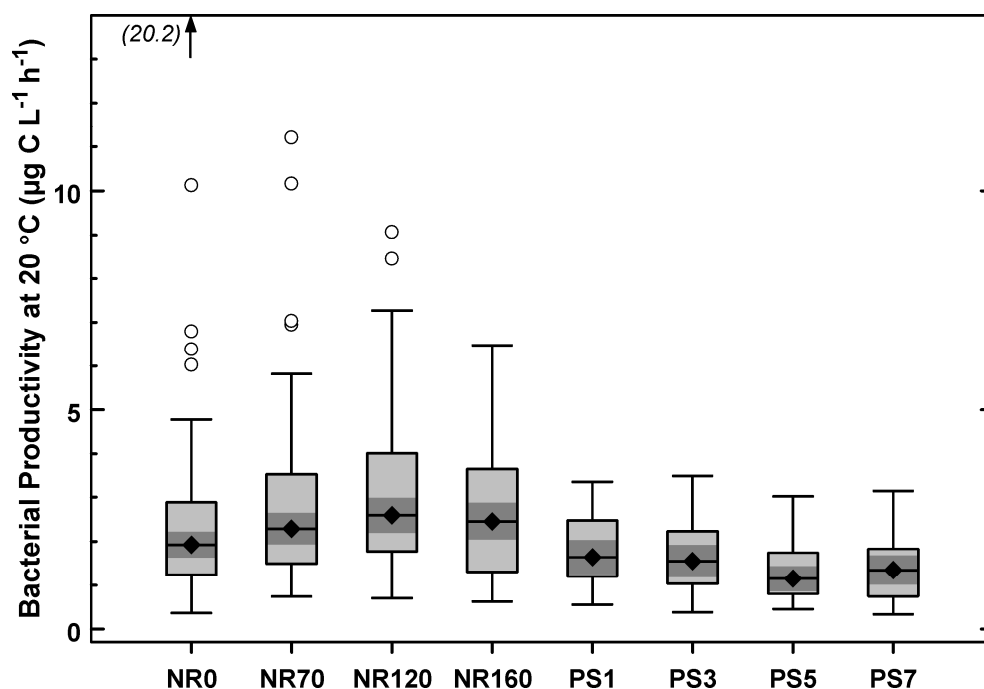


Figure 4.11 Surface bacterioplankton productivity normalized to 20 °C in  $\mu\text{g C L}^{-1} \text{h}^{-1}$  by station in NRPS during 2002-2005. Outlier at station NR0 indicated by arrow. Symbols as in Figure 4.1.

### 4.3.2 EFFECT OF DISCHARGE

The location of peak productivity varied by year, especially between 2002 and 2003. The major difference between years was discharge, which averaged 73.3, 184, 102, and  $82.6 \text{ m}^3 \text{s}^{-1}$  for 2002, 2003, 2004, and 2005, respectively. Peak median BP was at NR70 in 2002, a very dry year (Figure 4.12). The next year proved to be above normal discharge ( $124 \text{ m}^3 \text{s}^{-1}$ , 10-year mean) and the peak in BP appeared to move downstream to NR 120 and 160, although the difference by station was not significant at the chosen level ( $p = 0.09$ ). In 2004, peak median BP was at NR120, but high variability again obscured the difference by station ( $p = 0.68$ ). The same held true for 2005 ( $p = 0.21$ ), but the apparent peak in BP was at station NR70 during this dry year. The same movement of peak productivity with varying annual discharge was seen in the yearly PP spatial patterns as well (Figure 4.13). Each of the yearly distributions by station was



significantly different ( $p < 0.001$ ). The pattern in DOC concentration by station did not appear to change with varying discharge, although the overall levels of DOC were higher in 2003 than 2002 (Figure 4.14).

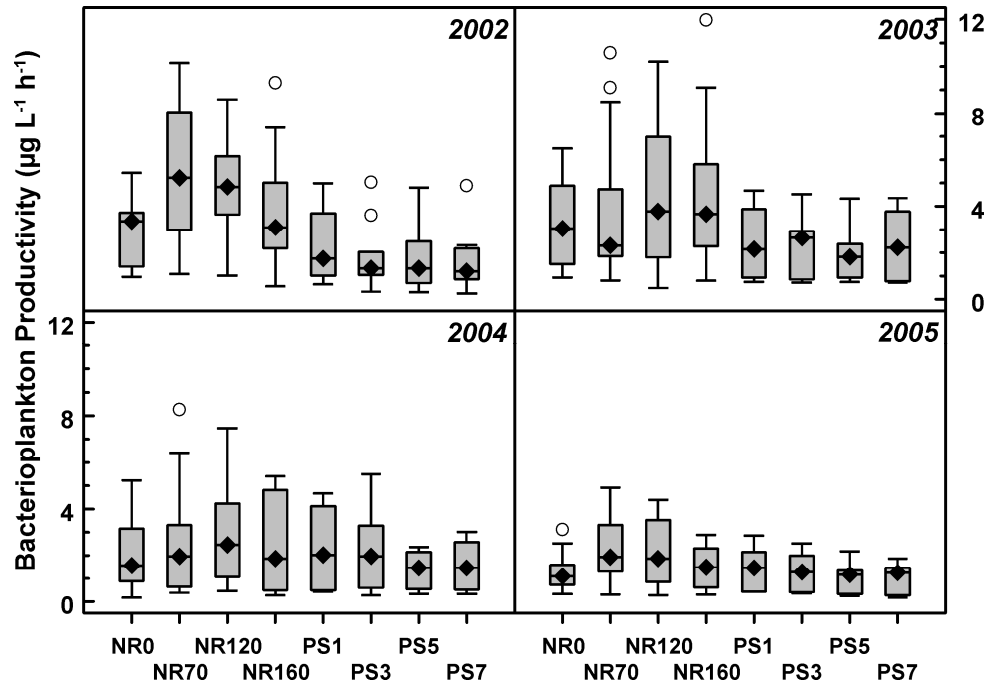


Figure 4.12 Surface bacterioplankton productivity in  $\mu\text{g C L}^{-1} \text{ h}^{-1}$  by station and year in the NRPS. Symbols as in Figure 4.1, except 95% confidence limits are not shown. Vertical scale limit is less than maximum value of 24.6

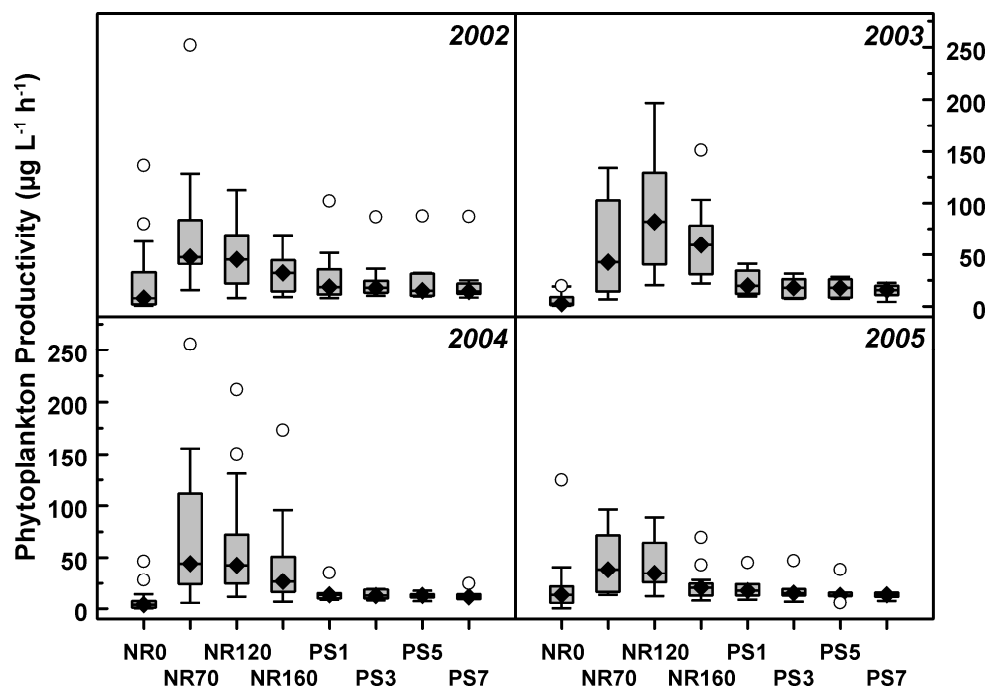


Figure 4.13 Surface phytoplankton productivity in  $\mu\text{g C L}^{-1} \text{ h}^{-1}$  by station and year in the NRPS. Symbols as in Figure 4.12.

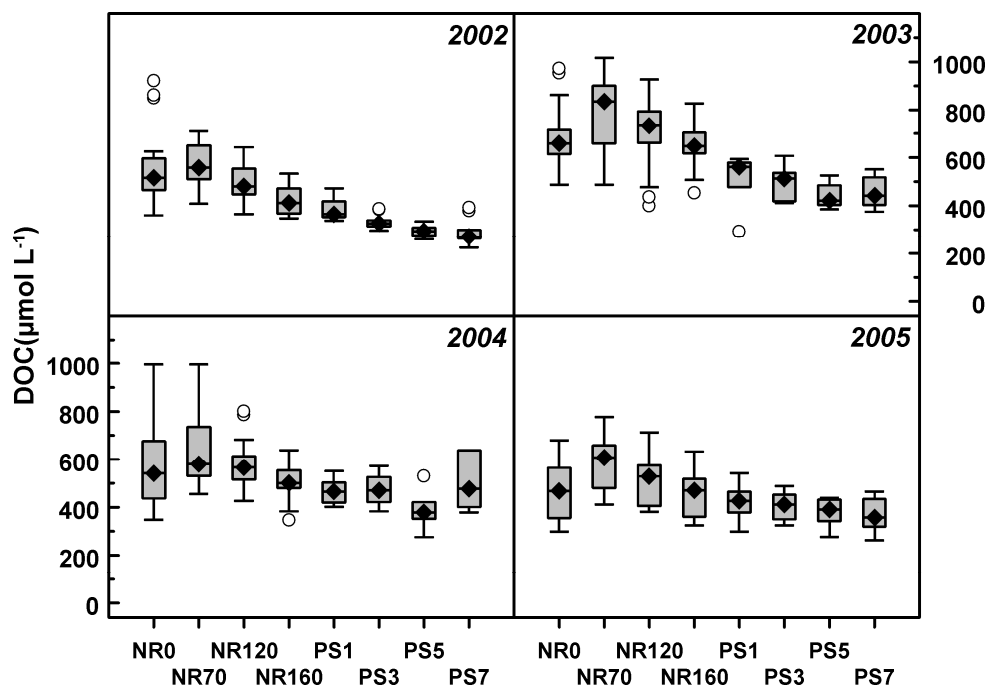


Figure 4.14 Surface DOC concentrations in  $\mu\text{mol L}^{-1}$  by station and year in the NRPS. Symbols as in Figure 4.12.

### 4.3.3 PROPERTY–SALINITY RELATIONSHIPS

Since salinity varies predictably across space, all measured variables were tested for correlation against salinity. Dissolved components showed a strong negative correlation with salinity (Table 4.1), while particulate components had only slight positive or no correlation with salinity. Salinity was not correlated with BP, but there was a slight negative correlation when BP was normalized to 20 °C (BP<sub>20</sub>). These correlation results mostly confirmed the spatial patterns shown in the previous sections.

Table 4.1 Correlation with salinity for measured chemical and biological variables. BP<sub>20</sub> is BP normalized to 20 °C. Coefficient is from the Spearman's rank correlation test.

| Variables        | Coefficient ( $\rho$ ) | p       | n   |
|------------------|------------------------|---------|-----|
| DOC              | -0.64                  | < 0.001 | 422 |
| CDOM             | -0.62                  | < 0.001 | 151 |
| DIN              | -0.72                  | < 0.001 | 426 |
| PO <sub>4</sub>  | -0.46                  | < 0.001 | 422 |
| POC              | 0.16                   | < 0.001 | 426 |
| PON              | 0.14                   | 0.0033  | 420 |
| Chla             | 0.03                   | 0.48    | 426 |
| PP               | 0.09                   | 0.059   | 425 |
| BA               | 0.20                   | 0.046   | 102 |
| BP               | 0.03                   | 0.53    | 428 |
| BP <sub>20</sub> | -0.12                  | 0.014   | 428 |

The property–salinity relationships for BP, PP, chlorophyll *a*, DOC, and POC were examined at the scale of individual research trips and compared with each other. Spatial coherence was considered to exist if the four station trend pattern for each variable against salinity matched on a particular date. When spatial coherence occurred between BP and other variables, it was often for only one variable as shown for PP (Figure 4.15) and DOC (Figure 4.16). On 26% of the 105 individual transects, BP

showed coherence with at least one variable; about 40 % of those transects had more than one variable matching at the same time. Property–salinity patterns for BP matched PP, chlorophyll *a*, DOC, and POC patterns 9, 16, 5, and 10 % of the time, respectively. When the pattern matching criterion was relaxed to include transects with at least two of three trends the same, the percentage of sampling dates showing coherence increased to 50 %, with individual variable matches increasing to between 16 and 31 %. BP showed partial coherence with DOC, but not PP or chlorophyll *a* (not shown), four days after category 2 Hurricane Isabel rapidly moved over the system, bringing 4 to 10 feet of storm surge (Figure 4.17).

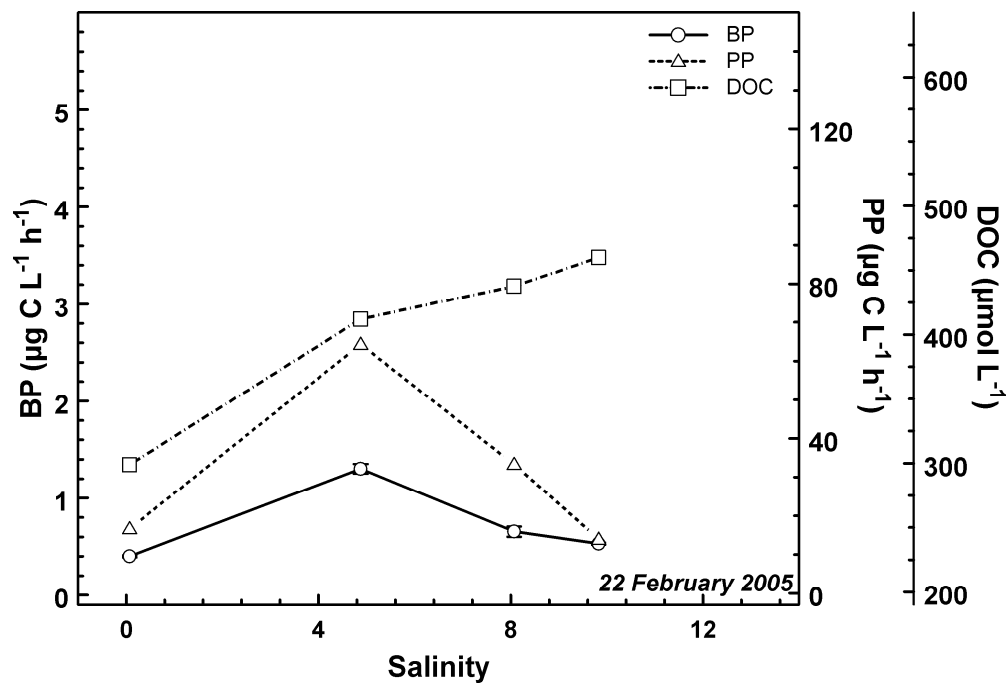


Figure 4.15 Property–salinity plot for bacterioplankton productivity (BP), phytoplankton productivity (PP), and DOC on 22 February 2005, units as before. Error bars for BP when visible indicate the 95% confidence interval around the mean.

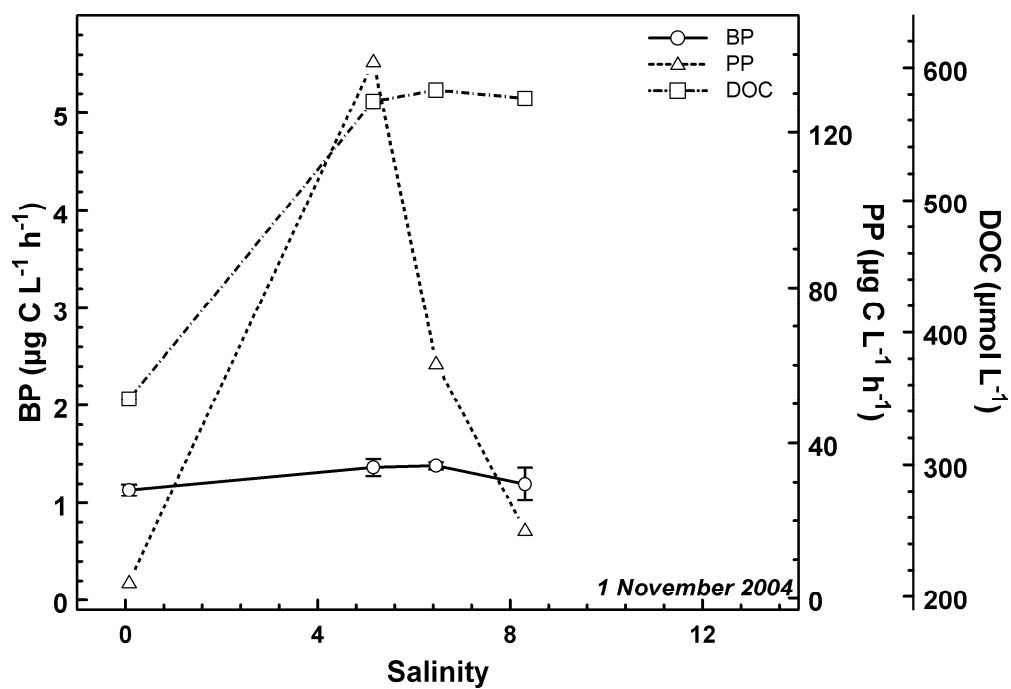


Figure 4.16 Property-salinity plot on 1 November 2004. All else as in Figure 4.15

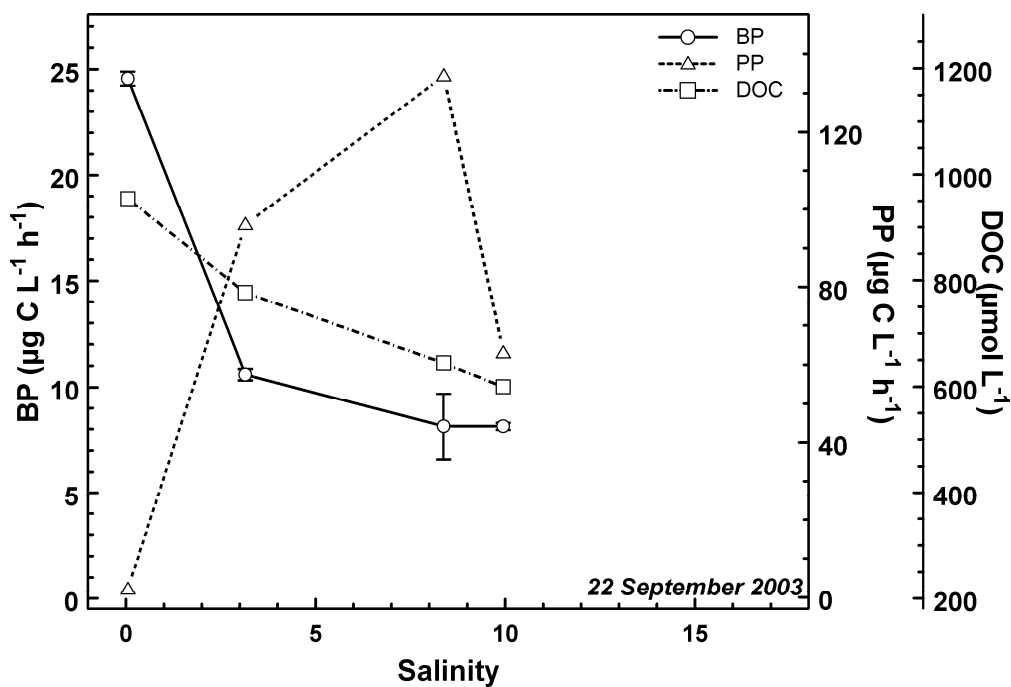


Figure 4.17 Property-salinity plot on 22 September 2003, four days after Hurricane Isabel crossed the system. Note change in BP and DOC scale. All else as in Figure 4.15

#### 4.3.4 EFFECT OF LOCATION

To examine the impact of space on the controls of BP, ANCOVA was used to determine the effect of station on the relationships between BP and other variables. Stations were considered independently or were grouped into freshwater (NR0) and marine (all others) stations. Individual stations had an effect on the regression slopes of BP versus chlorophyll *a* ( $p = 0.03$ ) and DIN ( $p = 0.0002$ ). The two station groups produced a significant interaction for temperature ( $p = 0.006$ ), DIN ( $p = 0.001$ ), chlorophyll *a* ( $p = 0.0004$ ), and PP ( $p = 0.008$ ), although only temperature explained any more than about 10 % of the variance in BP. The slope of BP on temperature for the freshwater station was lower than the slope for the marine stations (Figure 4.18). Group-wise  $Q_{10}$  values were 1.87 and 2.49 for fresh and marine station, respectively. To further investigate the difference by station, the most parsimonious multiple regression model using all the data (see Chapter 3) was fit using data from each station (Table 4.2). The temperature coefficient for NR0 was lower than for the other stations, although this was only significant ( $> 95$  % conf. limit) at NR160. Also, the coefficient for DOC was much higher for NR0 than for the other locations, none of which were different from zero. This means that for a given temperature, BP increased with increasing DOC only at NR0. Along the same lines, PON had the largest effect on BP at NR 70 assuming all else was fixed.

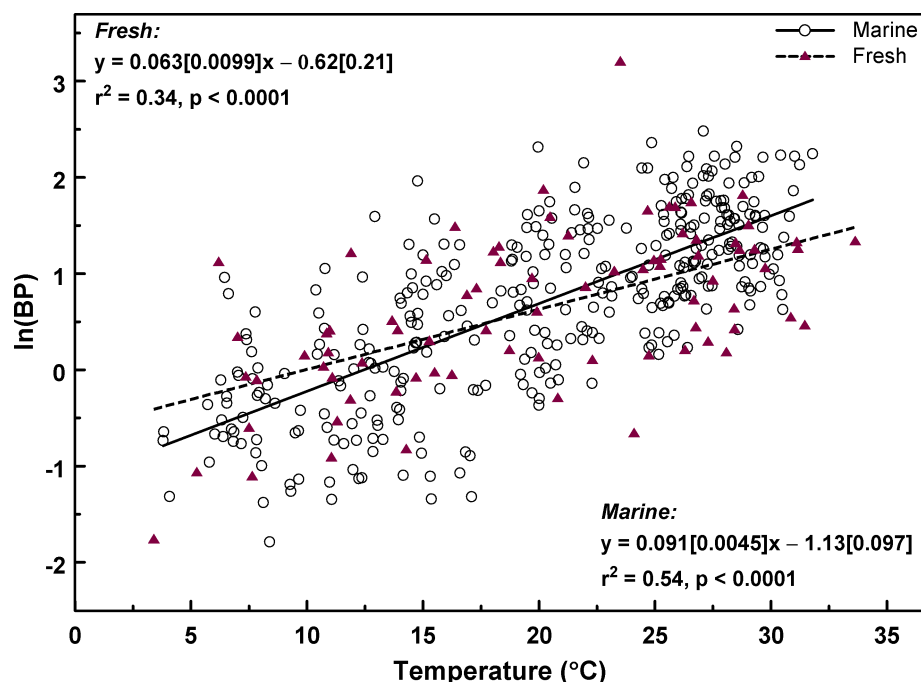


Figure 4.18 Linear regression of natural log-transformed surface BP versus temperature in the NRPS during 2002-2005. Symbols indicate either the freshwater station (NR0, triangles and dashed line) or the marine stations (all others, open circles and solid line). Bracketed numbers in equations are coefficient standard errors.

Table 4.2 Results of multiple regression analysis by station with BP as the response factor. Fitted model is  $\ln BP = B_0 + B_1 \text{Temp} + B_2 \ln \text{DOC} + B_3 \ln \text{PON}$ . Coefficients significantly different from zero are indicated with \* ( $p < 0.05$ ) or \*\* ( $p < 0.001$ ).

| Station | $B_0$  | $B_1$   | $B_2$ | $B_3$ | $r^2$ |
|---------|--------|---------|-------|-------|-------|
| NR0     | -8.8** | 0.058** | 1.2** | 0.22  | 0.54  |
| NR70    | -3.6   | 0.092** | 0.18  | 0.45* | 0.61  |
| NR120   | -3.0   | 0.086** | 0.26  | 0.19  | 0.58  |
| NR160   | -5.0*  | 0.10**  | 0.53  | 0.15  | 0.65  |
| PS1     | -3.3   | 0.089** | 0.30  | 0.072 | 0.69  |
| PS3     | -6.1   | 0.094** | 0.68  | 0.18  | 0.72  |
| PS5     | -4.3   | 0.086** | 0.40  | 0.18  | 0.66  |
| PS7     | -4.3*  | 0.090** | 0.33  | 0.27  | 0.67  |

#### 4.3.5 VERTICAL SCALE VARIABILITY

For a selection of stations and dates, both surface and bottom samples were collected. Bottom BP ranged from 0.6 to almost 12  $\mu\text{g C L}^{-1} \text{ h}^{-1}$  (median = 5.4). Median surface BP for the same locations and times was 3.3  $\mu\text{g C L}^{-1} \text{ h}^{-1}$ . The difference between bottom and surface was tested using a non-parametric comparison test ( $H_a: \mu > 0$ ) and was found to be significant ( $p = 0.042$ ,  $n = 31$ ). The only variables to have similar difference between surface and bottom were nutrient concentrations (DIN:  $p = 0.002$ ;  $\text{PO}_4$ :  $p = 0.03$ ;  $n = 31$ ). Surface DOC concentrations were higher than bottom concentrations ( $p = 0.025$ ;  $n = 31$ ).

The vertical structure of BP was examined in more detail during four sampling trips in June 2005 (Figure 4.19). Discrete depth profiles of BP showed that bottom and pycnocline samples often had greater rates than surface samples and the high rates sometimes corresponded with peaks in chlorophyll fluorescence (Figure 4.20). Rates of BP at depth were greater than surface rates in 6 out of 11 instances for pycnocline samples and 8 out of 12 instances for bottom. The difference appeared to be related to stratification as there were more positive differences between depth and surface rates with greater  $\Delta\text{salinity}$  (Figure 4.21). Productivity was also correlated with POC at depth ( $\rho = 0.59$ ,  $p = 0.0056$ ,  $n = 23$ ), but not in surface samples (Figure 4.22).



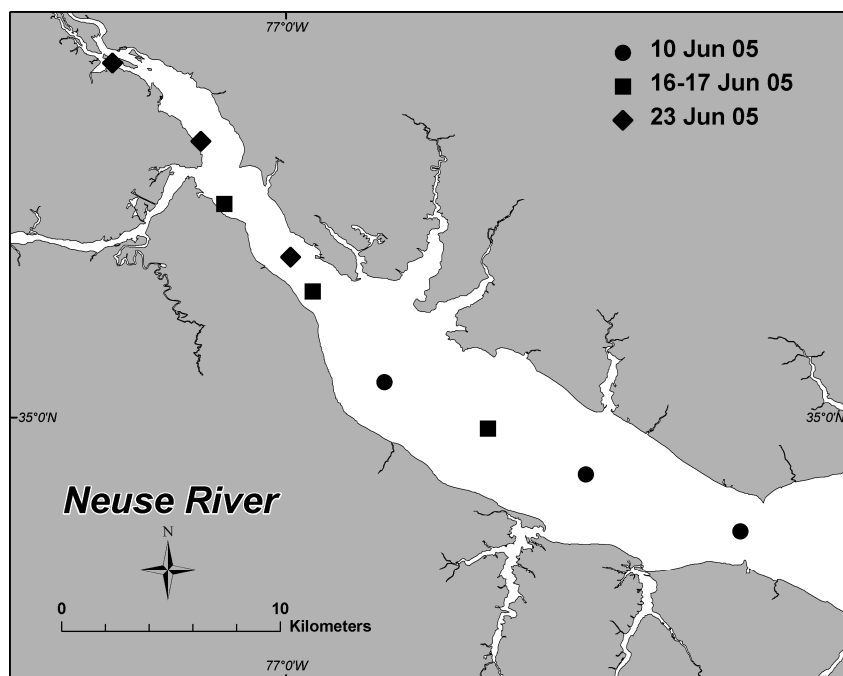


Figure 4.19 Location by date of BP profiles in Neuse River. The middle station of each grouping by date is the location of the chlorophyll maximum. The profiles collected 16–17 June were in the same location for a day and night sampling.

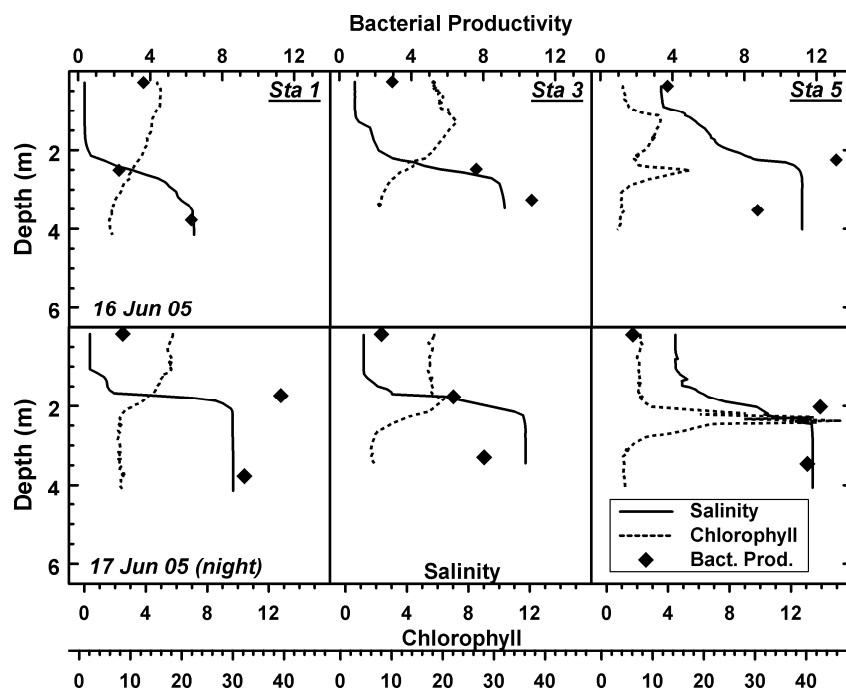


Figure 4.20 Vertical profiles of BP ( $\mu\text{g C L}^{-1} \text{h}^{-1}$ ), salinity (ppt), and in vivo chlorophyll fluorescence ( $\mu\text{g L}^{-1}$ ) at three stations in the Neuse River estuary on 16–17 June 2005 at mid-morning and just past midnight. Station 3 was at the location of the chlorophyll maximum for the estuary and Stations 1 and 5 were located upstream and downstream, respectively, from Station 3.

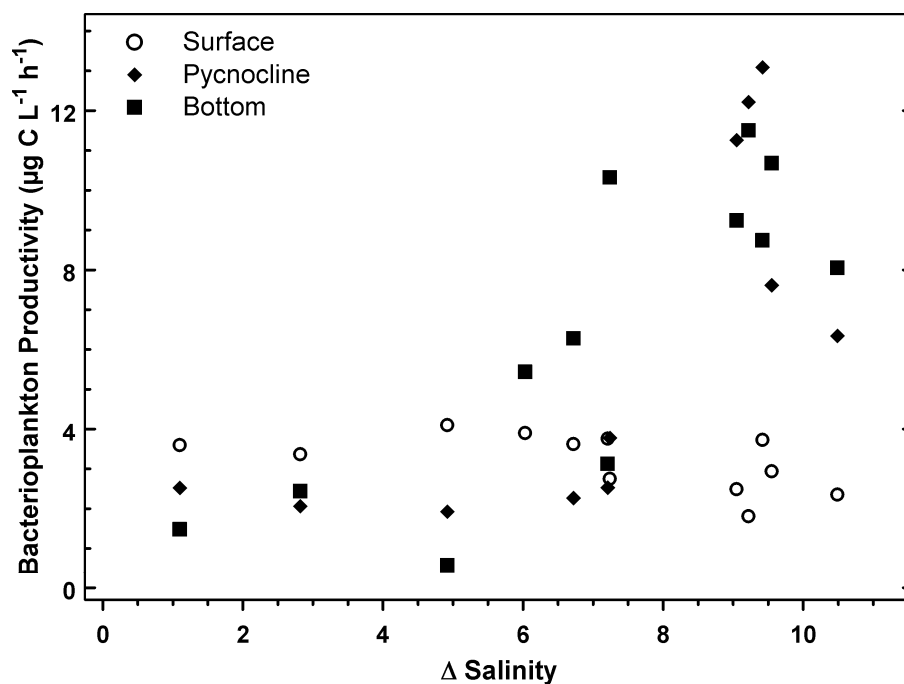


Figure 4.21 Comparison of BP versus  $\Delta$ salinity (bottom minus surface) in 12 vertical profiles in the Neuse River estuary during June 2005. Symbol type indicates sample depth location.

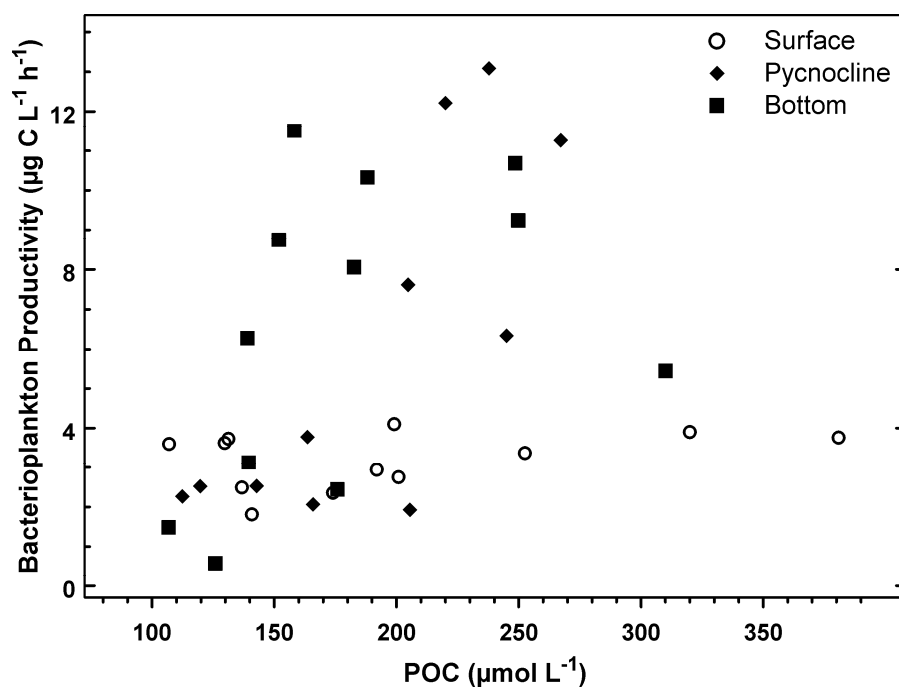


Figure 4.22 Comparison of BP versus POC in 12 vertical profiles in the Neuse River estuary during June 2005. Symbols as for Figure 4.21

#### 4.3.6 CROSS SYSTEM COMPARISON

Average station values for surface daily BP and PP were compared to the cross system analysis of Cole et al. (1988). The values for this study fell outside the confidence limits (calculated from data in their Table 2 and not shown in the original figure), but within the prediction limits for the log-log regression line based on all marine and freshwater data, excluding their validation set (Figure 4.23). The slope of the line through the points from this study, excluding the most upstream station (NR0), was similar to the slope for the Cole et al. regression ( $0.599 \pm 0.063$  vs.  $0.804 \pm 0.103$ , slope  $\pm$  SE). The same comparison was made for the relationship between bacterioplankton productivity and chlorophyll *a* (Figure 4.24) and between BA and chlorophyll *a* (Figure 4.25). All of the mean station values fell above the Cole et al. regression line. Again, except for station NR0, the trend from this study matched the Cole et al. slope for BP on chlorophyll *a* ( $0.506 \pm 0.059$  vs.  $0.618 \pm 0.087$ ) and BA on chlorophyll *a* ( $0.501 \pm 0.124$  vs.  $0.524 \pm 0.054$ , slope  $\pm$  SE). A similar comparison between BP and chlorophyll *a* was made by White et al. (1991) and their regression line corresponded very closely to the marine stations from this study; both were well removed from the Cole et al. regression line (Figure 4.24).

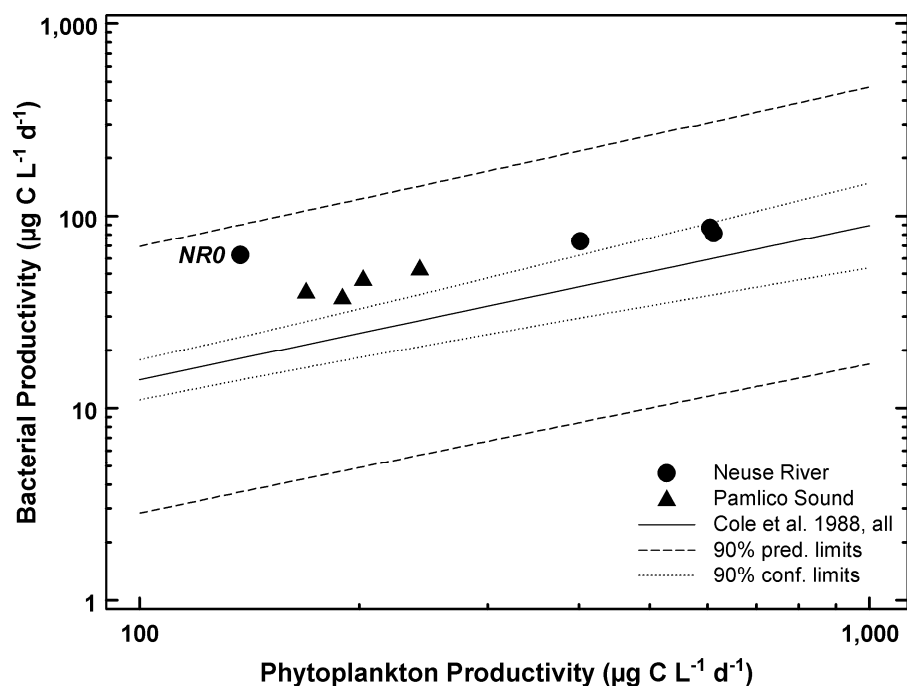


Figure 4.23 Relationship between daily surface bacterioplankton and phytoplankton productivity using station mean values. Shown is the regression line from Cole et al. 1988 for all data points excluding the validation data (their Fig. 1). Dotted and dashed lines are confidence and prediction limits respectively for the regression calculated from statistics in Cole et al. 1988 (their Table 2). Neuse River and Pamlico Sound stations are indicated by symbols and the most upstream station is labeled by NR0.

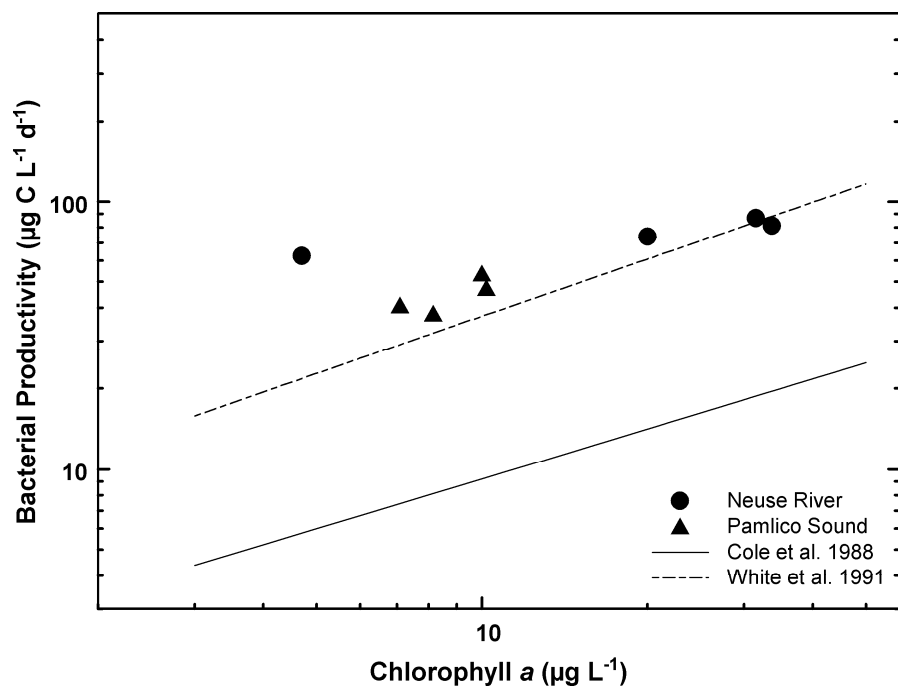


Figure 4.24 Relationship between daily surface bacterioplankton productivity and chlorophyll *a* using station mean values. Shown is the regression line from Cole et al. 1988 for all data points (solid,  $n = 41$ ) and the regression line from White et al. 1991 (dashed,  $n = 412$ ). Symbols as in Figure 4.23.

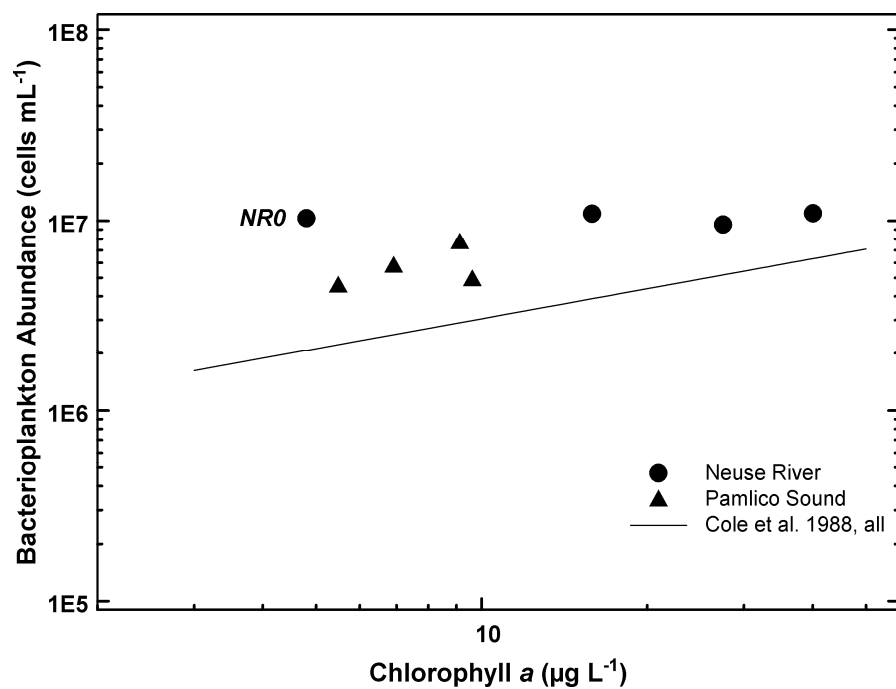


Figure 4.25 Relationship between bacterioplankton abundance and chlorophyll *a* using station mean values. Shown is the regression line from Cole et al. 1988 for all data points. Symbols as in Figure 4.23. Note  $n = 1$  to 2 for the Pamlico Sound station.

#### 4.4 DISCUSSION

Unlike in open ocean systems, the microbial loop in estuaries operates in an environment made up of a complex mixture of both autochthonous and allochthonous organic matter (Ducklow and Shiah 1993). It is well known that phytoplankton directly supply organic matter to heterotrophic bacterioplankton (Hobbie and Cole 1984), but much of the allochthonous pool of organic matter is available to estuarine bacteria as well (Findlay 2003). Potential bacterial resources in the NRPS system were examined at several spatial scales in order to understand the major factors driving bacterioplankton activity.

The strong salinity gradient across the study site means that the station locations can be used as a proxy for relative salinity and that distributions of data by station will give approximate property–salinity profiles. Dissolved organic matter (DOM) showed evidence of mostly conservative mixing, except between the first two stations where concentrations increased. This suggests a source of DOM to that area, which may be from the humic-laden Trent River entering upstream of NR70, from municipal wastewater treatment effluent, or from internal loading via sediment regeneration and cell exudation or lysis. Christian et al. (1984) did not observe significant mortality of phytoplankton triggered by the freshwater–seawater interface in this system. Bulk DOM quality appeared fairly constant across space based on the C:N pattern, and the amount of colored matter (CDOM) decreased in parallel with bulk DOM suggesting conservative behavior. The nonlinear pattern for dissolved nutrients indicates phytoplankton uptake in the middle to upper portion of the estuary, particularly for N. The pattern of phytoplankton biomass shown here and in previous work (Christian et al. 1991; Boyer et al. 1993; Paerl 2006) confirms this. Bacterioplankton also utilize dissolved nutrients, but

net uptake is dependent on organic matter C to N and C to P ratios (Kirchman 2000b). The particulate variables, including phytoplankton, all showed unimodal distributions with peak values in the NR70 to 120 region, proving that this area is a zone of high productivity and biomass.

The general spatial pattern for BP matched that of phytoplankton productivity and biomass, suggesting that bacterioplankton are coupled to phytoplankton at this broad spatial and temporal scale. This was apparent even across years with varying discharge. A similar mid-estuarine peak and coincident phytoplankton peak was reported for the Delaware Bay estuary during one season (Kirchman and Hoch 1988) and for the Chesapeake Bay where peak annual average abundance and productivity corresponded to the chlorophyll peak (Ducklow et al. 2000). The same pattern was seen in the Mississippi River plume, but there were no concurrent phytoplankton measurements (Chin-Leo and Benner 1992). This is not the general rule and there are systems where the coupling of bacterioplankton and phytoplankton is not always apparent. For example, in the Schelde estuary, DOC spatial gradients explained most of the variation in BP unlike PP, which correlated with BP only in the lower estuary (Goosen et al. 1997). A similar lack of correspondence to phytoplankton was found in the Ria de Aveiro in Portugal (Almeida et al. 2005).

The coupling between bacterioplankton and phytoplankton was less evident when examined for individual sampling trips. At this scale, spatial coherence was not consistent and there was often coherence between bacterioplankton and other variables or nothing at all. This lack of correspondence at seasonal and smaller scales, while showing coupled activity or biomass at larger scales, has been reported before (Hoch and Kirchman 1993;

Shiah and Ducklow 1995). Both bottom-up and top-down controls of bacterial activity vary differentially from small (single transect) to large (annual) scales, but the labile substrates driving metabolism are impossible to determine from bulk measures such as DOC and chlorophyll alone (Findlay 2003) and there was no estimate of grazing in this study. The potential grazing effect is also complicated by the production of DOM from the process that can fuel BP (Hoch and Kirchman 1993). The location of mean peak phytoplankton biomass and productivity must have on average more substrate for bacterial growth, perhaps through the integrating effect of the sediments as senescent algal material is continuously remineralized. This mean behavior will vary from day to day, particularly after an event such as the DOC loading from Hurricane Isabel; the pattern of BP shifted to match that of the storm surge organic matter.

To add to the complexity, the effect of different substrates was not always consistent through space. The relationship between BP and chlorophyll *a*, PP, or DIN differed depending on location, although the effect on BP was small. Temperature, which has the largest effect on BP (Chapter 3), also produced a differential response depending location. Temperature had less of an effect on BP at the upstream station (NR0) than at all other stations. In their cross-system analysis, White et al. (1991) found a similar situation in which freshwater systems showed less of a temperature response than marine systems, although they attributed that to more variable temperature in freshwater habitats. They also found that riverine systems, especially blackwater rivers, did not fit their temperature substrate model. Felip et al. (1996) presented a conceptual model which predicts the temperature effect on growth decreasing as the concentration of limiting resources increases. That would imply that available labile substrates are more



concentrated at station NR0, which seems unlikely given the relative productivity rates. More likely is that resources are more limiting at this site, thereby reducing the temperature limitation. This is analogous to the sometimes observed threshold in the productivity–temperature relationship, above which temperature has little or no effect on activity due to substrate limitation (Hoch and Kirchman 1993; Apple et al. 2006). In the multiple regression models by station, DOC had a significant effect on the temperature-BP relationship at NR0 only, reinforcing this idea of more substrate limitation at this location.

A less-intensive analysis of bacterioplankton activity with depth provided more insight into the importance of substrates. It was surprising that the variation between a relatively small number of surface and bottom samples was as great as the annual variation at the surface. Bottom rates were often higher than surface rates. This is counter to what was found in the Chesapeake Bay, where the limitation of production at depth was thought to be from anoxic conditions (Shiah and Ducklow 1994b). Perhaps the more ephemeral nature of anoxia in the NRPS (Buzzelli et al. 2002; Reynolds-Fleming et al. 2004) prevents that limitation from occurring. On the other hand, the June survey showed that the difference between bottom and surface BP was greatest with conditions of strong stratification, conditions which are more likely to be anoxic. Samples from the pycnocline also showed generally elevated productivity, especially when stratification was strong. These high rates were sometimes, but not always, associated with high chlorophyll concentrations. A more general particulate variable, POC, seemed to have a large effect on BP for the samples at depth, but not at the surface. The POC at these different depths could be different in quality, with the deeper samples more likely to have

stressed or senescing algal cells. The bottom samples are also closer to the sediments, which are a source of labile compounds and the density difference at the pycnocline might cause particulate accumulation.

Finally, the work from this study was compared with two cross system analyses of phytoplankton-bacterioplankton coupling. At a broad scale, primary productivity seems to control the magnitude of bacterial productivity (Cole et al. 1988; White et al. 1991). This broad scale correspondence also applies to biomass. Mean values from this study compared quite well to the reported cross-system regressions. In all cases, the data from the NRPS were above the various regression lines in Cole et al. (1988). White et al. (1991) also noted a difference in intercepts between their regressions and those of Cole et al., but did not give an explanation. It is possible the difference was caused by the differences in the mean trophic status of the surveyed systems. A larger intercept on the BP-PP regression implies more heterotrophic activity overall. The mean values at station NR0 stood out from the other stations on these comparison plots. In all cases, BP or BA was higher than would be predicted by the cross system slopes. This suggests that the microbial activity at this site is supplemented by allochthonous matter, although the possibility that the bacterioplankton are more efficient at this site can not be ruled out. The different performance of the bacteria in this freshwater location may also be due to community compositional differences; freshwater taxa may show different patterns of resource utilization from the estuarine community (Crump et al. 2004). The tendency for lower DO saturation at NR0 highlights the more heterotrophic nature of the site.

#### **4.5 CONCLUSIONS**

This extensive examination of bacterioplankton activity and abundance over different spatial scales in the NRPS estuary has provided some insight into the complexity of one particular estuarine microbial loop. The general patterns of productivity over space suggest at least a moderate coupling with phytoplankton biomass or activity, and little with dissolved organic matter and nutrients. This is in agreement with cross-system studies that included a variety of aquatic ecosystems. The coupling seemed less strong on any particular day or across depths, which indicates a different set of controls at those scales. The fact that POC correlated with BP only at depth points towards the importance of a different substrate source from active phytoplankton exudation. The effects of temperature and substrate concentration and type varied across space, with the freshwater station showing the most difference. This station was also an outlier from the other stations in the cross-system comparisons. This location appears to be different from the rest of the estuary, either in terms of available substrates or the community that utilizes them. Even with a study spanning four years and the entire estuarine salinity gradient, the factors controlling heterotrophic activities through time and space were not fully explained. Future research will require more monitoring across depths and at algal bloom sites, as well an evaluation of the top-down factors such as grazing.

## **CHAPTER 5**

### **RESPIRATION AND CARBON FLUXES**

#### **5.1 INTRODUCTION**

Estuaries are highly productive, land-margin ecosystems that function both as sites of organic matter production and sites where watershed-derived material is processed. Resident microbial communities drive that production and biogeochemical cycling, so to fully understand estuarine function, the microbial processes need to be well characterized. The fate of carbon (C) in an estuary depends on trophic transfer and microbial metabolism, or the microbial food web (Sherr and Sherr 2000). Even though determining rates of primary and secondary production is important to quantify the C cycle, respiration is also a necessary measurement as it is constrained by total C inputs and is an indicator of how much is lost or retained by the system (Strayer 1988; Jahnke and Craven 1995).

Until recently, however, respiration in planktonic environments has received much less attention than processes that deal with organic matter production (Williams and del Giorgio 2005). Williams and del Giorgio propose this was because the abundance and ecological importance of planktonic microbes has been overlooked historically. They note how past observations of water column dissolved oxygen (DO) declines were assumed to be from sediment oxygen consumption. Hopkinson and Smith (2005) point out that for estuaries, pelagic respiration has been measured much less than benthic respiration. Williams and del Giorgio (2005) also suggest that the introduction of the  $^{14}\text{C}$

technique for oceanic primary production stifled research on plankton respiration. With the recognition of the numerical importance of water column bacteria and metabolism, planktonic respiration measurements have begun to increase exponentially (Williams and del Giorgio 2005).

Bacterial growth efficiency (BGE) is the proportion of total bacterial carbon uptake, or bacterial carbon demand (BCD), that goes towards the production of biomass and by extension the amount of carbon that gets lost as CO<sub>2</sub> (del Giorgio and Cole 1998). In this way, measures of productivity can be used to estimate carbon fluxes mediated by the microbial loop community (Azam et al. 1983). Methods to estimate BGE vary, but the short-term methods typically involve the simultaneous measurement of bacterial productivity (BP) and bacterial respiration (del Giorgio and Cole 1998). The typical *in vitro* oxygen consumption technique for respiration is prone to bottle effects, does not distinguish between autotrophic and heterotrophic respiration, and is often on a different time scale from the BP measurement. Despite these problems, the advantages of the short-term method outweigh the constraints of the long-term methods.

The BP data set described previously (Chapter 3 and 4) could provide extensive insight into carbon fluxes in the Neuse River and Pamlico Sound (NRPS) estuary given valid estimates of BGE. It was with this in mind that several attempts were made to measure respiration on short time scales and, using concurrent BP rates, calculate BGE. Those efforts are discussed here along with the application of the larger BP data set towards an understanding of the NRPS carbon cycle.

## 5.2 METHODS

Planktonic respiration was measured using the DO changes in bottles incubated at *in situ* temperatures and in the dark (Hopkinson and Smith 2005). Sample water was prescreened through 200  $\mu\text{m}$  mesh in order to remove larger zooplankton. Incubation bottles were 300 mL BOD bottles or 125 mL Erlenmeyer flasks with ground glass stoppers. One incubation used 20 mL glass scintillation vials with polyethylene cone-lined caps. Incubations were done with the bottles submerged, and fixed bottles (i.e., before acidification) were kept submerged at the same temperature until all time points (two to three) were completed; two to six replicate bottles were collected at each time point. Incubations lasted from 2.9 to 24 hours, with a mean of 12 hours (median = 6.5).

Concentrations of DO were measured using an adaptation of the Winkler method that determines iodine spectrophotometrically (Labasque et al. 2004). Reagents were made following the advice in Carignan et al. (1998) except that a pre-made manganous sulfate solution was used instead of manganous chloride. All samples and standards were brought to room temperature and acid was added to samples within two hours of reading. Standards were made in 20 mL glass scintillation vials by adding the reagents in reverse order to sample water and then adding variable volumes of 0.025 N potassium iodate. Iodine was determined on standards and samples from the absorbance at 466 nm (Labasque et al. 2004) using a Shimadzu UV-160 spectrophotometer and corrected for turbidity using the absorbance at 750 nm (Roland et al. 1999). The readings were made in a flow through cell that was fed by a siphon-based sipper system (Pai et al. 1993) pulling samples from the bottom to avoid loss of iodine. Mean coefficient of variation for replicate bottles was 0.33%.

Respiration rate was calculated from the slope of the DO concentration over time. Uncertainty in the rate measurement was represented by the standard error of the DO slope. This is a community rate, but it was assumed to be dominated by bacterioplankton respiration for purposes of the BGE calculation. Hence, calculated BGE's represent lower limits. Respiration was converted to carbon units assuming a respiratory quotient of one. Rates of BP were determined by the leucine uptake technique already discussed (Chapter 3) and had a mean coefficient of variation of 3.9%. BGE is defined as BP divided by the sum of respiration and. Error in BGE was calculated by propagating error from BP and respiration through the function. Both BP and respiration were scaled to daily rates assuming a constant rate throughout the day. Volumetric primary productivity (PP) was scaled to a daily rate by multiplying by 10, representing mean hours of daylight. The sum of daily respiration and BP was the total carbon consumed by bacteria or BCD.

As a proxy for a field measurement of respiration, water column DO deficit was calculated. Profiles of DO, temperature, and salinity were determined using calibrated YSI 6600 sondes. At each 0.5 m depth intervals, the DO concentration was subtracted from the saturated DO concentration based on the *in situ* temperature and salinity. The profile of the differences was integrated using the trapezoidal rule resulting in areal DO deficit in units of  $\text{mmol m}^{-2}$ . Positive values imply a water column that is undersaturated and has more respiration than photosynthesis.

## 5.3 RESULTS AND DISCUSSION

### 5.3.1 RESPIRATION VALUES

Mean community respiration rate determined by dark bottle DO change was 28.8 mmol O<sub>2</sub> m<sup>-3</sup> d<sup>-1</sup> (median = 27.3) and ranged from 5 to 66 mmol O<sub>2</sub> m<sup>-3</sup> d<sup>-1</sup> (n = 12) for stations NR70 and NR160. This falls within a range of pelagic respiration estimates for estuaries world wide (Hopkinson and Smith 2005). For comparison, sediment oxygen consumption measured in the same system is 12–24 mmol O<sub>2</sub> m<sup>-2</sup> d<sup>-1</sup> (Rizzo and Christian 1996; Luettich et al. 2000; Fear et al. 2005). This means that a 1-m water column would have roughly the same pelagic and sediment respiration per m<sup>2</sup> of area. Given that the water column in the NRPS is deeper than 1 m on average, total planktonic respiration probably exceeds sediment respiration, thereby contributing significantly to overall system metabolism.

Since metabolic processes are strongly controlled by temperature, respiration should show some correlation. As shown in Figure 5.1, the exponential fit of respiration and temperature was non significant and the reported slope was lower than for a cross system comparison (Hopkinson and Smith 2005). Assuming the relationship was valid, the Q<sub>10</sub> calculated from the semi-log regression slope is 1.6, which happens to be the same value found for bacterial respiration from 0 to 30 °C in the Monie Bay estuary (Apple et al. 2006). Respiration was more predictable from BP, which explained 40 % of the variation (Figure 5.2). The data fall close to regressions published elsewhere (del Giorgio and Cole 1998; Roland and Cole 1999), but the regression using untransformed data was a better fit than the logarithmic equation reported.



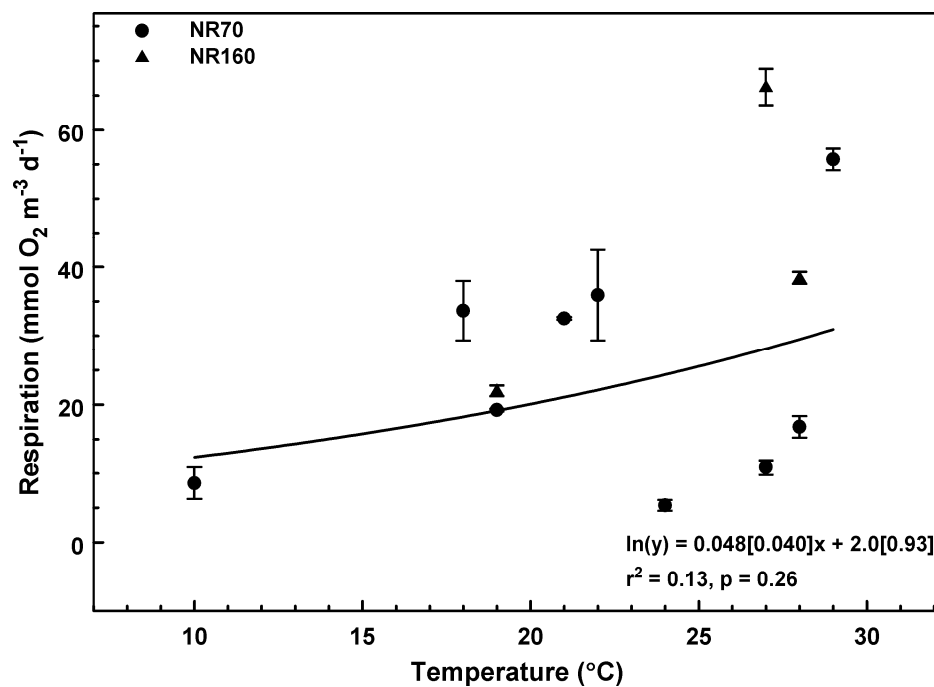


Figure 5.1 Daily volumetric respiration ( $\text{mmol O}_2 \text{ m}^{-3} \text{ d}^{-1}$ ) versus temperature in the Neuse River. Stations indicated by symbols and error bars are the standard errors of the oxygen change slope. Line is the exponential curve fit. Regression results are for the semi-log form and bracketed numbers are coefficient standard errors.

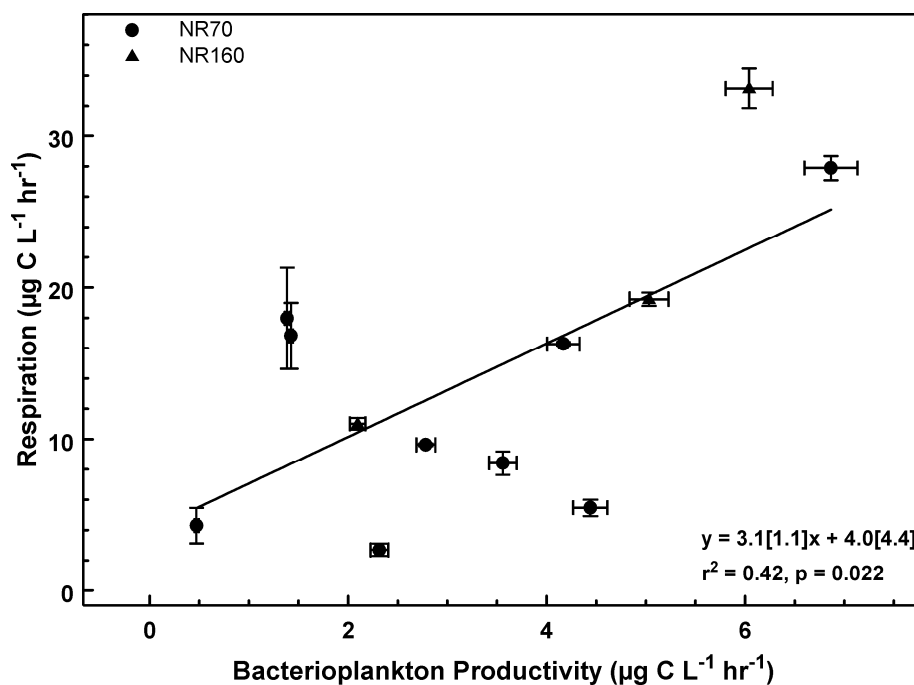


Figure 5.2 Linear regression of hourly volumetric respiration versus bacterioplankton productivity both in units of  $\mu\text{g L}^{-1} \text{ hr}^{-1}$  in the Neuse River. Line is the linear fit. Error bars for BP are standard deviations. All else as in Figure 5.1.

### 5.3.2 BACTERIAL GROWTH EFFICIENCY

Assuming all respiration measured was due to bacterioplankton, mean BGE was 0.22 (median = 0.20, range 0.072 to 0.46). This is comparable to a range of estuarine BGE, although the minimum from this study is lower than any reported (del Giorgio and Cole 1998; Apple et al. 2006). Mean estuarine BGE from a literature survey is 0.37 (del Giorgio and Cole 2000). The relationship between BGE and temperature was not significant, but it appeared positive (Figure 5.3). This is contrary to Apple et al. (2006), who found a negative slope for their regression and stated this was due to the difference in temperature relationships between respiration and BP. The lack of a significant relationship for this data prevents an evaluation of that finding.

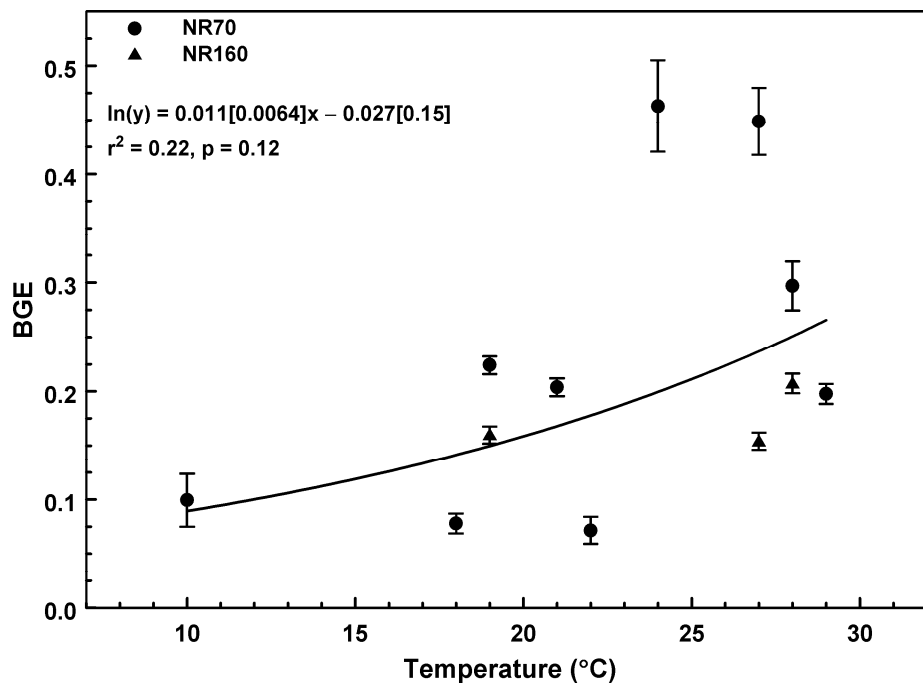


Figure 5.3 Bacterial growth efficiency versus temperature in the Neuse River. Error bars represent propagated errors from respiration and BP. All else as in Figure 5.1.

These are rough estimates of BGE and probably on the low side since the DO change included that from non-bacterial organisms present in the sample. Another

possible concern is that the respiration incubations were longer than those for BP. The BP incubations lasted 1 hour while the respiration assays were 12 hours on average. Despite the long incubations, the DO changes remained linear throughout.

### **5.3.3 BACTERIAL CARBON DEMAND**

The ratio of BP to PP is often used as an indicator of carbon fluxes in the microbial loop (Hoch and Kirchman 1993). The ratio of average daily BP to average daily PP is 0.18 or using median, 0.23. This is similar to the mean cross system ratio reported by Cole et al. (Cole et al. 1988) and to the ratios of annual BP and PP in the euphotic zone for a few estuaries summarized by Ducklow and Shiah (1993). The ratios found here would be higher if scaled on an areal basis, since PP is not constant with depth, and BP may even be greater at depth (see Chapter 4). When examined by station, the ratios show a distinct separation between the freshwater station, NR0, and the other, marine stations (Figure 5.4). The ratio of mean rates at NR0 was 0.45 (median = 0.82), while the ratios of mean and median rates at the other locations only ranged from 0.13 to 0.27.

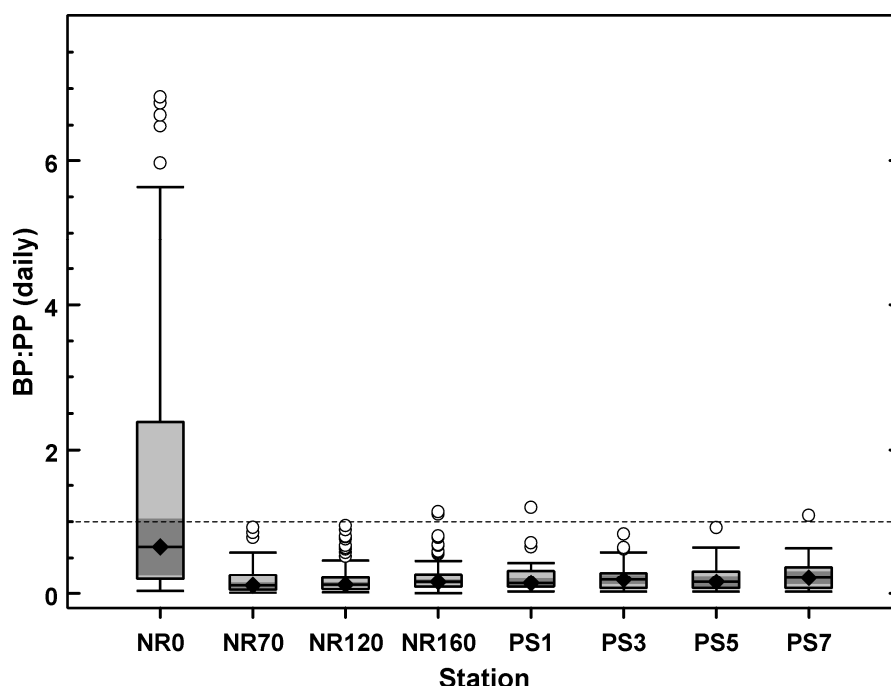


Figure 5.4 Ratio of daily bacterioplankton productivity (BP) to daily phytoplankton productivity (PP) by station in the NRPS. Ratios were calculated for each trip. Dotted line indicates a ratio of one. Some of the outliers (maximum ratio of 24) have been cut off by the y-axis scaling.

Using BCD determined from BP and the mean BGE, the percent of mean daily PP that could meet mean bacterioplankton carbon requirements was 82 %. The distribution of the ratio for each trip is shown in Figure 5.5. Station NR0 stands out again by having more BCD than can be provided by PP (ratio of mean values = 2.1). This means that the bacterioplankton must be utilizing allochthonous carbon at this freshwater location and that the system is probably locally net heterotrophic. Given that the empirically derived BGE is probably an underestimate, BCD based on a higher growth efficiency (and the BCD to PP ratio) would be lower. On the other hand, the BCD to PP ratio would be even higher if the whole water column was considered. The scaling of PP to daily rates was somewhat simplistic and a more realistic estimate of daily PP would need to include incident light, water transparency, and photosynthesis-irradiance relationships for the

phytoplankton community. Also, the PP method utilizes a variable light incubation (Mallin and Paerl 1992), which may or may not match field conditions at the time of collection. It is possible that fine tuning the PP estimate could lower the BCD to PP ratios, but the effect of those issues is unknown at this point. Given the opposite effect of the various corrections, BCD is still a significant proportion of PP, even at the marine stations.

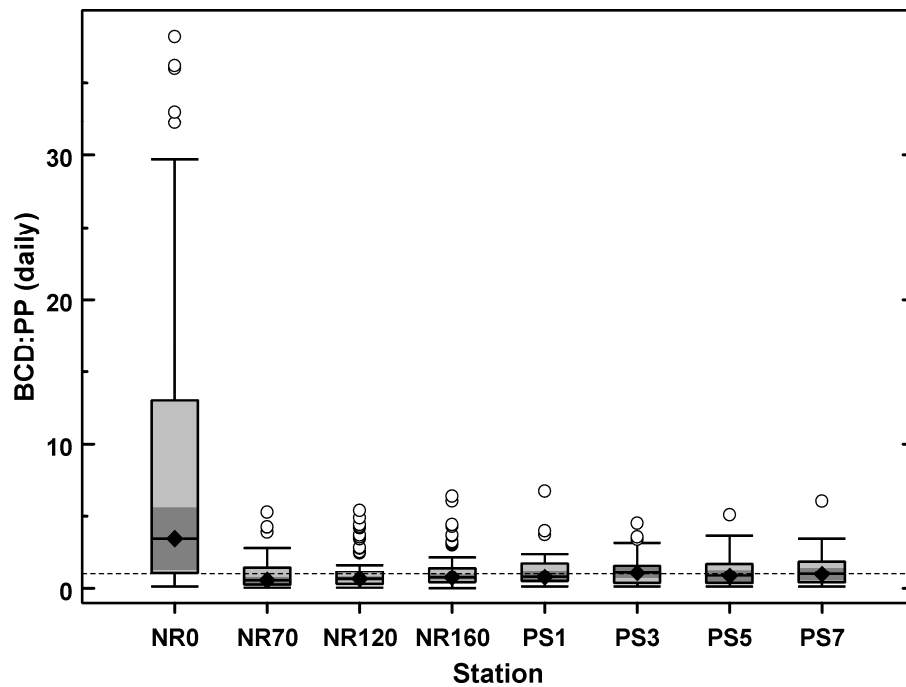


Figure 5.5 Ratio of daily bacterioplankton carbon demand (BCD) to daily phytoplankton productivity (PP) by station in the NRPS. Ratios were calculated for each trip. Dotted line indicates a ratio of one. Some of the outliers have been cut off by the y-axis scaling.

### 5.3.4 OXYGEN DEFICITS

Another way to estimate water column respiration is through field measurements of DO. The DO deficit calculation gives a snapshot of conditions that are responding to both respiration and photosynthesis. Most of the profiles were collected from mid-morning to mid-afternoon, a time when photosynthetic rates would be highest. Therefore,

any positive DO deficits should be close to minimum values and would indicate net oxygen consumption throughout the day. Mean DO deficit was 188 (median = 122) mmol O<sub>2</sub> m<sup>-2</sup> with a range from -252 to 1188 mmol O<sub>2</sub> m<sup>-2</sup>. When DO deficit was partitioned by station, several stations showed large deficits over the four years of the study, especially NR0, 120, and 160 (Figure 5.6). Station NR70 did not show as much oxygen deficit because it is quite shallow and tends to have high PP. The trend with increasing salinity was for oxygen deficit to approach zero, which could be related to the increased mixing at those stations nearest the ocean inlet. A seasonal pattern was evident in the DO deficit record with higher values in the warmer month (Figure 5.7). When Hurricane Isabel passed through the system and caused a large storm surge, DO deficit increased dramatically at NR0. The flooding of the land from the surge carried with it a large load of organic matter on its return to the estuary, driving up microbial respiration, but only at the upstream station. The DO deficit quickly returned to previous levels, just as BP did (Chapter 3).

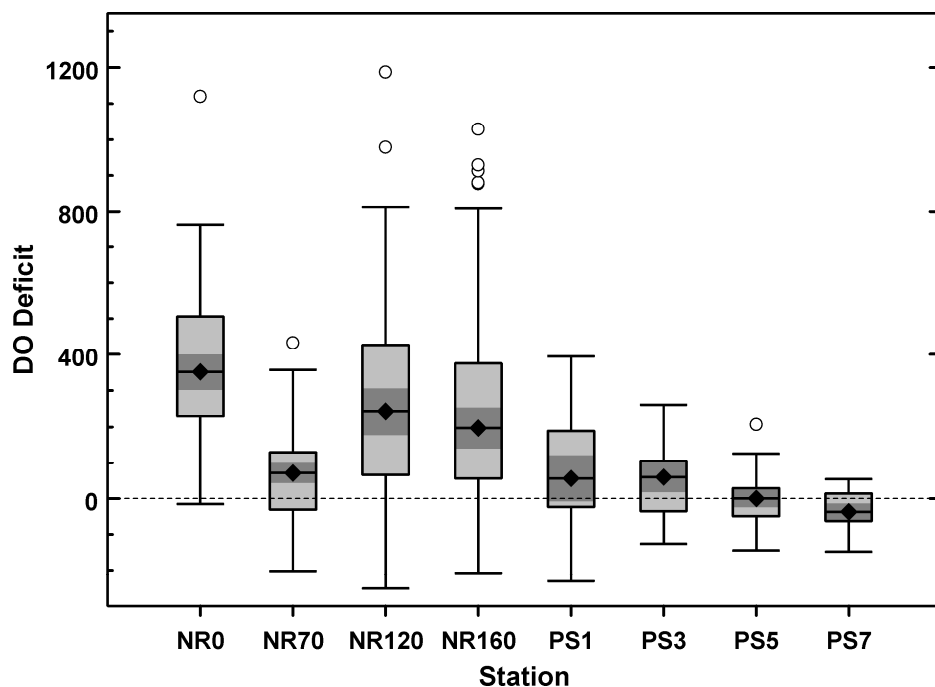


Figure 5.6 Integrated dissolved oxygen (DO) deficit in  $\text{mmol m}^{-2}$  by station in the NRPS. Dotted line indicates a deficit of zero, which means the whole water column was at saturation.

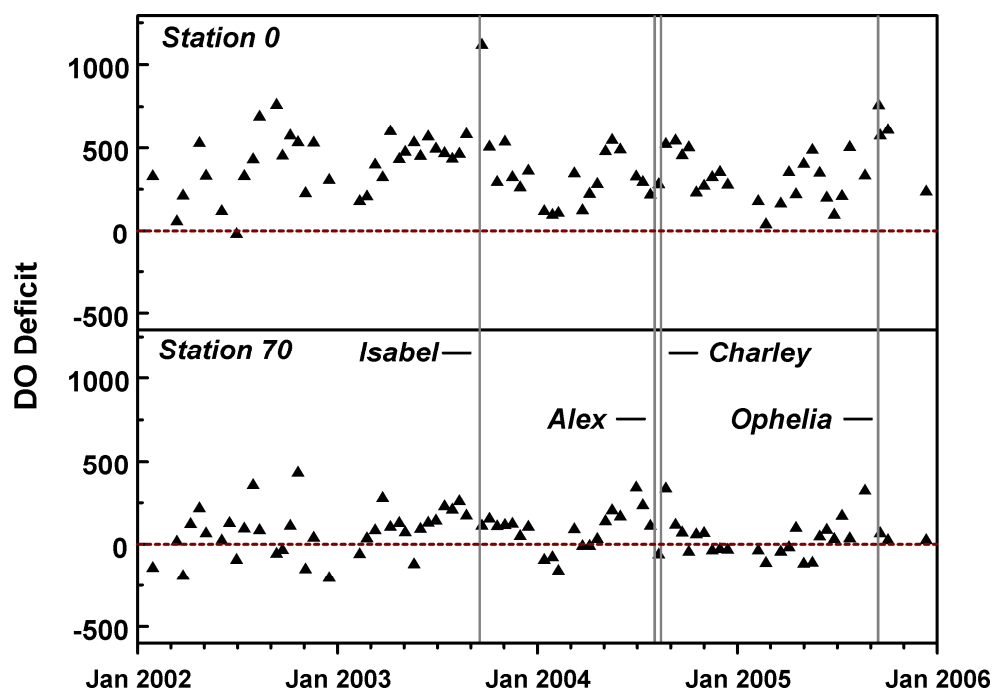


Figure 5.7 Integrated dissolved oxygen (DO) deficit in  $\text{mmol m}^{-2}$  by date at two stations in the Neuse River. Dotted line indicates a deficit of zero, which means the whole water column was at saturation. Significant tropical storms striking the area are indicated by vertical lines.

## 5.4 CONCLUSIONS

Respiration in aquatic ecosystems is difficult to quantify but provides important information about carbon fluxes in the microbial loop. A small set of DO consumption measurements in the NRPS showed that respiration rates for this system are typical for estuaries. The temperature effect on respiration was not significant, but the temperature signal may have been obscured by the relatively small data set and analytical uncertainty in the respiration data. BP turned out to be a good predictor of respiration. The simultaneous measures of BP rates allowed for the calculation of BGE, which was low, but again, within the range seen for other estuaries. Temperature also had no apparent effect on BGE. The extent of BCD met by phytoplankton was estimated using the mean BGE. The freshwater station stood out from the other marine locations by having more BCD than could be met by phytoplankton production alone. This implies that allochthonous material is supporting bacterial growth at this station and that the system may be net heterotrophic. Finally, system respiration could be gauged using water column DO deficit. This showed that several of the stations were sites of significant respiration and that the storm surge from Hurricane Isabel had a significant impact on the upstream microbial community.



## **CHAPTER 6**

### **SUMMARY**

Bacterioplankton and phytoplankton metabolism and biomass were examined over several years across the salinity gradient of the Neuse River and Pamlico Sound (NRPS) estuarine system. The results provide new insights into the dynamics and control of estuarine microbial communities across various spatial and temporal scales and in response to climatological events. These insights will be invaluable for a better understanding of this particular system's current conditions and response to future regional and global change.

Three successive hurricanes brought record flooding to the NRPS and the multi-year monitoring effort revealed both the time for recovery to pre-storm conditions and baseline water quality data for the sound, which had been sorely lacking. Salinity was abnormally low and nutrient and chlorophyll *a* concentrations were very high at the start of the study right after the storms. Recovery was fairly rapid (within a month) for some variables like nutrients, while salinity and chlorophyll *a* took several months to a year to return to pre-storm values. Phytoplankton community composition, based on taxonomic pigments, began to change after the perturbation and had yet to stop changing at the end of the study period. Other consequences of the flooding were changes to the stratification regime, advection of particles, and a bypassing of the sub-estuarine nutrient filtration leading to two to three times the inferred annual nitrogen loading to the sound.

The patterns and controls of heterotrophic bacterioplankton in the NRPS were the main focus of a separate long-term study. Sampling spanned four years that differed dramatically in annual discharge. Also, several tropical storms crossed or passed by the system, each having different paths and strengths. The system was found to be rich in organic matter and nutrients, the supply of which appeared to be controlled by discharge, but not temperature. There was little seasonal variation in phytoplankton biomass and productivity, and only chlorophyll *a* showed interannual variation that might have been related to nutrient loading. Bacterioplankton productivity, on the other hand showed strong positive correlation with temperature, but little correspondence with proxies for bacterial substrates such as dissolved organic matter and phytoplankton productivity. Somewhat less than half the variation in bacterioplankton productivity was left unexplained and could be due to factors not measured such as specific substrates or grazing. Absolute rates were typical of temperate estuaries around the world. Only one of the storms impacting the system had an effect (stimulating) on the microbial community and that effect was short lived.

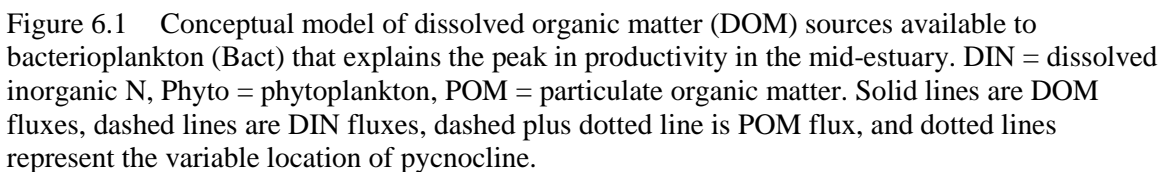
While bacterioplankton and phytoplankton appeared uncoupled at various temporal scales, the microbial variables had similar patterns along the salinity gradient suggesting a large scale coupling. Both autotrophic and heterotrophic productivity had tendencies for peak values in the middle portion of the estuary. The coherence between rates was much less strong when considering each sampling trip individually. The effect of temperature and substrate on bacterioplankton productivity differed only at the upstream, fresh water station. Variation in bacterioplankton productivity with depth was large and was related to stratification and particulate organic matter. From this it appears

that organic matter released from the sediments and particles at the pycnocline or deeper are important resources for bacteria.

Respiration measurements based on dissolved oxygen loss in bottles revealed planktonic rates that are comparable with sediment oxygen demand. The number of samples was small enough to obscure any temperature relationship, but bacterioplankton productivity did explain some of the variation in respiration. Bacterial growth efficiencies were estimated using respiration and concurrent productivity measurements and assuming that the respiration was all due to bacteria. The mean efficiency was low, but individual values fell within the range for estuaries. Growth efficiency was used to calculate total bacterial carbon demand or the sum of production and respiration. This carbon flux was compared to phytoplankton production, and for all stations except the fresh water end member, autochthonous carbon production can meet the needs of the heterotrophs. At the upstream site, a bacterial carbon demand several times primary production suggests that bacterioplankton depends on external carbon sources in this location.

The fact that phytoplankton and bacterioplankton covaried across large time and space scales, but are uncoupled at seasonal and smaller scales is somewhat of a paradox, although not unexpected (Hoch and Kirchman 1993). A simple conceptual model based on the work of Ducklow and Shiah (1993) was developed to provide a possible explanation (Figure 6.1). This model represents some of the major sources of DOM available to bacterioplankton, but it does not try to represent all the pathways of the microbial loop and food web. At the upstream site, bacteria primarily utilize allochthonous organic matter, since short residence times and possibly light limitation

keep primary production low. Bacteria and phytoplankton at this location may appear to be coupled at larger scales because of relatively smaller values for both variables. Phytoplankton production peaks in the mid-estuary fueled by nitrogen loading and aided by increased residence time, which is caused by the channel widening and the bidirectional estuarine circulation. The sediments in the area are enriched with particles from algal blooms and resuspended sediments (i.e., the turbidity maximum). The concentrating effects of circulation and the mineralization of those particles provides a steady supply of dissolved organic matter for the bacteria. Bacterioplankton productivity also peaks in the mid-estuary zone where a large supply and range of labile substrates is always available, even if direct release from phytoplankton is not constant. Thus, the bacterioplankton can be uncoupled from phytoplankton at small time scales, while covarying at the annual scale.



129

This study provided extensive multi-year, multi-seasonal coverage of microbial activity across the entire salinity range. Eight stations were spread out over more than 100 km, so more closely spaced sampling, especially in the upper estuary between the first two stations, could help to better characterize the spatial variability. Diel sampling could test the assumption that rates are constant throughout the day and not affected by light (Church et al. 2004). This study focused only on bottom-up controls of productivity, so estimates of grazing and other losses might explain more of the variation. Finally, since the respiration technique could not exclude any autotrophs and protists in the bottles, the rates of respiration were possibly overestimates. A method that could isolate bacterial respiration at the time scale of BP measurements would produce more accurate growth efficiencies and lead to a clearer understanding of the microbial community's role in the estuarine carbon cycle.

## APPENDIX

### LEUCINE UPTAKE KINETICS

One of the concerns with the leucine uptake method for determining bacterial productivity is the dilution of  $^3\text{H}$ -leucine additions by extracellular pools or intracellular synthesis (Roberts 1998). Initial tests showed that  $20 \text{ nmol L}^{-1}$  additions of  $^3\text{H}$ -leucine produced saturated uptake, minimizing any isotope dilution. Further kinetic tests demonstrated that this concentration was not sufficient to saturate uptake rates (Figure A.1). None of the experiments reach saturated uptake, as determined by the non-linear least squares regression fits to the following model:  $V = \frac{V_{\max} \times S}{K + S}$ , where  $V$  is measured uptake,  $V_{\max}$  is estimated maximum uptake,  $S$  is the leucine concentration, and  $K$  is the half-saturation constant. The isotope dilution factor (ID) is defined as estimated  $V_{\max}$  divided by measured uptake ( $V$ ). This factor is part of the equation for converting leucine uptake rates to bacterial productivity. Uptake rates close to  $V_{\max}$  will have ID close to 1 and therefore will have no correction for isotope dilution.

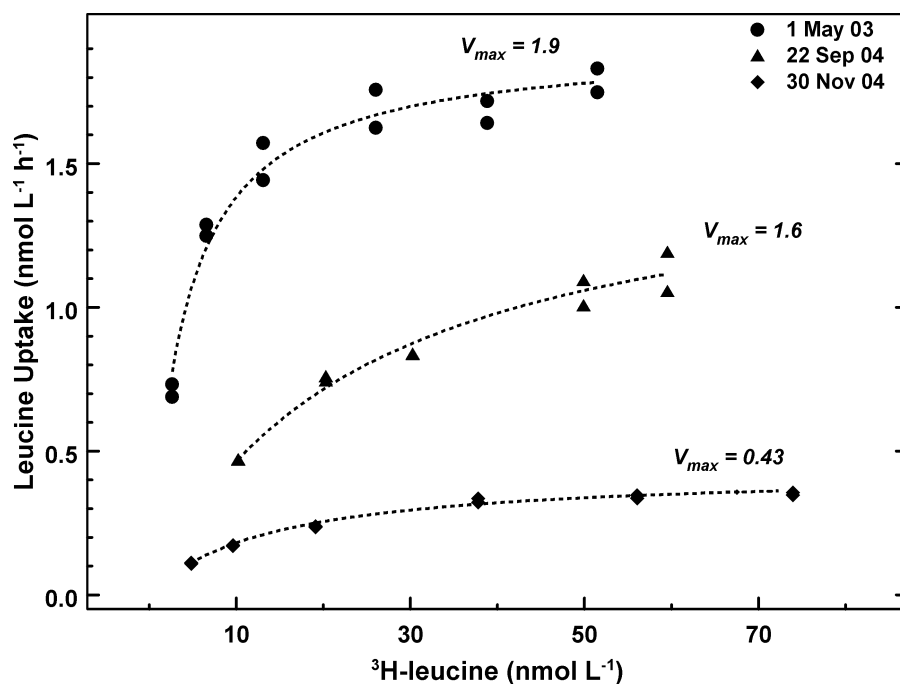


Figure A.1 Examples of  $^3\text{H-leucine}$  uptake kinetics using Neuse River water. Dotted lines are the non-linear least square regressions model fits. Estimated maximum uptake rate,  $V_{\max}$ , is indicated for each date.

Leucine uptake kinetic experiments were conducted for 44 separate station and date combinations in the NRPS study area. For each measurement replicate, ID was calculated from the estimated  $V_{\max}$  and the measured  $V$ . These individual ID values were plotted against added  $^3\text{H-leucine}$  concentration (Figure A.2). These data were fit to a power function model using non-linear least squares regression. This model was used to correct all other leucine uptake assays where isotope dilution was not known.



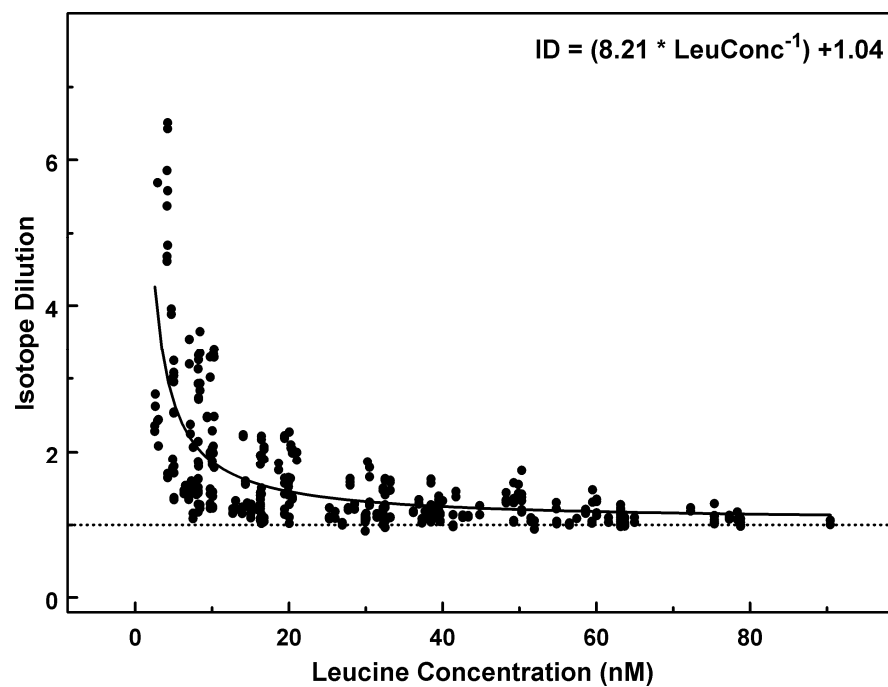


Figure A.2 Isotope dilution (ID) versus  $^3\text{H}$ -leucine concentration from 44 uptake kinetic experiments. ID is the ratio of maximum uptake ( $V_{\max}$ ) to measured uptake for each experimental replicate. The solid line is the non-linear least squares regression line with the model and estimated parameters shown. The dotted line is  $ID = 1$ .

## LITERATURE CITED

- Almeida, M. A., M. A. Cunha, and F. Alcântara. 2005. Relationship of bacterioplankton production with primary production and respiration in a shallow estuarine system (Ria de Aveiro, NW Portugal). *Microbiological Research* 160:315-328.
- Alonso-Sáez, L., E. Vázquez-Domínguez, C. Cardelús, J. Pinhassi, M. M. Sala, I. Lekunberri, V. Balagué, M. U. F. Vila-Costa, R. Massana, R. Simó, and J. M. Gasol. 2008. Factors controlling the year-round variability in carbon flux through bacteria in a coastal marine system. *Ecosystems* 11:397-409.
- Apple, J. K., P. A. del Giorgio, and R. I. E. Newell. 2004. The effects of system-level nutrient enrichment on bacterioplankton production in a tidally influenced estuary. *Journal of Coastal Research* 110-133.
- Apple, J. K., P. A. del Giorgio, and W. M. Kemp. 2006. Temperature regulation of bacterial production, respiration, and growth efficiency in a temperate salt-marsh estuary. *Aquatic Microbial Ecology* 43:243-254.
- Arar, E. J., W. L. Budde, and T. D. Behymer. 1997. Methods for the determination of chemical substances in marine and environmental matrices. EPA/600/R-97/072. National Exposure Research Laboratory, U.S. Environmental Protection Agency, Cincinnati, OH.
- Attrill, M. J. and S. D. Rundle. 2002. Ecotone or ecocline: ecological boundaries in estuaries. *Estuarine Coastal and Shelf Science* 55:929-936.
- Azam, F., T. Fenchel, J. G. Field, J. S. Gray, L. A. Meyer-Reil, and F. Thingstad. 1983. The ecological role of water-column microbes in the sea. *Marine Ecology Progress Series* 10:257-263.
- Bales, J. D. 2003. Effects of Hurricane Floyd inland flooding, September-October 1999, on tributaries to Pamlico Sound, North Carolina. *Estuaries* 26:1319-1328.
- Bales, J. D., C. J. Oblinger, and A. H. Sallenger, Jr. 2000. Two months of flooding in eastern North Carolina, September-October 1999. Water-Resources Investigations Report 00-4093. U.S. Geological Survey, Raleigh, NC.
- Balls, P. W. 1994. Nutrient inputs to estuaries from nine Scottish east coast rivers; influence of estuarine processes on inputs to the North Sea. *Estuarine Coastal and Shelf Science* 39:329-352.
- Barrera-Alba, J. J., S. M. F. Gíanesella, G. A. O. Moser, and F. M. P. Saldanha-Corrêa. 2008. Bacterial and phytoplankton dynamics in a sub-tropical estuary. *Hydrobiologia* 598:229-246.

- Bell, C. R. and L. J. Albright. 1981. Attached and free-floating bacteria in the Fraser River estuary, British Columbia, Canada. *Marine Ecology-Progress Series* 6:317-327.
- Boyer, J. N., R. R. Christian, and D. W. Stanley. 1993. Patterns of phytoplankton primary productivity in the Neuse River estuary, North Carolina, USA. *Marine Ecology Progress Series* 97:287-297.
- Boyer, J. N., D. W. Stanley, and R. R. Christian. 1994. Dynamics of  $\text{NH}_4^+$  and  $\text{NO}_3^-$  uptake in the water column of the Neuse River Estuary, North Carolina. *Estuaries* 17:361-371.
- Brown, J. H., J. F. Gillooly, A. P. Allen, V. M. Savage, and G. B. West. 2004. Toward a metabolic theory of ecology. *Ecology* 85:1771-1789.
- Buzzelli, C. P., J. Ramus, and H. W. Paerl. 2003. Ferry-based monitoring of surface water quality in North Carolina estuaries. *Estuaries* 26:975-984.
- Buzzelli, C. P., R. A. Luettich Jr., S. P. Powers, C. H. Peterson, J. E. McNinch, J. L. Pinckney, and H. W. Paerl. 2002. Estimating the spatial extent of bottom-water hypoxia and habitat degradation in a shallow estuary. *Marine Ecology Progress Series* 230:103-112.
- Carignan, R., A.-M. Blais, and C. Vis. 1998. Measurement of primary production and community respiration in oligotrophic lakes using the Winkler method. *Canadian Journal of Fisheries and Aquatic Sciences* 55:1078-1084.
- Chan, T. U. and D. P. Hamilton. 2001. Effect of freshwater flow on the succession and biomass of phytoplankton in a seasonal estuary. *Marine and Freshwater Research* 52:869-884.
- Chesapeake Research Consortium. 1976. The effects of tropical storm Agnes on the Chesapeake Bay estuarine system. The Johns Hopkins University Press, Baltimore, MD.
- Chin-Leo, G. and R. Benner. 1992. Enhanced bacterioplankton production and respiration at intermediate salinities in the Mississippi River plume. *Marine Ecology Progress Series* 87:87-103.
- Christian, R. R., J. N. Boyer, and D. W. Stanley. 1991. Multi-year distribution patterns of nutrients within the Neuse River Estuary, North Carolina. *Marine Ecology Progress Series* 71:259-274.
- Christian, R. R., J. N. Boyer, D. W. Stanley, and W. M. Rizzo. 1992. Network analysis of nitrogen cycling in an estuary, p. 217-247. *In* C. Hurst (ed.), Modeling the metabolic and physiologic activities of microorganisms. Wiley, New York.

- Christian, R. R., D. W. Stanley, and D. A. Daniel. 1984. Microbiological changes occurring at the freshwater-seawater interface of the Neuse River Estuary, North Carolina, p. 349-365. *In* V. S. Kennedy (ed.), *The Estuary as a Filter*. Academic Press, New York.
- Christian, R. R. and C. R. Thomas. 2000. Neuse River Estuary modeling and monitoring project stage 1: Network analysis for evaluating the consequences of nitrogen loading. Water Resources Research Institute Report No. 325-F. Water Resources Research Institute of the University of North Carolina, Raleigh.
- Christian, R. R. and C. R. Thomas. 2003. Network analysis of nitrogen inputs and cycling in the Neuse River Estuary, North Carolina, USA. *Estuaries* 26:815-828.
- Church, M. J., H. W. Ducklow, and D. M. Karl. 2004. Light dependence of [<sup>3</sup>H]leucine incorporation in the oligotrophic North Pacific Ocean. *Applied and Environmental Microbiology* 70:4079-4087.
- Cloern, J. E. 1996. Phytoplankton bloom dynamics in coastal ecosystems: A review with some general lessons from sustained investigations of San Francisco Bay, California. *Reviews of Geophysics* 34:127-168.
- Cloern, J. E. 2001. Our evolving conceptual model of the coastal eutrophication problem. *Marine Ecology Progress Series* 210:223-253.
- Cole, J. J., S. Findlay, and M. L. Pace. 1988. Bacterial production in fresh and saltwater ecosystems: a cross-system overview. *Marine Ecology Progress Series* 43:1-10.
- Collos, Y. 1986. Time-lag algal growth dynamics: biological constraints on primary production in aquatic environments. *Marine Ecology Progress Series* 33:193-206.
- Costanza, R., W. M. Kemp, and W. R. Boynton. 1993. Predictability, scale and biodiversity in coastal and estuarine ecosystems: Implication for management. *Ambio* 22:88-96.
- Cotner, J. B., T. H. Johengen, and B. A. Biddanda. 2000. Intense winter heterotrophic production stimulated by benthic resuspension. *Limnology and Oceanography* 45:1672-1676.
- Crump, B. C., C. S. Hopkinson, M. L. Sogin, and E. Hobbie. 2004. Microbial biogeography along an estuarine salinity gradient: combined influences of bacterial growth and residence time. *Applied and Environmental Microbiology* 70:1494-1505.
- Cunha, M. A., M. A. Almeida, and F. Alcântara. 2000. Patterns of ectoenzymatic and heterotrophic bacterial activities along a salinity gradient in a shallow tidal estuary. *Marine Ecology Progress Series* 204:1-12.

- Day, J. W., Jr., C. A. S. Hall, W. M. Kemp, and A. Yáñez-Arancibia. 1989. *Estuarine Ecology*. John Wiley & Sons, New York.
- del Giorgio, P. A. and J. J. Cole. 1998. Bacterial growth efficiency in natural aquatic systems. *Annual Review of Ecology and Systematics* 29:503-541.
- del Giorgio, P. A. and J. J. Cole. 2000. Bacterial energetics and growth efficiency, p. 289-325. *In* D. L. Kirchman (ed.), *Microbial Ecology of the Oceans*. Wiley-Liss, Inc., New York.
- del Giorgio, P. A. and G. Scarborough. 1995. Increase in the proportion of metabolically active bacteria along gradients of enrichment in freshwater and marine plankton: implications for estimates of bacterial growth and production rates. *Journal of Plankton Research* 17:1905-1924.
- Ducklow, H. W., G. Schultz, P. Raymond, J. Bauer, and F. Shiah. 2000. Bacterial dynamics in large and small estuaries, p. 105-111. *In* C. R. Bell, M. Brylinsky, and P. Johnson-Green (eds.), *Microbial Biosystems: New Frontiers, Proceedings of the 8th International Symposium on Microbial Ecology*. Atlantic Canada Society for Microbial Ecology, Kentville, Canada.
- Ducklow, H. W. and F.-K. Shiah. 1993. Bacterial production in estuaries, p. 261-287. *In* T. E. Ford (ed.), *Aquatic Microbiology*. Blackwell Scientific Publications, Boston.
- Eby, L. and L. Crowder. 2002. Hypoxia-based habitat compression in the Neuse River Estuary: context-dependent shifts in behavioral avoidance thresholds. *Canadian Journal of Fisheries and Aquatic Sciences* 59:952-965.
- Elliott, M. and D. S. Mclusky. 2002. The need for definitions in understanding estuaries. *Estuarine Coastal and Shelf Science* 55:815-827.
- Elliott, M. and V. Quintino. 2007. The Estuarine Quality Paradox, Environmental Homeostasis and the difficulty of detecting anthropogenic stress in naturally stressed areas. *Marine Pollution Bulletin* 54:640-645.
- Epperly, S. P. and S. W. Ross. 1986. Characterization of the North Carolina Pamlico-Albemarle estuarine complex. NOAA Technical Memorandum NMFS-SEFC-175. National Oceanographic and Atmospheric Administration, Beaufort, N.C.
- Eyre, B. and P. Balls. 1999. A comparative study of nutrient behavior along the salinity gradient of tropical and temperate estuaries. *Estuaries* 22:313-326.
- Eyre, B. and C. Twigg. 1997. Nutrient behavior during post-flood recovery of the Richmond River Estuary northern NSW, Australia. *Estuarine Coastal and Shelf Science* 44:311-326.

- Eyre, B. D. 2000. Regional evaluation of nutrient transformation and phytoplankton growth in nine river-dominated sub-tropical east Australian estuaries. *Marine Ecology Progress Series* 205:61-83.
- Fear, J. M., S. P. Thompson, T. E. Gallo, and H. W. Paerl. 2005. Denitrification rates measured along a salinity gradient in the eutrophic Neuse River Estuary, North Carolina, USA. *Estuaries* 28:608-619.
- Felip, M., M. L. Pace, and J. J. Cole. 1996. Regulation of planktonic bacterial growth rates: The effects of temperature and resources. *Microbial Ecology* 31:15-28.
- Findlay, S. 2003. Bacterial response to variation in dissolved organic matter, p. 363-379. In S. E. G. Findlay and R. L. Sinsabaugh (eds.), *Aquatic Ecosystems: Interactivity of Dissolved Organic Matter*. Academic Press, San Diego.
- Findlay, S., M. L. Pace, D. Lints, J. J. Cole, N. F. Caraco, and B. Peierls. 1991. Weak coupling of bacterial and algal production in a heterotrophic ecosystem: the Hudson River estuary. *Limnology and Oceanography* 36:268-278 .
- Fukuda, R., H. Ogawa, T. Nagata, and I. Koike. 1998. Direct determination of carbon and nitrogen contents of natural bacterial assemblages in marine environments. *Applied and Environmental Microbiology* 64:3352-3358.
- Gasol, J. M., J. Pinhassi, L. Alonso-Sáez, H. Ducklow, G. J. Herndl, M. Koblížek, M. Labrenz, Y. Luo, X. A. G. Moran, T. Reinthaler, and M. Simon. 2008. Towards a better understanding of microbial carbon flux in the sea. *Aquatic Microbial Ecology* 53:21-38.
- Giese, G. L., H. B. Wilder, and G. G. Parker, Jr. 1985. Hydrology of major estuaries and sounds of North Carolina. U.S. Geological Survey Water-Supply Paper 2221. U. S. Geological Survey, Alexandria, Virginia.
- Gillooly, J. F., J. H. Brown, G. B. West, V. M. Savage, and E. L. Charnov. 2001. Effects of size and temperature on metabolic rate. *Science* 293:2248-2251.
- Goldenberg, S. B., C. W. Landsea, A. M. Mestas-Núñez, and W. M. Gray. 2001. The recent increase in Atlantic hurricane activity: causes and implications. *Science* 293:474-479.
- Goosen, N. K., P. van Rijswijk, J. Kromkamp, and J. Peene. 1997. Regulation of annual variation in heterotrophic bacterial production in the Schelde estuary (SW Netherlands). *Aquatic Microbial Ecology* 12:223-232.
- Heip, C. H. R., N. K. Goosen, P. M. J. Herman, J. Kromkamp, J. J. Middelburg, and K. Soetaert. 1995. Production and consumption of biological particles in temperate tidal estuaries. *Oceanography and Marine Biology: an Annual Review* 33:1-149.

- Hietanen, S., J. M. Lehtimäki, L. Tuominen, K. Sivonen, and J. Kuparinen. 2002. Nodularia spp. (Cyanobacteria) incorporate leucine but not thymidine: importance for bacterial-production measurements. *Aquatic Microbial Ecology* 28:99-104.
- Hobbie, J. E. and J. J. Cole. 1984. Response of a detrital foodweb to eutrophication. *Bulletin of Marine Science* 35:357-363.
- Hoch, M. P. and D. L. Kirchman. 1993. Seasonal and inter-annual variability in bacterial production and biomass in a temperate estuary. *Marine Ecology Progress Series* 98:283-295.
- Hopkinson, C. S., Jr. and E. M. Smith. 2005. Estuarine respiration: an overview of benthic, pelagic, and whole system respiration, p. 122-146. In P. A. del Giorgio and P. J. I. B. Williams (eds.), *Respiration in Aquatic Ecosystems*. Oxford University Press, Oxford.
- Jahnke, R. A. and D. B. Craven. 1995. Quantifying the role of heterotrophic bacteria in the carbon cycle: A need for respiration rate measurements. *Limnology and Oceanography* 40:436-441.
- Jeffrey, S. W. and G. F. Humphrey. 1975. New spectrophotometric equations for determining chlorophylls *a*, *b*, *c*<sub>1</sub> and *c*<sub>2</sub> in higher plants, algae and natural phytoplankton. *Biochimie und Physiologie der Pflanzen* 167:191-194.
- Jeffrey, S. W., R. F. C. Mantoura, and S. W. Wright. 1997. Phytoplankton pigments in oceanography: Guidelines to modern methods. UNESCO Publishing, Paris.
- Jensen, L. M., K. Sand-Jensen, S. Marcher, and M. Hansen. 1990. Plankton community respiration along a nutrient gradient in a shallow Danish estuary. *Marine Ecology Progress Series* 61:75-85.
- Kirchman, D. 2001. Measuring bacterial biomass production and growth rates from leucine incorporation in natural aquatic environments, p. 227-237. In J. H. Paul (ed.), *Marine Microbiology*. Academic Press, San Diego.
- Kirchman, D., E. K'Neas, and R. Hodson. 1985. Leucine incorporation and its potential as a measure of protein synthesis by bacteria in natural aquatic systems. *Applied and Environmental Microbiology* 49:599-607.
- Kirchman, D. L. 1993. Leucine incorporation as a measure of biomass production by heterotrophic bacteria, p. 509-512. In P. F. Kemp, B. F. Sherr, E. B. Sherr, and J. J. Cole (eds.), *Handbook of Methods in Aquatic Microbial Ecology*. Lewis Publishers, Boca Raton.
- Kirchman, D. L. 2000a. *Microbial Ecology of the Oceans*. Wiley-Liss, Inc., New York.

- Kirchman, D. L. 2000b. Uptake and regeneration of inorganic nutrients by marine heterotrophic bacteria, p. 261-288. *In* D. L. Kirchman (ed.), *Microbial Ecology of the Oceans*. Wiley-Liss, Inc., New York.
- Kirchman, D. L. and M. P. Hoch. 1988. Bacterial production in the Delaware Bay estuary estimated from thymidine and leucine incorporation rates. *Marine Ecology Progress Series* 45:169-178.
- Kristiansen, S. 1998. Impact of increased river discharge on the phytoplankton community in the outer Oslofjord, Norway. *Hydrobiologia* 363:169-177.
- Labasque, T., C. Chaumery, A. Aminot, and G. Kergoat. 2004. Spectrophotometric Winkler determination of dissolved oxygen: re-examination of critical factors and reliability. *Marine Chemistry* 88:53-60.
- Lackey, G. J. 1992. The effects of light and nutrient availability on primary productivity across the freshwater-saltwater interface of the Neuse River Estuary, North Carolina. M.S. Thesis, East Carolina University, Greenville, NC.
- Litaker, R. W., P. A. Tester, C. S. Duke, B. E. Kenney, J. L. Pinckney, and J. S. Ramus. 2002. Seasonal niche strategy of the bloom-forming dinoflagellate *Heterocapsa triquetra*. *Marine Ecology Progress Series* 232:45-62.
- Luettich, R. A. Jr., S. D. Carr, J. V. Reynolds-Fleming, C. W. Fulcher, and J. E. Mcninch. 2002. Semi-diurnal seiching in a shallow, micro-tidal lagoonal estuary. *Continental Shelf Research* 22:1669-1681.
- Luettich, R. A., Jr., J. E. McNinch, H. W. Paerl, C. H. Peterson, J. T. Wells, M. Alperin, C. S. Martens, and J. L. Pinckney. 2000. Neuse River Estuary modeling and monitoring project stage 1: Hydrography and circulation, water column nutrients and productivity, sedimentary processes and benthic-pelagic coupling, and benthic ecology. Water Resources Research Institute Report No. 325-B. Water Resources Research Institute of the University of North Carolina, Raleigh, NC.
- Mackey, M. D., D. J. Mackey, H. W. Higgins, and S. W. Wright. 1996. CHEMTAX - a program for estimating class abundances from chemical markers: application to HPLC measurements of phytoplankton. *Marine Ecology Progress Series* 144:265-283.
- Mallin, M. A. and C. A. Corbett. 2006. How hurricane attributes determine the extent of environmental effects: multiple hurricanes and different coastal systems. *Estuaries and Coasts* 29:1046-1061.
- Mallin, M. A. and H. W. Paerl. 1992. Effects of variable irradiance on phytoplankton productivity in shallow estuaries. *Limnology and Oceanography* 37:54-62.



- Mallin, M. A., H. W. Paerl, J. Rudek, and P. W. Bates. 1993. Regulation of estuarine primary production by watershed rainfall and river flow. *Marine Ecology Progress Series* 93:199-203.
- Mallin, M. A., M. H. Posey, M. R. McIver, D. C. Parsons, S. H. Ensign, and T. D. Alphin. 2002. Impacts and recovery from multiple hurricanes in a Piedmont-coastal plain river system. *Bioscience* 52:999-1010.
- Mallin, M. A., M. H. Posey, G. C. Shank, M. R. McIver, S. H. Ensign, and T. D. Alphin. 1999. Hurricane effects on water quality and benthos in the Cape Fear watershed: Natural and anthropogenic impacts. *Ecological Applications* 9:350-362.
- McKee, L. J., B. D. Eyre, and S. Hossain. 2000. Transport and retention of nitrogen and phosphorus in the sub-tropical Richmond River estuary, Australia - a budget approach. *Biogeochemistry* 50:241-278.
- McManus, G. B., P. M. Griffin, and J. R. Pennock. 2004. Bacterioplankton abundance and growth in a river-dominated estuary: relationships with temperature and resources. *Aquatic Microbial Ecology* 37:23-32.
- Mitchell, A. W., R. G. V. Bramley, and A. K. L. Johnson. 1997. Export of Nutrients and Suspended Sediment During a Cyclone- Mediated Flood Event in the Herbert River Catchment, Australia. *Marine and Freshwater Research* 48:79-88.
- Nixon, S. W., J. W. Ammerman, L. P. Atkinson, V. M. Berounsky, G. Billen, W. C. Boicourt, W. R. Boynton, T. M. Church, D. M. DiToro, R. Elmgren, J. H. Garber, A. E. Giblin, R. A. Jahnke, N. J. P. Owens, M. E. Q. Pilson, and S. P. Seitzinger. 1996. The fate of nitrogen and phosphorus at the land-sea margin of the North Atlantic Ocean. *Biogeochemistry* 35:141-180.
- Nixon, S. W. 1995. Coastal marine eutrophication: a definition, social causes, and future concerns. *Ophelia* 41:199-219.
- Noble, R. T. and J. A. Fuhrman. 1998. Use of SYBR Green I for rapid epifluorescence counts of marine viruses and bacteria. *Aquatic Microbial Ecology* 14:113-118.
- Noble, R. T. and J. A. Fuhrman. 2000. Rapid virus production and removal as measured with fluorescently labeled viruses as tracers. *Applied and Environmental Microbiology* 66:3790-3797.
- Odum, E. P. and G. W. Barrett. 2005. Fundamentals of Ecology, Fifth Edition ed. Thomson Brooks/Cole, Belmont, CA.
- Pace, M. L., P. del Giorgio, D. Fischer, R. Condon, and H. Malcom. 2004. Estimates of bacterial production using the leucine incorporation method are influenced by differences in protein retention of microcentrifuge tubes. *Limnology and Oceanography: Methods* 2:55-61.

- Paerl, H. W. 1988. Nuisance phytoplankton blooms in coastal, estuarine, and inland waters. *Limnology and Oceanography* 33:823-847.
- Paerl, H. W. 1999. Physical-chemical constraints on cyanobacterial growth in the oceans, p. 319-349. *In* L. Charpy and A. W. D. Larkum (eds.), *Marine Cyanobacteria*. Musée Océanographique, Monaco.
- Paerl, H. W. 2006. Assessing and managing nutrient-enhanced eutrophication in estuarine and coastal waters: Interactive effects of human and climatic perturbations. *Ecological Engineering* 26:40-54.
- Paerl, H. W., J. D. Bales, L. W. Ausley, C. P. Buzzelli, L. B. Crowder, L. A. Eby, J. M. Fear, M. Go, B. L. Peierls, T. L. Richardson, and J. S. Ramus. 2001. Ecosystem impacts of three sequential hurricanes (Dennis, Floyd, and Irene) on the United States' largest lagoonal estuary, Pamlico Sound, NC. *Proceedings of the National Academy of Sciences of the United States of America* 98:5655-5660.
- Paerl, H. W., J. L. Pinckney, J. M. Fear, and B. L. Peierls. 1998. Ecosystem responses to internal and watershed organic matter loading: consequences for hypoxia in the eutrophying Neuse River Estuary, North Carolina, USA. *Marine Ecology Progress Series* 166:17-25.
- Paerl, H. W., L. M. Valdes, A. R. Joyner, B. L. Peierls, M. F. Piehler, S. R. Riggs, R. R. Christian, L. A. Eby, L. B. Crowder, J. S. Ramus, E. J. Clesceri, C. P. Buzzelli, and R. A. Luetlich Jr. 2006a. Ecological response to hurricane events in the Pamlico Sound System, North Carolina, and implications for assessment and management in a regime of increased frequency. *Estuaries and Coasts* 29:1033-1045.
- Paerl, H. W., L. M. Valdes, M. F. Piehler, and C. A. Stow. 2006b. Assessing the Effects of Nutrient Management in an Estuary Experiencing Climatic Change: the Neuse River Estuary, North Carolina. *Environmental Management* 37:422-436.
- Paerl, H. W., L. M. Valdes-Weaver, A. R. Joyner, and V. Winkelmann. 2007. Phytoplankton indicators of ecological change in the eutrophying Pamlico Sound system, North Carolina. *Ecological Applications* 17:S88-S101.
- Pai, S.-C., G.-C. Gong, and K.-K. Liu. 1993. Determination of dissolved oxygen in seawater by direct spectrophotometry of total iodine. *Marine Chemistry* 41:343-351.
- Painchaud, J., D. Lefavre, and J.-C. Therriault. 1987. Box model analysis of bacterial fluxes in the St. Lawrence Estuary. *Marine Ecology Progress Series* 41:241-252.
- Painchaud, J., D. Lefavre, J.-C. Therriault, and L. Legendre. 1996. Bacterial dynamics in the upper St. Lawrence estuary. *Limnology and Oceanography* 41:1610-1618.

- Palumbo, A. V. and R. L. Ferguson. 1978. Distribution of suspended bacteria in the Newport River Estuary, North Carolina. *Estuarine and Coastal Marine Science* 7:521-529.
- Peierls, B. L., N. F. Caraco, M. L. Pace, and J. J. Cole. 1991. Human influence on river nitrogen. *Nature* 350:386-387.
- Peierls, B. L., R. R. Christian, and H. W. Paerl. 2003. Water quality and phytoplankton as indicators of hurricane impacts on a large estuarine ecosystem. *Estuaries* 26:1329-1343.
- Pietrafesa, L. J., G. S. Janowitz, T.-Y. Chao, R. H. Weisberg, F. Askari, and E. Noble. 1986. The physical oceanography of Pamlico Sound. UNC Sea Grant Publication UNC-WP-86-5. UNC Sea Grant, Raleigh, N.C.
- Pinckney, J. L., D. F. Millie, K. E. Howe, H. W. Paerl, and J. P. Hurley. 1996. Flow scintillation counting of  $^{14}\text{C}$ -labeled microalgal photosynthetic pigments. *Journal of Plankton Research* 18:1867-1880.
- Pinckney, J. L., H. W. Paerl, M. B. Harrington, and K. E. Howe. 1998. Annual cycles of phytoplankton community-structure and bloom dynamics in the Neuse River Estuary, North Carolina. *Marine Biology* 131:371-381.
- Pinckney, J. L., H. W. Paerl, and M. B. Harrington. 1999. Responses of the phytoplankton community growth rate to nutrient pulses in variable estuarine environments. *Journal of Phycology* 35:1455-1463.
- Pinckney, J. L., T. L. Richardson, D. F. Millie, and H. W. Paerl. 2001. Application of photopigment biomarkers for quantifying microalgal community composition and in situ growth rates. *Organic Geochemistry* 32:585-595.
- Pomeroy, L. R. and W. J. Wiebe. 2001. Temperature and substrates as interactive limiting factors for marine heterotrophic bacteria. *Aquatic Microbial Ecology* 23:187-204.
- Ramus, J., L. A. Eby, C. M. McClellan, and L. B. Crowder. 2003. Phytoplankton forcing by a record freshwater discharge event into a large lagoonal estuary. *Estuaries* 26:1344-1352.
- Revilla, M., A. Iriarte, I. Madariaga, and E. Orive. 2000. Bacterial and phytoplankton dynamics along a trophic gradient in a shallow temperate estuary. *Estuarine Coastal and Shelf Science* 50:297-313.
- Reynolds-Fleming, J. V., Luettich, and R. A. Luettich, Jr. 2004. Wind-driven lateral variability in a partially mixed estuary. *Estuarine Coastal and Shelf Science* 60:395-407.

- Riemann, B. and F. Azam. 1992. Measurements of bacterial protein synthesis in aquatic environments by means of leucine incorporation. *Marine Microbial Food Webs* 6:91-105.
- Rizzo, W. M. and R. R. Christian. 1996. Significance of subtidal sediments to heterotrophically-mediated oxygen and nutrient dynamics in a temperate estuary. *Estuaries* 19:475-487.
- Rizzo, W. M., G. J. Lackey, and R. R. Christian. 1992. Significance of euphotic, subtidal sediments to oxygen and nutrient cycling in a temperate estuary. *Marine Ecology Progress Series* 86:51-61.
- Roberts, R. D. 1998. Incorporation of radioactive precursors into macromolecules as measures of bacterial growth: problems and pitfalls, p. 471-486. In K. E. Cooksey (ed.), *Molecular Approaches to the Study of the Ocean*. Chapman & Hall, London.
- Roland, F., N. F. Caraco, J. J. Cole, and P. del Giorgio. 1999. Rapid and precise determination of dissolved oxygen by spectrophotometry: Evaluation of interference from color and turbidity. *Limnology and Oceanography* 44:1148-1154.
- Roland, F. and J. J. Cole. 1999. Regulation of bacterial growth efficiency in a large turbid estuary. *Aquatic Microbial Ecology* 20:31-38.
- Rudek, J., H. W. Paerl, M. A. Mallin, and P. W. Bates. 1991. Seasonal and hydrological control of phytoplankton nutrient limitation in the lower Neuse River Estuary, North Carolina. *Marine Ecology Progress Series* 75:133-142.
- Sañudo-Wilhelmy, S. A. and G. T. Taylor. 1999. Bacterioplankton dynamics and organic carbon partitioning in the lower Hudson River estuary. *Marine Ecology Progress Series* 182:17-27.
- Schultz, G. E., E. D. White III, and H. W. Ducklow. 2003. Bacterioplankton dynamics in the York River estuary: primary influence of temperature and freshwater inputs. *Aquatic Microbial Ecology* 30:135-148.
- Sharp, J. H., J. R. Pennock, T. M. Church, J. M. Tramontano, and L. A. Cifuentes. 1984. The estuarine interaction of nutrients, organics, and metals: a case study in the Delaware Estuary, p. 241-258. In V. S. Kennedy (ed.), *The Estuary as a Filter*. Academic Press, New York.
- Sherr, E. and B. Sherr. 2000. Marine microbes: an overview, p. 13-46. In D. L. Kirchman (ed.), *Microbial Ecology of the Oceans*. Wiley-Liss, New York.
- Shiah, F.-K., S.-W. Chung, S.-J. Kao, G.-C. Gong, and K.-K. Liu. 2000. Biological and hydrographical responses to tropical cyclones (typhoons) in the continental shelf of the Taiwan Strait. *Continental Shelf Research* 20:2029-2044.

- Shiah, F.-K. and H. W. Ducklow. 1994a. Temperature and substrate regulation of bacterial abundance, production and specific growth-rate in Chesapeake Bay, USA. *Marine Ecology Progress Series* 103:297-308.
- Shiah, F.-K. and H. W. Ducklow. 1994b. Temperature regulation of heterotrophic bacterioplankton abundance, production, and specific growth-rate in Chesapeake Bay. *Limnology and Oceanography* 39:1243-1258.
- Shiah, F.-K. and H. W. Ducklow. 1995. Multiscale variability in bacterioplankton abundance, production, and specific growth-rate in a temperate salt-marsh tidal creek. *Limnology and Oceanography* 40:55-66.
- Smith, D. C. and F. Azam. 1992. A simple, economical method for measuring bacterial protein synthesis rates in seawater using  $^3\text{H}$ -leucine. *Marine Microbial Food Webs* 6:107-114.
- Staroscik, A. M. and D. C. Smith. 2004. Seasonal patterns in bacterioplankton abundance and production in Narragansett Bay, Rhode Island, USA. *Aquatic Microbial Ecology* 35:275-282.
- Steel, J. 1991. Albemarle-Pamlico estuarine system: technical analysis of status and trends. Albemarle-Pamlico Estuarine Study Report No. 91-01. N.C. Department of Environment, Health, and Natural Resources, Albemarle-Pamlico Estuarine Study, Raleigh, NC.
- Steemann Nielsen, E. 1952. The use of radio-active carbon ( $\text{C}^{14}$ ) for measuring organic production in the sea. *Journal du Conseil permanent international pour L'Exploration de la Mer* 18:117-140.
- Stow, C. A., M. E. Borsuk, and D. W. Stanley. 2001. Long-term changes in watershed nutrient inputs and riverine exports in the Neuse River, North Carolina. *Water Research* 35:1489-1499.
- Strayer, D. L. 1988. On the limits to secondary production. *Limnology and Oceanography* 33:1217-1220.
- Strayer, D. L., M. E. Power, W. F. Fagan, S. T. A. Pickett, and J. Belnap. 2003. A classification of ecological boundaries. *Bioscience* 53:723-729.
- Summers, K. 2001. National Coastal Condition Report. EPA-620/R-01/005. US Environmental Protection Agency, Washington, D.C.
- Tabb, D. C. and A. C. Jones. 1962. Effect of Hurricane Donna on the aquatic fauna of north Florida Bay. *Transactions of the American Fisheries Society* 91:375-378.
- Tester, P. A., S. M. Varnam, M. E. Culver, D. L. Eslinger, R. P. Stumpf, R. N. Swift, J. K. Yungel, M. D. Black, and R. W. Litaker. 2003. Airborne detection of ecosystem responses to an extreme event: phytoplankton displacement and

- abundance after hurricane induced flooding in the Pamlico-Albemarle Sound system, North Carolina. *Estuaries* 26:1353-1364.
- Troussellier, M., H. Schäfer, N. Batailler, L. Bernard, C. Courties, P. Lebaron, G. Muyzer, P. Servais, and J. Vives-Rego. 2002. Bacterial activity and genetic richness along an estuarine gradient (Rhône River plume, France). *Aquatic Microbial Ecology* 28:13-24.
- U.S. Environmental Protection Agency. 2000. Ambient aquatic life water quality criteria for dissolved oxygen (saltwater): Cape Cod to Cape Hatteras. EPA-822-R-00-012. U.S. Environmental Protection Agency, Washington, D.C.
- Ulanowicz, R. E. 1987. NETWRK4: A package of computer algorithms to analyze ecological flow networks. University of Maryland, Chesapeake Biological Laboratory, Solomons, Maryland.
- Valiela, I., P. Peckol, C. D'Avanzo, J. Kremer, D. Hersh, K. Foreman, K. Lajtha, B. Seely, W. R. Geyer, T. Isaji, and R. Crawford. 1998. Ecological effects of major storms on coastal watersheds and coastal waters: Hurricane Bob on Cape Cod. *Journal of Coastal Research* 14:218-238.
- Van Dolah, R. F. and G. S. Anderson. 1991. Effects of Hurricane Hugo on salinity and dissolved oxygen conditions in the Charleston Harbor estuary, p. 83-94. In C. W. Finkl and O. H. Pilkey (eds.), Impacts of Hurricane Hugo: September 10-22, 1989. Coastal Education and Research Foundation, Fort Lauderdale, Florida.
- White, P. A., J. Kalff, J. B. Rasmussen, and J. M. Gasol. 1991. The effect of temperature and algal biomass on bacterial production and specific growth rate in freshwater and marine habitats. *Microbial Ecology* 21:99-118.
- Williams, A. B., G. S. Posner, W. J. Woods, and E. E. Deubler, Jr. 1973. A hydrographic atlas of larger North Carolina sounds. Sea Grant Publication UNC-SG-73-02. University of North Carolina Sea Grant Program, Chapel Hill.
- Williams, C. J., J. N. Boyer, and F. J. Jochem. 2008. Indirect hurricane effects on resource availability and microbial communities in a subtropical wetland-estuary transition zone. *Estuaries and Coasts* 31:204-214.
- Williams, P. J. I. B. and P. A. del Giorgio. 2005. Respiration in aquatic ecosystems: history and background, p. 1-17. In P. A. del Giorgio and P. J. I. B. Williams (eds.), Respiration in Aquatic Ecosystems. Oxford University Press, Oxford.
- Wilson, J. G. 2002. Productivity, fisheries and aquaculture in temperate estuaries. *Estuarine, Coastal and Shelf Science* 55:953-967.
- Woods, W. J. 1967. Hydrographic studies in Pamlico Sound, p. 105-114. In Proceedings of Symposium on Hydrology of the Coastal Waters of North Carolina. Water Resources Research Institute of the University of North Carolina, Raleigh.

Wright, R. T. and R. B. Coffin. 1983. Planktonic bacteria in estuaries and coastal waters of northern Massachusetts: spatial and temporal distribution. *Marine Ecology Progress Series* 11:205-216.